PRODUCT STUDIES OF THE ATMOSPHERICALLY-IMPORTANT REACTIONS OF ALKENES AND AROMATIC HYDROCARBONS

Final Report

Contract No. 94-311

Prepared for:

California Air Resources Board
Research Division
2020 L Street
Sacramento, CA 95814

Prepared by:

Roger Atkinson, Janet Arey and Ernesto C. Tuazon
Co-Principal Investigators

Statewide Air Pollution Research Center
University of California
Riverside, CA 92521

May 1997

Disclaimer

The statements and conclusions in this Report are those of the contractor and not necessarily those of the California Air Resources Board. The mention of commercial products, their source, or their use in connection with material reported herein is not to be construed as actual or implied endorsement of such products.

Acknowledgments

The Principal Investigators thank Ms. Sara M. Aschmann, Mr. Andrew A. Chew and Dr. Jennifer Sasaki for their invaluable contributions to the experimental work described in this report. In particular, the work described in Section 5 fulfilled a part of the Ph.D. requirement for Dr. Jennifer Sasaki, and the work described in Section 2 will fulfill part of the thesis dissertation of Andrew A. Chew.

This Report was submitted in fulfillment of ARB Contract No. 94-311, "Product Studies of the Atmospherically-Important Reactions of Alkenes and Aromatic Hydrocarbons," by the Statewide Air Pollution Research Center, University of California, Riverside, CA, under the partial sponsorship of the California Air Resources Board. Work was completed as of January 15, 1997.

Table of Contents

Disclaimer ii

Acknowledgments iii

List of Figures vi

List of Tables xi

Abstract xii

Executive Summary xiii

1. INTRODUCTION AND BACKGROUND OF PROJECT 1

2. OH RADICAL FORMATION YIELDS FROM THE REACTIONS OF O_3 WITH ALKENES 9
   - Introduction 9
   - Experimental 11
   - Results and Discussion 14

3. PRODUCTS OF THE GAS-PHASE REACTIONS OF O_3 WITH A SERIES OF METHYL-SUBSTITUTED ETHENES 22
   - Introduction 22
   - Experimental 23
   - Results 26
   - Discussion 45

4. PRODUCTS OF THE GAS-PHASE REACTIONS OF A SERIES OF METHYL-SUBSTITUTED ETHENES WITH THE OH RADICAL 51
   - Introduction 51
   - Experimental 53
   - Results 56
   - Discussion 74

5. PRODUCTS OF THE GAS-PHASE OH AND NO_3 RADICAL-INITIATED REACTIONS OF NAPHTHALENE 78
   - Introduction 78
   - Experimental 79
   - Results 83
   - Conclusions 101

6. PRODUCTS OF THE GAS-PHASE OH AND NO_3 RADICAL-INITIATED REACTIONS OF BIPHENYL AND 1- AND 2-METHYLNAPHTHALENE . . 104
Introduction 104
Experimental 104
Results and Discussion 107

7. CONCLUSIONS 116

References 118

Glossary of Terms, Abbreviations and Symbols 126

List of Figures

Figure 1. Plot of Equation (I) for the gas-phase reaction of the OH radical with 2-butanol, with cyclohexane as the reference organic 15

Figure 2. Plot of the amount of 2-butanone formed, corrected for reaction with the OH radical, against the amount of 2-butanol reacted with the OH radical in irradiated CH_3ONO - NO - 2-butanol - air and CH_3ONO - NO - 2-butanol - cyclohexane - air mixtures 16

Figure 3. Plots of the amounts of 2-butanone formed against the amounts of 2,3-dimethyl-2-butene, 2-methyl-2-butene, α-pinene and sabinene reacted with O_3 in the presence of sufficient 2-butanol to scavenge $\geq$95% of the OH radicals formed. The data for 2,3-dimethyl-2-butene and 2-methyl-2-butene have been displaced vertically by 5.0×10^{12} molecule cm^{-3} and 1.0×10^{13} molecule cm^{-3}, respectively, for clarity 19

Figure 4. Plots of the amounts of acetaldehyde and acetone formed against the amounts of 2-methyl-2-butene with O_3 in the presence of sufficient cyclohexane to scavenge $\geq$95% of the OH radicals formed . . . 27

Figure 5. Plots of the amounts of acetone formed against the amounts of 2-methylpropene and 2,3-dimethyl-2-butene reacted with O_3 in the presence of sufficient cyclohexane to scavenge $\geq$95% of the OH radicals formed 28

Figure 6. FT-IR spectra from the reaction of O_3 with propene in air in the presence of excess cyclohexane. (A) Reaction mixture with 51.6% of propene consumed. (B) From (A) after subtraction of absorptions by propene, HCHO, CO, and CO_2. (C) Residual spectrum after subtraction of absorptions by the known compounds, except ketene; subtraction of CH_3CHO was based on the yield measured by GC-FID. The discontinuities in the spectra represent regions severely distorted by strong absorptions of the added cyclohexane 33

Figure 7. FT-IR spectra from the reaction of O_3 with 2-methylpropene in air in the presence of excess cyclohexane. (A) Reaction mixture with 53.9% of 2-methylpropene consumed. (B) From (A) after subtraction of absorptions by 2-methylpropene, HCHO, CO, and CO_2. (C) Residual spectrum after subtraction of absorptions by the known compounds. The discontinuities in the spectra represent regions severely distorted by strong absorptions of the added cyclohexane 34

Figure 8. FT-IR spectra from the reaction of O_3 with *cis*-2-butene in air in the presence of excess cyclohexane. (A) Reaction mixture with 59.5% of *cis*-2-butene consumed. (B) From (A) after subtraction of absorptions by *cis*-2-butene, HCHO, CO, and CO_2. (C) Residual spectrum after subtraction of absorptions by the known compounds, except ketene and glyoxal. The discontinuities in the spectra represent regions severely distorted by strong absorptions of the added cyclohexane 35

Figure 9. FT-IR spectra from the reaction of O_3 with 2-methyl-2-butene in air in the presence of excess cyclohexane. (A) Reaction mixture with 58.6% of 2-methyl-2-butene consumed. (B) From (A) after subtraction of absorptions by 2-methyl-2-butene, HCHO, CO, and CO_2. (C) Residual spectrum after subtraction of absorptions by the known compounds, except ketene; CH_3CHO absorptions was also subtracted based on the yield measured by GC-FID. The discontinuities in the spectra represent regions severely distorted by strong absorptions of the added cyclohexane 36

Figure 10. FT-IR spectra from the reaction of O_3 with 2,3-dimethyl-2-butene in air in the presence of excess cyclohexane. (A) Reaction mixture with 53.2% of 2,3-dimethyl-2-butene consumed. (B) From (A) after subtraction of absorptions by HCHO and CO_2. (C) Residual spectrum after subtraction of absorptions by the known compounds. The discontinuities in the spectra represent regions severely distorted by strong absorptions of the added cyclohexane 37

Figure 11. Plots of the amounts of products formed against the amounts of propene reacted with O_3 in the presence of sufficient cyclohexane to scavenge $\geq$95% of the OH radicals formed. Data from two separate experiments are combined in each plot (except for CO_2 and glyoxal where data from one experiment were excluded because of background interference) 38

Figure 12. Plots of the amounts of products formed against the amounts of 2-methylpropene reacted with O_3 in the presence of sufficient cyclohexane to scavenge $\geq$95% of the OH radicals formed. Data from two separate experiments are combined in each plot 39

Figure 13. Plots of the amounts of products formed against the amounts of *cis*-2-butene reacted with O_3 in the presence of sufficient cyclohexane to scavenge $\geq$95% of the OH radicals formed. Data from two separate experiments are combined in each plot 40

Figure 14. Plots of the amounts of products formed against the amounts of *trans*-2-butene reacted with O_3 in the presence of sufficient cyclohexane to scavenge ≥95% of the OH radicals formed. Data from two separate experiments are combined in each plot 41

Figure 15. Plots of the amounts of products formed against the amounts of 2-methyl-2-butene reacted with O_3 in the presence of sufficient cyclohexane to scavenge ≥95% of the OH radicals formed. Data from two separate experiments are combined in each plot 42

Figure 16. Plots of the amounts of products formed against the amounts of 2,3-dimethyl-2-butene reacted with O_3 in the presence of sufficient cyclohexane to scavenge ≥95% of the OH radicals formed. Data from two separate experiments are combined in each plot 43

Figure 17. Plots of the amounts of acetone formed, corrected for reaction with the OH radical, against the amounts of 2-methyl-2-butene and 2,3-dimethyl-2-butene reacted with the OH radical in the presence of NO 57

Figure 18. Infrared spectrum from a 2-methylpropene - CH_3CH_2ONO - NO irradiation experiment. (A) Initial reactant mixture. (B) Difference spectrum: spectrum of mixture after 3.25 min of photolysis minus that of reaction mixture prior to irradiation. (C) Residual spectrum 61

Figure 19. Infrared spectra from a *cis*-2-butene - CH_3ONO - NO irradiation experiment. (A) Initial alkene. (B) Mixture after 3.5 min of irradiation. (C) Product spectrum from (B). (D) Residual spectrum 62

Figure 20. Infrared spectra from a 2-methyl-2-butene - CH_3ONO - NO irradiation experiment. (A) Initial alkene. (B) Mixture after 3.0 min of irradiation. (C) Product spectrum from (B). (D) Residual spectrum 63

Figure 21. Infrared spectra from a 2,3-dimethyl-2-butene - CH_3ONO - NO irradiation experiment. (A) Initial alkene. (B) Mixture after 2.7 min of irradiation. (C) Product spectrum from (B). (D) Residual spectrum 64

Figure 22. Plots of the amounts of HCHO and acetone formed, corrected for reaction with the OH radical, against the amounts of 2-methylpropene reacted with the OH radical in irradiated CH_3ONO (or C_2H_5ONO) - NO - 2-methylpropene - air mixtures. The HCHO data are from an experiment using ethyl nitrite as the OH radical precursor 65

Figure 23. Plots of the amounts of CH_3CHO formed, corrected for reaction with the OH radical, against the amounts of *cis*-2-butene reacted with the OH radical in irradiated CH_3ONO - NO - *cis*-2-butene - air mixtures 66

Figure 24. Plots of the amounts of CH_3CHO and $CH_3C(O)CH_3$ formed, corrected for reaction with the OH radical, against the amounts of 2-methyl-2-butene reacted with the OH radical in irradiated CH_3ONO - NO - 2-methyl-2-butene - air mixtures 67

Figure 25. Plots of the amounts of $CH_3C(O)CH_3$ formed, corrected for reaction with the OH radical, against the amounts of 2,3-dimethyl-2-butene reacted with the OH radical in irradiated CH_3ONO - NO - 2,3-dimethyl-2-butene - air mixtures 68

Figure 26. GC-FID chromatogram of the diethyl ether eluate of a sample collected on Tenax solid adsorbent from the gas-phase OH radical-initiated reaction of naphthalene 84

Figure 27. API-MS spectra of irradiated CH_3ONO - NO - naphthalene - air (A) and CH_3ONO - NO - naphthalene-d_8 - air (B) mixtures 85

Figure 28. API-MS/MS collision induced dissociation (CAD) spectra of the 161 u (A) and 169 u (B) ion peaks observed in the OH radical-initiated reaction of naphthalene and naphthalene-d_8, respectively 87

Figure 29. Plots of the amounts of the molecular weight 176 products and 1,4-naphthoquinone against the amounts of naphthalene reacted with the OH radical. The measured concentrations of the two products were corrected for reaction with the OH radical as noted in the text and footnotes d and j of Table 7 91

Figure 30. Plots of the measured amount of 2-formyl-*cis*-cinnamaldehyde (○, ●) and 2-formyl-*trans*-cinnamaldehyde (Δ, ▲) against the amounts of naphthalene reacted with the OH radical 94

Figure 31. Plots of the amounts of 2-formylcinnamaldehyde (*cis* + *trans*) against the amounts of naphthalene reacted with the OH radical 96

Figure 32. GC-FID chromatogram of the diethyl ether eluate of a sample collected on Tenax solid adsorbent from the gas-phase NO_3 radical-initiated reaction of naphthalene 98

Figure 33. Plots of the amounts of 1- and 2-nitronaphthalene formed, corrected for reaction with the NO_3 radical (see text), against the amounts of naphthalene reacted with the NO_3 radical 100

Figure 34. GC-FID chromatogram of the diethyl ether eluate of a sample collected on Tenax solid adsorbent from the gas-phase OH radical-initiated reaction of 1-methylnaphthalene 110

Figure 35. GC-FID chromatogram of the diethyl ether eluate of a sample collected on Tenax solid adsorbent from the gas-phase OH radical-initiated reaction of 2-methylnaphthalene 111

Figure 36. GC-FID chromatogram of the diethyl ether eluate of a sample collected on Tenax solid adsorbent from the gas-phase NO_3 radical-initiated reaction of 1-methylnaphthalene 113

Figure 37. GC-FID chromatogram of the diethyl ether eluate of a sample collected on Tenax solid adsorbent from the gas-phase NO_3 radical-initiated reaction of 2-methylnaphthalene 114

List of Tables

Table 1. 2-Butanone and OH radical formation yields from the gas-phase reactions of O_3 with 2,3-dimethyl-2-butene, 2-methyl-2-butene, α-pinene, and sabinene at 296 $\pm$ 2 K and atmospheric pressure in the presence of sufficient 2-butanol to scavenge $\geq$95% of the OH radicals 20

Table 2. Products and their yields from the reaction of O_3 with alkenes in the presence of an OH radical scavenger at room temperature and one atmosphere of air 29

Table 3. Formation yields of the "primary" carbonyls from the gas-phase reactions of O_3 with a series of methyl-substituted ethenes at room temperature and atmospheric pressure of air in the presence of an OH radical scavenger 46

Table 4. Products and their formation yields observed from the reactions of the OH radical with alkenes in the presence of NO at 296 $\pm$ 2 K and 740 Torr total pressure of air 59

Table 5. Products formed from the gas-phase reactions of the OH radical with methyl-substituted ethenes in the absence of NO, as observed by API-MS and API-MS/MS analyses 76

Table 6. ^{1}H NMR chemical shifts, multiplicities, and coupling constants for 2-formyl-*trans*-cinnamaldehyde (I) and *trans*-cinnamaldehyde (II) in $CDCl_3$, GE 300 MHz NMR 89

Table 7. Products observed, and their formation yields, from the gas-phase OH radical- and NO_3 radical-initiated reactions of naphthalene 92

Abstract

Alkenes and aromatic hydrocarbons are important constituents of ambient air in polluted urban areas, and their atmospheric reactions in the presence of oxides of nitrogen lead to the formation of ozone and other manifestations of photochemical air pollution. During this Contract, the products and mechanisms of the gas-phase OH radical-initiated and O_3 reactions of a series of alkenes and of the gas-phase OH radical- and NO_3 radical-initiated reactions of four two-ring aromatic hydrocarbons have been investigated. The two-ring aromatic hydrocarbons were studied because it was anticipated that their reaction products would be more amenable to analysis using conventional gas chromatographic techniques than would the corresponding products formed from the monocyclic aromatic hydrocarbons such as benzene, toluene and the xylenes; this was found to be the case. Experiments were carried out in 5800-7900 liter volume Teflon or Teflon-coated chambers, and products were analyzed using gas chromatography with flame ionization detection, mass spectrometry, and Fourier transform infrared spectroscopy, by *in situ* Fourier transform infrared absorption spectroscopy, and by direct air sampling, atmospheric pressure ionization tandem mass spectrometry. The results of these experiments have better characterized the reactions in the atmosphere of simple alkenes and of aromatic hydrocarbons, and the reaction mechanisms determined in this study will be used in state-of-the-science detailed chemical mechanisms for the formation of ozone in urban and regional airshed models currently under development.

Executive Summary

Background

Alkenes and aromatic hydrocarbons are important constituents of ambient air in polluted urban areas, and their atmospheric reactions in the presence of oxides of nitrogen lead to the formation of ozone and other manifestations of photochemical air pollution. Despite some two decades of research by numerous groups throughout the world, there are still significant areas of uncertainty concerning the reactions in the atmosphere of alkenes and, especially, aromatic hydrocarbons. These uncertainties translate into uncertainties in the chemical mechanisms used in urban and regional air quality simulation models used to investigate optimum strategies for the control of ozone in these areas. During this Contract, the products and mechanisms of the gas-phase OH radical-initiated and O_3 reactions of a series of alkenes and of the gas-phase OH radical- and NO_3 radical-initiated reactions of four two-ring aromatic hydrocarbons have been investigated. The two-ring aromatic hydrocarbons were studied because it was anticipated that their reaction products would be more amenable to analysis using conventional gas chromatographic techniques than would the corresponding products formed from the monocyclic aromatic hydrocarbons such as benzene, toluene and the xylenes; and this was found to be the case.

Methods

Experiments were carried out in 5800-7900 liter volume Teflon or Teflon-coated chambers, with irradiation provided by blacklamps or by a point source xenon arc, and products were analyzed using gas chromatography with flame ionization detection, mass spectrometry, and Fourier transform infrared spectroscopy, by *in situ* Fourier transform infrared (FT-IR) absorption spectroscopy, and by direct air sampling, atmospheric pressure ionization tandem mass spectrometry (API-MS).

Results

The results of these studies, discussed in Sections 2 through 6 in the report, have advanced our knowledge of the atmospheric reactions of alkenes and aromatic hydrocarbons.

Alkene Chemistry. We have developed an improved method for determining the yields of OH radicals from the reactions of O_3 with alkenes, utilizing 2-butanol to scavenge OH radicals and determining the OH radical formation yields from the amounts of 2-butanone formed. We have shown that this more accurate technique agrees well with the results of previous studies from our laboratory using cyclohexane to scavenge OH radicals and deriving the OH radical formation yields from the amounts of cyclohexanone plus cyclohexanol formed (Atkinson *et al.*, 1992; Atkinson and Aschmann, 1993).

Product studies of the reactions of O_3 with a series of methyl-substituted ethenes shows that the sum of the primary carbonyls is unity (except where HCHO can be formed from secondary reactions of the biradical co-products), and a number of additional products (methane, methanol, ketene, glyoxal, CO and CO_2) were identified and quantified by *in situ* FTIR absorption spectroscopy. The yields of these products allows certain biradical decomposition pathways to be delineated.

Product studies of the reactions of the OH radical with 2-methylpropene, *cis*-2-butene, 2-methyl-2-butene and 2,3-dimethyl-2-butene in the presence of NO showed the formation of small amounts of organic nitrates from the $R\dot{O}_2$ + NO reactions, and the carbonyl products formed and their formation yields showed that the intermediate β-hydroxyalkoxy radicals undergo dominantly decomposition. API-MS analyses of the reacted mixtures showed no evidence for the formation of the β-hydroxycarbonyls which would be formed from reactions of the intermediate β-hydroxyalkoxy radicals with O_2. In the absence of NO_x, API-MS analyses indicated the formation of the products expected from the reactions of β-hydroxyalkyl peroxy radicals with organic peroxy radicals and HO_2 reactions (carbonyls, hydroxycarbonyls, dihydroxyalkanes and hydroxyhydroperoxides).

Aromatic Chemistry. Identification and quantification of the products of the reactions of the OH radical with naphthalene, 1- and 2-methylnaphthalene and biphenyl in the presence of NO_x showed that these reactions are analogous to the OH radical-initiated reactions of monocyclic aromatic hydrocarbons, in that a major reaction pathway(s) lead to the formation of ring-opened products. The formation of 2-formylcinnamaldehyde from naphthalene was observed in high ($\sim$35%) yield, together with a number of other ring-opened and ring-retaining products. Although most of the products from the methylnaphthalene and biphenyl reactions were not specifically identified, the reactions appear to be quite similar to that for naphthalene. The NO_3 radical-initiated reactions of naphthalene and 1- and 2-methylnaphthalene lead to the formation of nitronaphthalenes and methylnitronaphthalenes in significant ($\sim$25-30%) yield. These product studies of two-ring polycyclic aromatic hydrocarbons reinforce recent product data obtained in our laboratories for the monocyclic aromatic hydrocarbons using API-MS analyses of reaction products.

Conclusions

The results of these experiments have better characterized the reactions in the atmosphere of simple alkenes and of aromatic hydrocarbons, and the reaction mechanisms determined in this study will be used in state-of-the-science detailed chemical mechanisms for the formation of ozone in urban and regional airshed models currently under development.

1. INTRODUCTION AND BACKGROUND TO THE PROJECT

A large number of volatile non-methane organic compounds (NMOC) are emitted into the atmosphere from anthropogenic and biogenic sources. The estimated emissions of NMOC from anthropogenic and biogenic sources are of similar magnitude for the U.S.A., ~22 million tons per year for anthropogenic NMOC emissions *versus* ~29 million tons per year for biogenic NMOC (Lamb *et al.*, 1993). Anthropogenic NMOCs are therefore expected to dominate over biogenic NMOCs in urban areas while the reverse is the case in non-urban and rural areas, and this is borne out by ambient atmospheric measurements (see, for example, Martin *et al.*, 1991; Lurmann and Main, 1992; Montzska *et al.*, 1993; Riemer *et al.*, 1994). In urban areas the NMOCs are mainly comprised of alkanes, alkenes, aromatic hydrocarbons and carbonyl compounds (Lurmann and Main, 1992).

In urban areas, the most abundant alkenes are typically ethene and propene from anthropogenic sources and the most abundant aromatic hydrocarbons are benzene, toluene and the xylenes (Lurmann and Main, 1992). In the Los Angeles air basin, the measured alkene and aromatic hydrocarbon concentrations account for ~10% and ~18%, respectively, of ambient NMOCs (with 15% being unidentified) (Lurmann and Main, 1992). The high reactivities of aromatic hydrocarbons and, especially, the alkenes with respect to ozone formation (Carter, 1994) make these two classes of NMOC important in the formation of photochemical air pollution in urban and rural areas.

Despite some two decades of research into the atmospheric chemistry of the alkenes and aromatic hydrocarbons, at the start of this program there were still significant discrepancies in our knowledge of the reaction mechanisms and products formed (Atkinson, 1994), and hence in the representation of these NMOCs in the chemical mechanisms used in urban airshed computer models (Carter, 1994). The atmospheric chemistry of the alkanes and aromatic hydrocarbons (including of 2-ring polycyclic aromatic hydrocarbons) are briefly discussed below. More detailed discussions are given with each of the individual sections of the report, below.

Atmospheric Chemistry of Alkenes

The atmospherically-important reactions of the alkenes are with OH radicals, NO_3 radicals and O_3 (Atkinson, 1994), with the NO_3 reactions being important only during nighttime hours.

Ozone Reactions. The reactions of alkenes with O_3 proceed by initial addition of O_3 to the >C=C< bond(s) to form an energy-rich primary ozonide which is then believed to decompose to form, in general, two sets of (carbonyl + biradical) products (Reaction Scheme 1):

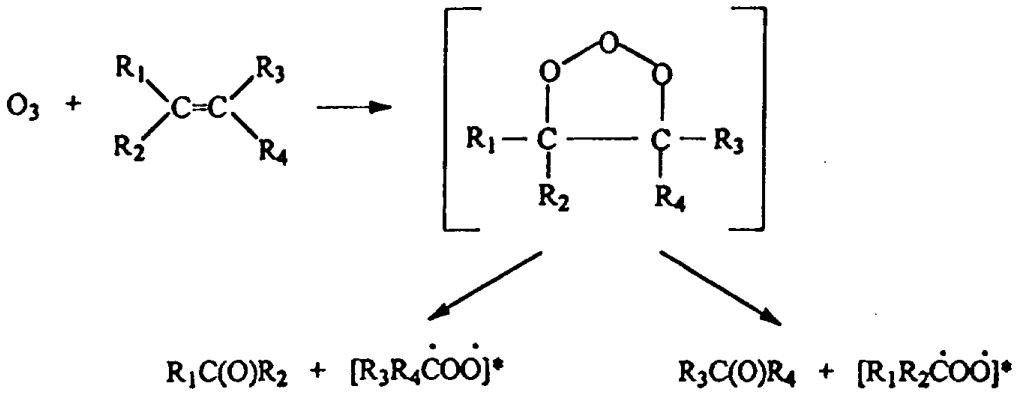

Reaction Scheme 1

The reactions of the initially energy-rich biradicals are not well understood, but are expected to include the following reactions (Reaction Scheme 2):

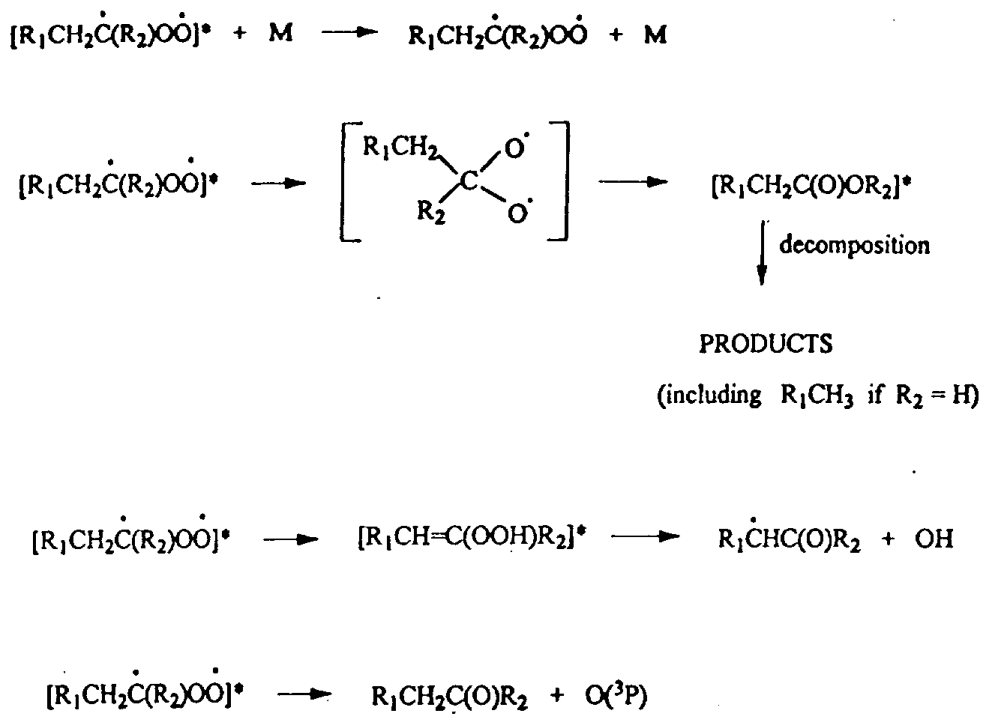

Reaction Scheme 2

$O(^3P)$ atom formation from acyclic alkenes and dienes has been shown to be insignificant (Atkinson *et al.*, 1994a,b), although the direct formation of epoxides from the O_3 reactions with the conjugated dienes 1,3-butadiene and isoprene has been observed in small yield (~2-5%) (Atkinson *et al.*, 1994a,b)]. However, OH radicals are formed from the gas-phase reactions of O_3 with alkenes (including isoprene, monoterpenes and sesquiterpenes), often in close to unit yield (Atkinson *et al.*, 1992, 1995a; Atkinson and Aschmann, 1993; Shu and Atkinson, 1994), and unless these OH radicals are scavenged the products observed are formed from both the OH radical and O_3 reactions with the alkene.

The reaction sequence shown above predicts that in the presence of an OH radical scavenger, the overall carbonyl yield (i.e., $R_1C(O)R_2$ + $R_3C(O)R_4$) will be 100%. The measured yield of carbonyls can be >100% if the biradicals decompose or react to form the same carbonyl products as formed from decomposition of the primary ozonide. This expectation

has been confirmed by recent product studies carried out in this laboratory (Atkinson *et al.*, 1995a) under our previous CRC-funded program, and more recently by Grosjean and co-workers (Grosjean and Grosjean, 1996a,b,c,d; Grosjean *et al.*, 1996a,b). At the time that this program started, reliable product yield data in the presence of an OH radical scavenger had not been obtained for the reactions of O_3 with simple methyl-substituted ethenes.

OH Radical Reactions. The OH radical reactions with alkenes in the presence of NO_x are postulated to proceed by the reaction scheme (Atkinson, 1994), taking internal OH radical addition to 1-pentene as the example (Reaction Scheme 3):

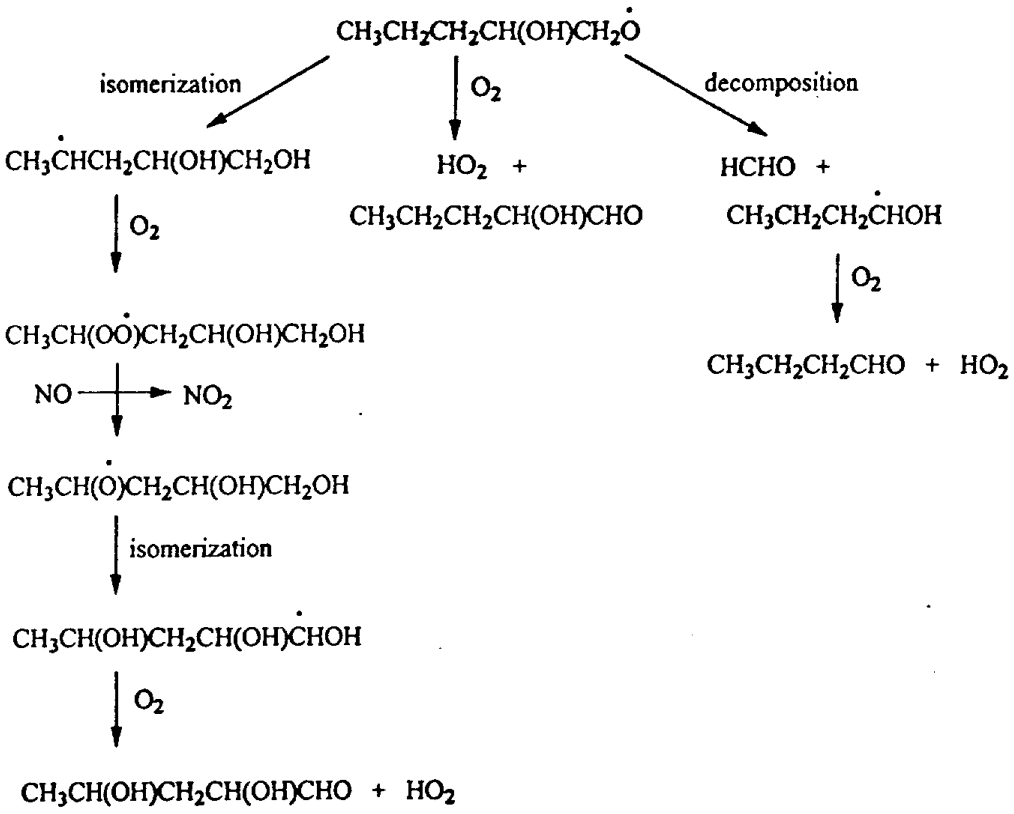

Reaction Scheme 3

leading to either the carbonyls $R_1C(O)R_2$ + $R_3C(O)R_4$ from the alkene $R_1R_2C=CR_3R_4$ or the β-hydroxycarbonyl (Atkinson, 1994). For alkenes with longer alkyl side-chains, alkoxy radical

isomerization also occurs, leading to dihydroxycarbonyls (Atkinson *et al.*, 1995b; Kwok *et al.*, 1996a; Atkinson, 1997a,b). Among the simpler acyclic alkenes, carbonyl product data are available for ethene (Niki *et al.*, 1981), propene (Niki *et al.*, 1978), 1-butene (Atkinson *et al.*, 1985), *trans*-2-butene (Niki *et al.*, 1978) and the C_5-C_8 1-alkenes and 2,3-dimethyl-1-butene (Atkinson *et al.*, 1995b). However, no product data are available for the relatively simple alkenes *cis*-2-butene (although expected to be identical to *trans*-2-butene), 2-methylpropene, 2-methyl-2-butene or 2,3-dimethyl-2-butene.

Aromatic Hydrocarbons

The aromatic hydrocarbons benzene and the alkyl-substituted benzenes and the simple polycyclic aromatic hydrocarbons (PAH) [such as naphthalene, biphenyl, and 1- and 2-methylnaphthalene] react with OH radicals and NO_3 radicals in the atmosphere (Atkinson, 1989, 1991, 1994; Atkinson and Arey, 1994). The OH radical reaction is calculated to dominate as the tropospheric loss process for the monocyclic and most of the polycyclic aromatic hydrocarbons (Arey *et al.*, 1989; Atkinson, 1994; Atkinson and Arey, 1994). The OH radical and NO_3 radical reactions proceed by two pathways: initial OH radical or NO_3 radical addition to the aromatic ring(s) to form an OH-aromatic or NO_3-aromatic adduct, and H-atom abstraction from the alkyl-substituent groups. The initial reaction pathways are shown in Reaction Scheme 4 below for the OH radical reaction with toluene.

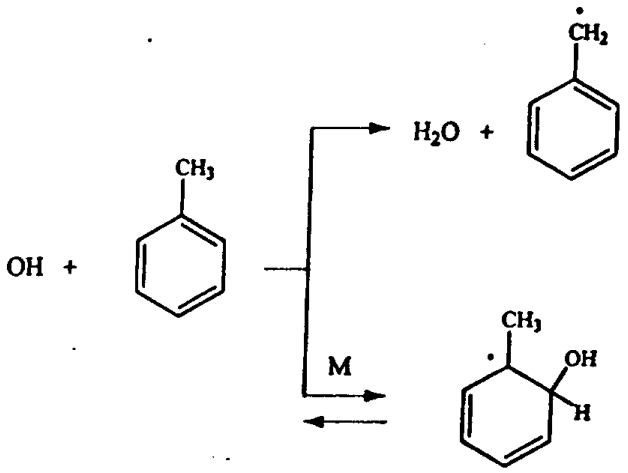

Reaction Scheme 4

The initial addition of OH radicals and, especially, NO_3 radicals to the aromatic ring(s) is reversible. For the OH radical reactions, at and below room temperature the OH-aromatic adducts are effectively thermally "stable" (Atkinson, 1989, 1994), while the NO_3-aromatic adducts thermally decompose back to reactants rapidly (Atkinson, 1991).

For the monocyclic aromatic hydrocarbons (for example, toluene and the xylenes), the only observable pathway for the NO_3 radical reactions is via the H-atom abstraction pathway leading to the formation of the benzyl radical from toluene and the methylbenzyl radicals from the xylenes. The H-atom abstraction channel is minor for the OH radical reactions, accounting for $\leq 10\%$ of the overall OH radical reaction (Atkinson, 1989, 1994). The major reaction pathway for the OH radical reactions therefore involves the formation of the hydroxycyclohexadienyl-type radicals (Atkinson, 1989, 1994), which then react with O_2 or NO_2 (Knispel *et al.*, 1990; Atkinson and Aschmann, 1994; Atkinson, 1994). Kinetic (Knispel *et al.*, 1990) and product (Atkinson and Aschmann, 1994) studies show that the hydroxycyclohexadienyl radicals formed from OH radical addition to benzene, toluene and the xylenes react predominantly with O_2 in the atmosphere, with a rate constant ratio of $k_{O2}/k_{NO2} \sim 1 \times 10^{-5}$ at 298 K (where k_{O2} and k_{NO2} are the rate constants for the reactions of the adduct with O_2 and NO_2, respectively). It should be noted, however, that in laboratory product studies carried out at elevated NO_x concentrations reaction of the hydroxycyclohexadienyl radical with NO_2 can be important or indeed dominant, possibly leading to product distributions and yields which differ from those in the atmosphere. In contrast, we have shown that for the reactions of O_2 and NO_2 with the nitrooxycyclohexadienyl radical formed from NO_3 radical addition to naphthalene, $k_{O2}/k_{NO2} < 4 \times 10^{-7}$ (Atkinson *et al.*, 1994c). The radical adducts formed from the PAH therefore appear more likely to react with NO_2 under tropospheric conditions than those formed from the monocyclic aromatics, explaining the observed formation of nitro-PAH in the atmosphere (Atkinson and Arey, 1994).

At the present time, we have a good understanding of the rate constants and reaction mechanisms of the initial OH radical (and NO_3 radical) reactions with aromatic hydrocarbons (Atkinson, 1989, 1991, 1994; Atkinson and Arey, 1994). Furthermore, the reaction mechanisms and products formed after the H-atom abstraction channel from the alkyl substituent groups are understood, at least in the presence of NO (Atkinson, 1994). However, while rate constants (or

rate constant ratios) for the reactions of the hydroxycyclohexadienyl and methyl-substituted hydroxycyclohexadienyl radicals with O_2 and NO_2 are now available (Knispel *et al.*, 1990; Atkinson and Aschmann, 1994; Atkinson, 1994), the detailed reaction mechanisms and products of these reactions are presently not known. Furthermore, there is still an incomplete knowledge of the products formed from the atmospheric OH radical-initiated reactions of benzene and the alkyl-substituted benzenes, with typically $\leq 50\%$ of the carbon being accounted for (Atkinson, 1994). While it is possible that the "missing" products are dicarbonyls and/or di- or multi-functional compounds (Dumdei and O'Brien, 1984) [as we have recently observed from the OH radical reactions with the three xylene isomers (xylenes, xylenes-d_6 and xylenes-d_{10}) using atmospheric pressure ionization tandem mass spectrometry], present analytical methods do not appear suitable for quantifying these compounds.

To answer several of the uncertainties noted above, during this two-year experimental study we used *in situ* FT-IR absorption spectroscopy and direct air sampling with atmospheric pressure ionization mass spectrometry (API-MS) in conjunction with chromatographic techniques (HPLC, GC-FID, GC-FTIR and GC-MS) to study selected aspects of the atmospheric chemistry of alkenes and aromatic hydrocarbons. Two cooperative and integrated experimental programs were carried out; one supported by the California Air Resources Board and the other by the Coordinating Research Council, Inc. The objectives of these two combined programs were:

- To investigate the products of the gas-phase reactions of O_3 with propene, 2-methylpropene, *cis*-2-butene, *trans*-2-butene, 2-methyl-2-butene and 2,3-dimethyl-2-butene in the presence of sufficient cyclohexane (or other alkane) to scavenge the OH radicals formed. The 2-methylpropene, *trans*-2-butene and 2,3-dimethyl-2-butene reactions were studied under this CARB contract.

- To investigate the products of the gas-phase reactions of the OH radical (in the presence of NO_x) with *cis*-2-butene, 2-methylpropene, 2-methyl-2-butene and 2,3-dimethyl-2-butene to determine the reaction products and the reaction pathways of the intermediate β-hydroxyalkoxy radicals under atmospheric conditions. The SCIEX API MS/MS instrument was also used to study the products formed from

the reactions of OH radicals with these alkenes in the absence of NO_x. The *cis*-2-butene and 2,3-dimethyl-2-butene reactions were studied in this CARB contract.

- To investigate the products formed from the gas-phase reactions of OH radicals, in the presence of NO_x, and NO_3 radicals with biphenyl [the OH radical reaction only since no reaction with the NO_3 radical has been observed (Atkinson, 1991)], naphthalene, 1- and 2-methylnaphthalene, acenaphthene and acenaphthylene. The data obtained from these studies was expected to provide product identification data which will be applicable to the monocyclic aromatic hydrocarbons and allow the products formed from their reactions to be predicted and targeted for analysis. Naphthalene was studied in detail under this CARB contract.

The experimental methods used and the data obtained are discussed in the following five sections. For completeness and to allow for a more meaningful discussion of the data obtained, the studies carried out under the complementary program funded by the Coordinating Research Council, Inc., are included in their entirety.

2. OH RADICAL FORMATION YIELDS FROM THE REACTIONS OF O_3 WITH ALKENES

Introduction

It is now recognized that the gas-phase reactions of O_3 with alkenes, including with isoprene, monoterpenes, sesquiterpenes and oxygenates emitted from vegetation, lead to the formation of hydroxyl (OH) radicals (Niki *et al.*, 1987; Paulson *et al.*, 1992a; Atkinson *et al.*, 1992, 1995a,c; Paulson and Seinfeld, 1992; Atkinson and Aschmann, 1993; Shu and Atkinson, 1994; Aschmann *et al.*, 1996). The formation of OH radicals from these O_3 reactions with alkenes is potentially a dark nighttime source of OH radicals (Hu and Stedman, 1995), which then initiate the oxidation of other volatile organic compounds present.

However, accurate measurements of OH radical formation yields from these O_3 reactions are difficult. Niki *et al.* (1987) derived the OH radical formation yield from the reaction of O_3 with the symmetrical alkene 2,3-dimethyl-2-butene from a comprehensive product study, and specifically from the measured stoichiometry of (Δ[2,3-dimethyl-2-butene]/$\Delta[O_3]$) = 1.7 and the observation that addition of formaldehyde scavenged the stabilized $(CH_3)_2\dot{C}O\dot{O}$ biradical to form the secondary ozonide in 28-30% yield. More recent OH radical formation yield measurements have used a tracer compound to measure the OH radical concentrations during the reactions in conjunction with computer modeling of the reaction systems (Paulson *et al.*, 1992a; Paulson and Seinfeld, 1992) or have used cyclohexane to scavenge >90-95% of the OH radicals formed and monitored the cyclohexanone and cyclohexanol formed from the OH radical reaction with cyclohexane (Atkinson *et al.*, 1992, 1995a,c; Atkinson and Aschmann, 1993; Shu and Atkinson, 1994; Aschmann *et al.*, 1996). Both of these methods have problems.

The use of a tracer compound to measure the OH radical concentration requires a tracer which is reactive towards OH radicals but which does not react with O_3, together with a knowledge of all of the OH radical loss processes in reacting O_3 - alkene - tracer - air mixtures. This necessitates a quantitative understanding of the products of the reactions of O_3 and OH radicals with the alkene and potentially also of the reactions of the OH radical with the products of these OH radical and O_3 reactions.

The use of cyclohexane to scavenge OH radicals assumes that the cyclohexanone plus cyclohexanol formation yield from the reaction of the OH radical with cyclohexane in the

absence of NO is both known and is a constant for all O_3 - organic reactions. However, as discussed previously (Atkinson *et al.*, 1992; Atkinson and Aschmann, 1993), the reactions of the cyclohexyl peroxy radicals formed after O_2 addition to the cyclohexyl radicals produced in the reaction of OH radicals with cyclohexane are complex,

$$C_6H_{11}\dot{O}_2 + R\dot{O}_2 \rightarrow \alpha \text{ cyclohexanone} + (1-\alpha) \text{ cyclohexanol} + R\dot{O}_2 \text{ products} + O_2 \quad (1a)$$

$$C_6H_{11}\dot{O}_2 + R\dot{O}_2 \rightarrow C_6H_{11}\dot{O} + R\dot{O} + O_2 \quad (1b)$$

$$C_6H_{11}\dot{O}_2 + HO_2 \rightarrow C_6H_{11}OOH + O_2 \quad (2)$$

$$C_6H_{11}\dot{O} + O_2 \rightarrow \text{cyclohexanone} + HO_2 \quad (3)$$

$$C_6H_{11}\dot{O} \rightarrow \text{isomerization and/or decomposition products} \quad (4)$$

with $k_3[O_2]/(k_3[O_2] + k_4) = 0.42 \pm 0.05$ at 296 ± 2 K and 740 Torr total pressure of air (Atkinson *et al.*, 1992) and where $R\dot{O}_2$ can be the cyclohexyl peroxy radical or other organic peroxy radicals. Thus the formation of cyclohexanone and cyclohexanol from the cyclohexyl peroxy radical arises from reaction (1a), and/or reaction (1b) followed by reaction (3). The occurrence of reactions (2) and (4) results in a less than unit yield of cyclohexanone plus cyclohexanol from the OH radical reaction with cyclohexane in reacting O_3 - alkene - cyclohexane - air mixtures (Atkinson *et al.*, 1992; Atkinson and Aschmann, 1993). Furthermore, the yield of cyclohexanone plus cyclohexanol from the reaction of the OH radical with cyclohexane in such reaction systems is expected to depend on the identities and relative concentrations of the various organic peroxy radicals present as well as on the relative concentrations of HO_2 and $R\dot{O}_2$ radicals, and hence the yields of cyclohexanone plus cyclohexanol are expected, *a priori*, to be dependent on the specific reaction system. There is evidence that this is indeed the case, with Rowley *et al.* (1991) measuring a formation yield of cyclohexanone plus cyclohexanol of 0.67 ± 0.04 in irradiated Cl_2 - cyclohexane - N_2 (550 Torr) - O_2 (150 Torr) mixtures at 295 ± 2 K while Atkinson *et al.* (1992) and Atkinson and

Aschmann (1993) have measured formation yields of cyclohexanone plus cyclohexanol from the reaction of the OH radical with cyclohexane in reacting O_3 - alkene - cyclohexane - air mixtures at 296 ± 2 K of 0.55 ± 0.09 and 0.50 ± 0.07, respectively.

We have explored another scavenger for OH radicals which leads to the formation of a readily measured product formed with a yield which is invariant of the specific reaction system investigated. Specifically, we investigated the use of 2-butanol to scavenge OH radicals. The OH radical reaction with 2-butanol is expected to proceed mainly by H-atom abstraction from the tertiary C-H bond (Carter *et al.*, 1979; Atkinson, 1994; Kwok and Atkinson, 1995), followed by reaction of the α-hydroxyalkyl radical $CH_3\dot{C}(OH)CH_2CH_3$ with O_2 to form 2-butanone (Carter *et al.*, 1979; Atkinson, 1994).

$$OH + CH_3CH(OH)CH_2CH_3 \rightarrow H_2O + CH_3\dot{C}(OH)CH_2CH_3 \quad (5)$$

$$CH_3\dot{C}(OH)CH_2CH_3 + O_2 \rightarrow CH_3C(O)CH_2CH_3 + HO_2 \quad (6)$$

We measured the formation yield of 2-butanone from the OH radical reaction with 2-butanol and, because no measurements of the rate constant for the reaction of the OH radical with 2-butanol have been reported to date, we have determined the rate constant for this reaction. The use of 2-butanol to scavenge OH radicals in the gas-phase reactions of O_3 has then been used in the reactions of O_3 with 2,3-dimethyl-2-butene, 2-methyl-2-butene, α-pinene and sabinene, with the OH radical formation yields being obtained from the amounts of 2-butanone formed.

Experimental

All experiments were carried out in a 7900 liter Teflon chamber equipped with two parallel banks of blacklamps and a Teflon-coated fan to ensure rapid mixing of reactants during their introduction into the chamber.

Kinetics and Products of the Reactions of OH Radicals with 2-Butanol

The rate constant for the gas-phase reaction of the OH radical with 2-butanol was measured using a relative rate method (Atkinson *et al.*, 1981, 1995c), in which the relative disappearance rates of 2-butanol and cyclohexane (the reference organic) were measured in the presence of OH radicals. Provided that the 2-butanol and cyclohexane were removed from the gas phase only by reaction with OH radicals, then,

$$\ln\left\{\frac{[2\text{-}butanol]_{t_o}}{[2\text{-}butanol]_t}\right\} = \frac{k_7}{k_8} \ln\left\{\frac{[cyclohexane]_{t_o}}{[cyclohexane]_t}\right\} \qquad \text{(I)}$$

where $[2\text{-butanol}]_{t_o}$ and $[\text{cyclohexane}]_{t_o}$ are the concentrations of 2-butanol and cyclohexane at time t_o, $[2\text{-butanol}]_t$ and $[\text{cyclohexane}]_t$ are the corresponding concentrations at time t, and k_7 and k_8 are the rate constants for reactions (7) and (8), respectively.

$$\text{OH} + \text{2-butanol} \rightarrow \text{products} \qquad (7)$$

$$\text{OH} + \text{cyclohexane} \rightarrow \text{products} \qquad (8)$$

A plot of $\ln([2\text{-butanol}]_{t_o}/[2\text{-butanol}]_t)$ against $\ln([\text{cyclohexane}]_{t_o}/[\text{cyclohexane}]_t)$ should therefore be a straight line with slope of k_7/k_8 and zero intercept. The formation of 2-butanone from the reaction of the OH radical with 2-butanol was measured in similar experiments in the absence of cyclohexane.

OH radicals were generated by the photolysis of methyl nitrite (CH_3ONO) in air at wavelengths >300 nm, and NO was added to the reactant mixture to suppress the formation of O_3 and NO_3 radicals (Atkinson *et al.*, 1981). The initial reactant concentrations in these irradiations of CH_3ONO - NO - 2-butanol - cyclohexane - air and CH_3ONO - NO - 2-butanol - air mixtures were (in molecule cm^{-3} units): CH_3ONO, $\sim 2.4 \times 10^{14}$; NO, $\sim 2.4 \times 10^{14}$; 2-butanol, $(2.21\text{-}2.67) \times 10^{13}$; cyclohexane (when present), $\sim 2.4 \times 10^{13}$; and irradiations were carried out resulting in up to 42-50% consumption of the initially present 2-butanol.

The concentrations of 2-butanol, cyclohexane and 2-butanone were measured during the experiments by gas chromatography with flame ionization detection (GC-FID). Cyclohexane

was analyzed using a 30 m DB-5 megabore column as described previously (Atkinson and Aschmann, 1993). For the analyses of 2-butanol and 2-butanone, 100 cm^3 volume gas samples were collected from the chamber onto Tenax-TA solid adsorbent, with subsequent thermal desorption at ~225 °C onto a 30 m DB-1701 megabore column held at -20 °C and then temperature programmed to 200 °C at 8 °C min^{-1}.

Formation Yields of OH Radicals from the Reactions of O_3 with Alkenes

The amounts of 2-butanone formed in the reactions of O_3 with alkenes were measured in the presence of sufficient 2-butanol to scavenge ≥95% of any OH radicals formed from the O_3 radical reaction with the alkene. The initial reactant concentrations were (in molecule cm^{-3} units): alkene, (2.55-5.59) x 10^{13}; 2-butanol, ~1.2 x 10^{16}; and 5 additions of 50 cm^3 volume of O_3 in O_2 diluent (each O_3/O_2 addition corresponding to an initial concentration of O_3 in the chamber of ~6 x 10^{12} molecule cm^{-3}) were made to the chamber during an experiment. The concentrations of 2-butanone, α-pinene and sabinene were measured during the experiments by GC-FID as described above for the analyses of 2-butanone. The DB-1701 column provided complete separation between the 2-butanone formed (≤3.0 x 10^{13} molecule cm^{-3}) and 2-butanol, even at the 2-butanol concentrations of ~1.2 x 10^{16} molecule cm^{-3} used in these experiments. 2-Methyl-2-butene and 2,3-dimethyl-2-butene were analyzed using the 30 m DB-5 megabore column as described previously (Atkinson and Aschmann, 1993).

Chemicals

The chemicals used, and their stated purities, were: cyclohexane (high-purity solvent grade), American Burdick and Jackson; 2-butanol (99.5%), 2-butanone (99+%), 2,3-dimethyl-2-butene (99+%), 2-methyl-2-butene (99+%), α-pinene (99+%), and sabinene (99%), Aldrich Chemical Company; and NO (≥99.0%), Matheson Gas Products. Methyl nitrite was prepared and stored as described previously (Atkinson *et al.*, 1981), and O_3 in O_2 diluent was prepared as needed using a Welsbach T-408 ozone generator.

Results and Discussion

Rate Constant for the Reaction of the OH Radical with 2-Butanol

The data obtained from irradiated CH_3ONO - NO - 2-butanol - cyclohexane - air mixtures are plotted in accordance with Equation (I) in Figure 1. A least-squares analysis of these data leads to the rate constant ratio $k_7/k_8 = 1.24 \pm 0.07$, where the indicated error is two least-squares standard deviations. Using a rate constant k_8 for the reaction of the OH radical with cyclohexane at 296 K of 7.45×10^{-12} cm^3 $molecule^{-1}$ s^{-1} ($\pm 25\%$) (Atkinson, 1989, 1994) results in a rate constant of

$$k_7(OH + \text{2-butanol}) = (9.2 \pm 2.4) \times 10^{-12} \text{ cm}^3 \text{ molecule}^{-1} \text{ s}^{-1} \text{ at } 296 \pm 2 \text{ K},$$

where the indicated error is two least-squares standard deviations combined with the estimated overall uncertainties in the rate constant k_8 (and is largely due to the uncertainties in the rate constant k_8). This measured rate constant is in excellent agreement with that of 1.00×10^{-11} cm^3 $molecule^{-1}$ s^{-1} at 298 K calculated using the estimation method of Kwok and Atkinson (1995).

Products of the OH Radical Reactions with 2-Butanol

GC-FID and GC-MS analyses of irradiated CH_3ONO - NO - 2-butanol - air and CH_3ONO - NO - 2-butanol - cyclohexane - air mixtures showed the formation of 2-butanone. The measured amounts of 2-butanone were corrected for secondary reaction with the OH radical as described previously (Atkinson *et al.*, 1982), using a rate constant for the reaction of the OH radical with 2-butanone at 296 K of 1.15×10^{-12} cm^3 $molecule^{-1}$ s^{-1} (Atkinson, 1994). Corrections for secondary reactions of 2-butanone were $<5\%$. The amounts of 2-butanone formed, corrected for reaction with the OH radical, are plotted against the amounts of 2-butanol reacted with the OH radical in irradiated CH_3ONO - NO - 2-butanol - air and CH_3ONO - NO - 2-butanol - cyclohexane - air mixtures in Figure 2, with the presence or absence of cyclohexane having no effect. A least-squares analysis of these data leads to a formation yield of 2-butanone from 2-butanol of 0.695 ± 0.073, where the indicated error is two least-squares standard deviations combined with estimated overall uncertainties in the GC-FID response factors for 2-butanone and 2-butanol of $\pm 5\%$ each.

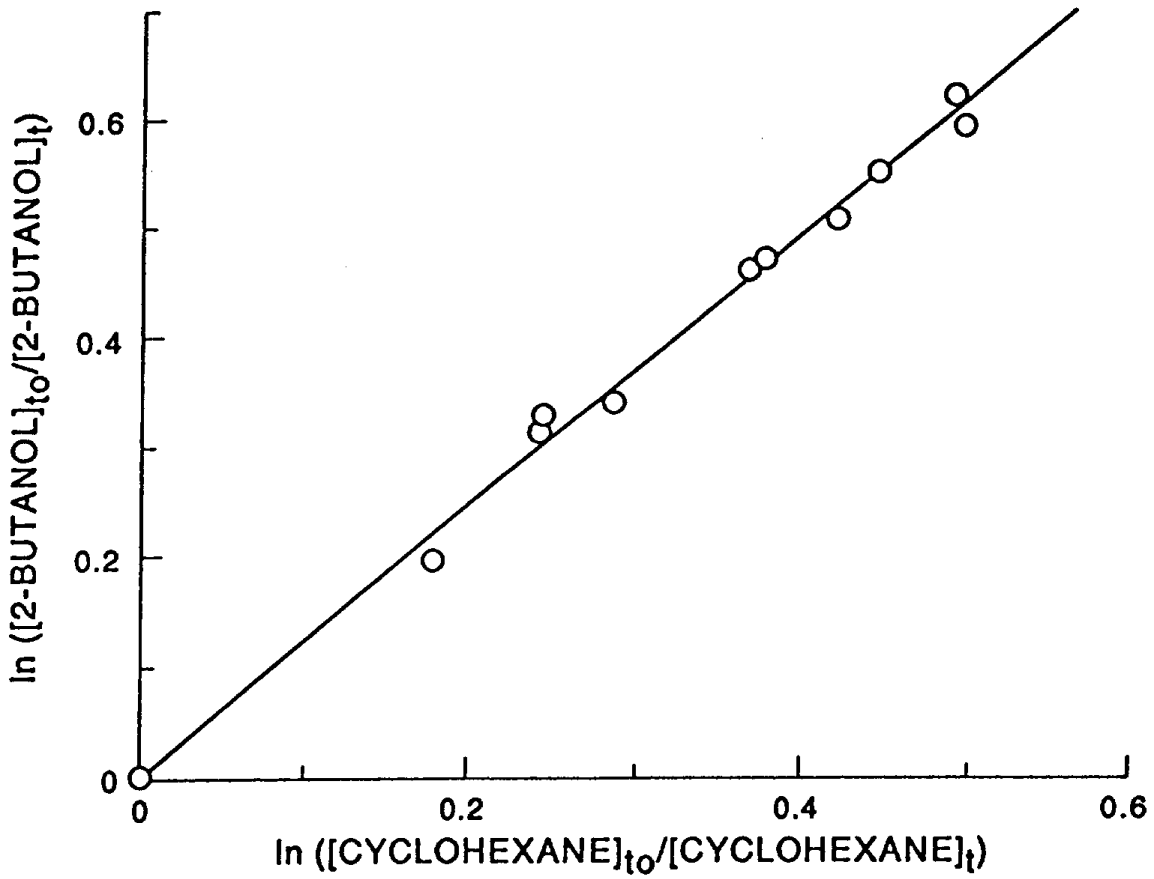

Figure 1. Plot of Equation (I) for the gas-phase reaction of the OH radical with 2-butanol, with cyclohexane as the reference organic.

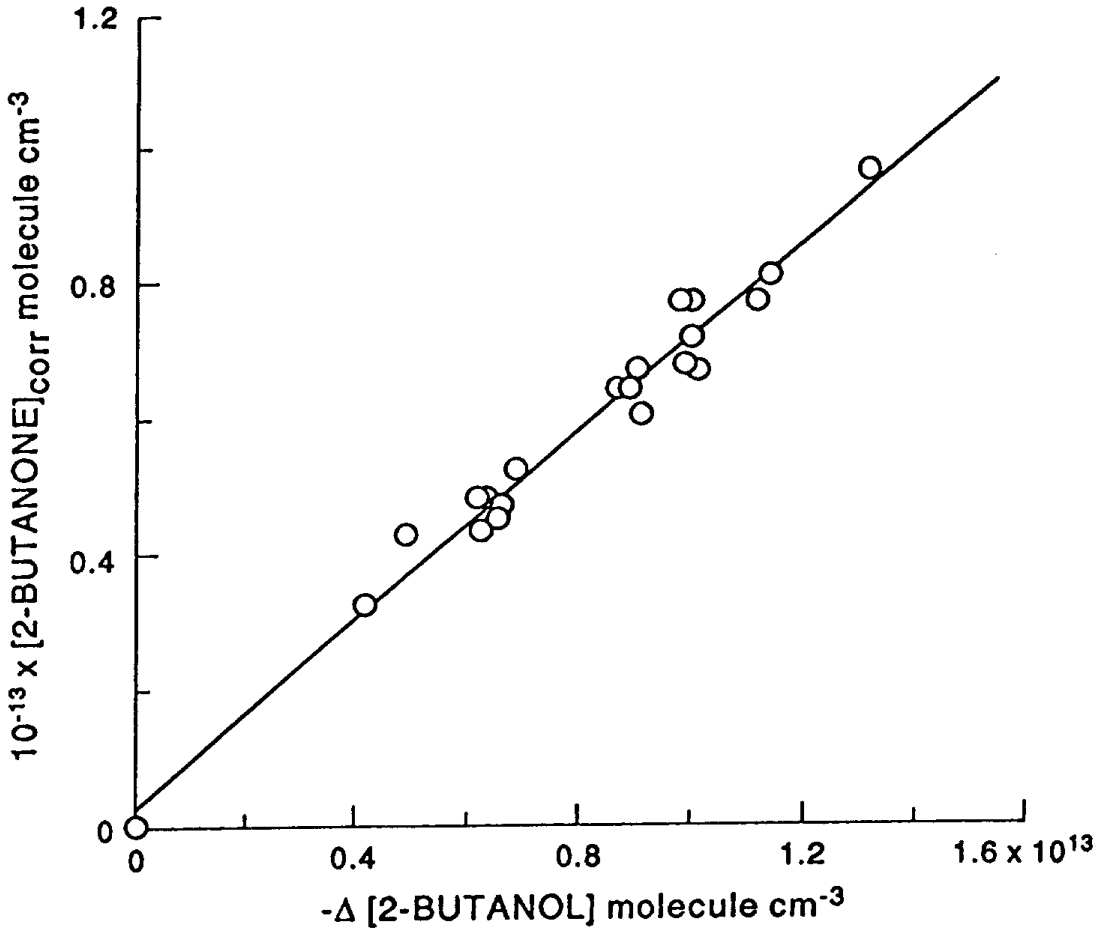

Figure 2. Plot of the amount of 2-butanone formed, corrected for reaction with the OH radical, against the amount of 2-butanol reacted with the OH radical in irradiated CH_3ONO - NO - 2-butanol - air and CH_3ONO - NO - 2-butanol - cyclohexane - air mixtures.

Our 2-butanone formation yield from the OH radical reaction with 2-butanol of 0.695 ± 0.073 is in reasonable agreement with the formation yield of 0.74-0.81 obtained by Carter *et al.* (1979) [which is actually an upper limit because Carter *et al.* (1979) used too high a rate constant for the reaction of 2-butanone with the OH radical to correct the measured 2-butanone concentrations for secondary reactions]. Our 2-butanone formation yield is somewhat lower than the fraction of the OH radical calculated to proceed by H-atom abstraction from the tertiary C-H bond in 2-butanol, of 0.84 (Kwok and Atkinson, 1995), suggesting that the activating effects of the -OH substituent group in 2-butanol extend beyond the α- >CH- group, as previously concluded by Wallington *et al.* (1988) and Nelson *et al.* (1990). Thus, while the overall OH radical reaction rate constant may be reliably estimated (Kwok and Atkinson, 1995), the calculated relative importance of the various reaction pathways may not be correct, as also observed by Atkinson *et al.* (1995d) for the OH radical reaction with *n*-pentane. H-atom abstraction from the -OH group, forming the $CH_3CH(\dot{O})CH_2CH_3$ radical, is predicted to account for ~1.4% of the overall OH radical reaction with 2-butanol (Kwok and Atkinson, 1995), and this pathway is estimated to contribute an additional 2-butanone yield of ~0.01 (Atkinson, 1994).

OH Radical Formation Yields from the Reactions of O_3 with Alkenes

Ten separate introductions of 1.2 x 10^{16} molecule cm^{-3} of 2-butanol (the concentration required to scavenge ≥95% of the OH radicals formed in the reactions of O_3 with the alkenes studied at the initial alkene concentrations employed) into the chamber showed the presence of (1.21-1.69) x 10^{12} molecule cm^{-3} of 2-butanone. This concentration of 2-butanone corresponds to 0.010-0.014% of 2-butanone impurity in the 2-butanol samples used, and suggests that an OH radical formation yield of ~0.1 should be measurable for ~2 x 10^{13} molecule cm^{-3} of alkene reacted. It is interesting to note that our previous study of OH radical formation from the reactions of O_3 with alkenes using (7-10.6) x 10^{15} molecule cm^{-3} of high-purity solvent grade cyclohexane (Atkinson *et al.*, 1995a) resulted in initial cyclohexanone plus cyclohexanol concentrations in the chamber of typically (0.7-1.7) x 10^{11} molecule cm^{-3} (some of which may have been due to "carry-over" from previous O_3 - alkene - cyclohexane - air reactions), corresponding to only 0.001-0.002% of cyclohexanone plus cyclohexanol impurity in the

cyclohexane (and a factor of 10 lower than the case for the 2-butanone in the 2-butanol samples used here).

Preliminary experiments showed that in O_3 [(1.0-1.2) x 10^{13} molecule cm^{-3}] - 2-butanol ($\sim$1.2 x 10^{16} molecule cm^{-3}) - air mixtures in the absence of added alkene, $\sim$1.8 x 10^{12} molecule cm^{-3} of 2-butanone was formed during the first 30-40 min, followed by a slower formation of $\sim$7 x 10^{9} molecule cm^{-3} min^{-1} of 2-butanone over the next 200 min (with an overall amount of 2-butanone formed of (2.9-3.4) x 10^{12} molecule cm^{-3} over 220-230 min). This formation of 2-butanone in O_3 - 2-butanol - air mixtures was presumably due to the presence of small amounts of impurities in the 2-butanol which reacted with O_3 to form OH radicals, which in turn reacted with 2-butanol to form 2-butanone. We therefore limited the alkenes studied to those with O_3 reaction rate constants >8 x 10^{-17} cm^3 $molecule^{-1}$ s^{-1} to minimize the O_3 concentrations and exposure of 2-butanol to O_3 during the experiments.

The amounts of 2-butanone formed are plotted against the amounts of 2,3-dimethyl-2-butene, 2-methyl-2-butene, α-pinene and sabinene reacted in Figure 3. Good straight line plots are observed, with zero intercepts within two least-squares standard deviations for all four alkenes studied. The ratios {([2-butanone] formed)/([alkene] reacted)} obtained from least-squares analyses of the data shown in Figure 3 are given in Table 1, together with the OH radical formation yields calculated using our measured formation yield of 2-butanone from the OH radical reaction with 2-butanol of 0.695 $\pm$ 0.073. For the experiments with 2-methyl-2-butene and 2,3-dimethyl-2-butene, with rate constants for their reactions with O_3 at 296 K of 1.12 x 10^{-15} cm^3 $molecule^{-1}$ s^{-1} and 3.96 x 10^{-16} cm^3 $molecule^{-1}$ s^{-1}, respectively (Atkinson, 1994)], the calculated lifetimes of O_3 were always $\leq$1 min and $<$5 mins, respectively (and were longest for the fifth addition of O_3 in each case), and exposures of 2-butanol to O_3 were minimal. For the experiments with α-pinene and sabinene, with rate constants for their reactions with O_3 of (8.5-8.6) x 10^{-17} cm^3 $molecule^{-1}$ s^{-1} (Atkinson, 1994), the O_3 lifetimes varied from $\sim$7 min for the first O_3 addition to $\sim$20 min for the fourth O_3 addition, with only the last data point for each experiment being obtained under conditions such that 2-butanol was exposed to O_3 at concentrations of $\sim$6 x 10^{12} molecule cm^{-3} for $\sim$30 min.

Table 1 shows that the OH radical formation yields measured using 2-butanol to scavenge OH radicals are in good agreement with those we have previously reported using cyclohexane

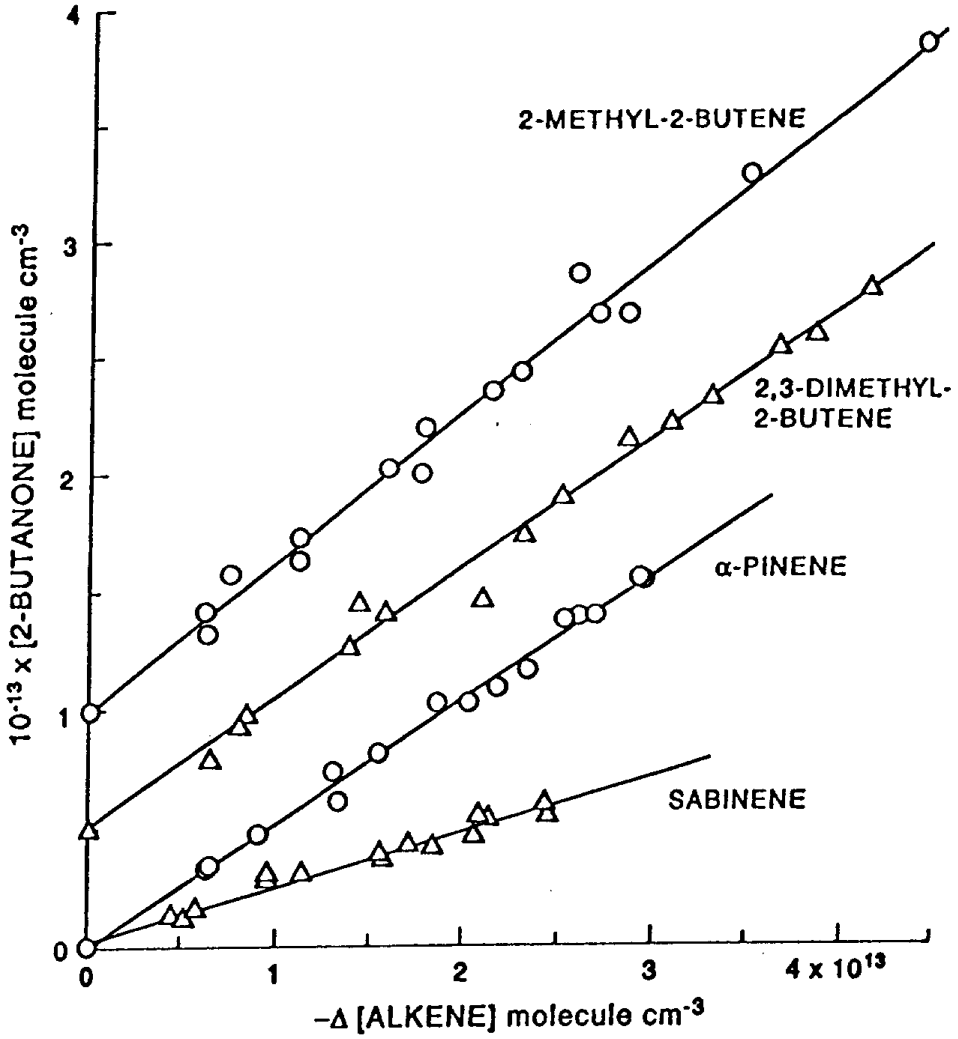

Figure 3. Plots of the amounts of 2-butanone formed against the amounts of 2,3-dimethyl-2-butene, 2-methyl-2-butene, α-pinene and sabinene reacted with O_3 in the presence of sufficient 2-butanol to scavenge ≥95% of the OH radicals formed. The data for 2,3-dimethyl-2-butene and 2-methyl-2-butene have been displaced vertically by 5.0 x 10^{12} molecule cm^{-3} and 1.0 x 10^{13} molecule cm^{-3}, respectively, for clarity.

Table 1. 2-Butanone and OH radical formation yields from the gas-phase reactions of O_3 with 2,3-dimethyl-2-butene, 2-methyl-2-butene, α-pinene, and sabinene at 296 ± 2 K and atmospheric pressure in the presence of sufficient 2-butanol to scavenge ≥95% of the OH radicals

Alkene	2-Butanone Yield[a]	OH Radical Yield	Reference
2,3-dimethyl-2-butene	0.553 ± 0.050	0.80 ± 0.12	This work
		$1.00^{+0.50}_{-0.34}$	Atkinson and Aschmann (1993)
		0.7 ± 0.1	Niki *et al.* (1987)
2-methyl-2-butene	0.649 ± 0.062	0.93 ± 0.14	This work
		$0.89^{+0.45}_{-0.30}$	Atkinson and Aschmann (1993)
α-pinene	0.530 ± 0.045	0.76 ± 0.11	This work
		$0.85^{+0.43}_{-0.29}$	Atkinson *et al.* (1992)
sabinene	0.228 ± 0.027	0.33 ± 0.06	This work
		$0.26^{+0.13}_{-0.09}$	Atkinson *et al.* (1992)

[a]Errors are two least-squares standard deviations combined with the estimated overall uncertainties in the GC-FID response factors for the alkene and 2-butanone of ±5% each.

to scavenge OH radicals (Atkinson *et al.*, 1992; Atkinson and Aschmann, 1993). Furthermore, our present OH radical formation yield from 2,3-dimethyl-2-butene is in excellent agreement with the value reported by Niki *et al.* (1987). 2,3-Dimethyl-2-butene forms only one initially energy-rich biradical, $[(CH_3)_2\dot{C}O\dot{O}]^*$, which appears to be either thermally stabilized or isomerizes to the hydroperoxide with decomposition to form an OH radical,

$$[(CH_3)_2\dot{C}O\dot{O}]^* + M \rightarrow (CH_3)_2\dot{C}O\dot{O} + M \quad (9)$$

$$[(CH_3)_2\dot{C}O\dot{O}]^* \rightarrow [CH_3C(OOH)=CH_2]^* \rightarrow OH + CH_3C(O)\dot{C}H_2 \quad (10)$$

with the OH radical then reacting further (with 2,3-dimethyl-2-butene, reaction products and/or an OH radical scavenger). Niki *et al.* (1987) observed the formation of isobutene ozonide with a yield of 0.28-0.30 upon addition of formaldehyde to O_3 - 2,3-dimethyl-2-butene - N_2 - O_2 mixtures, indicating a stabilization yield of the biradical via reaction (9) of $\sim$0.29. This biradical stabilization yield together with the measured stoichiometry of (Δ[2,3-dimethyl-2-butene]/$\Delta[O_3]$) = 1.7 $\pm$ 0.1 in the absence of an OH radical scavenger led Niki *et al.* (1987) to conclude that the OH radical formation yield from the reaction of O_3 with 2,3-dimethyl-2-butene is 0.7.

The good agreement of the OH radical formation yields from the gas-phase reactions of O_3 with the four alkenes studied here using both cyclohexane and 2-butanol to scavenge the OH radicals (and measuring the amounts of (cyclohexanone plus cyclohexanol) and 2-butanone formed, respectively) suggests that the OH radical formation yields measured previously using cyclohexane as an OH radical scavenger (Atkinson *et al.*, 1992, 1995a,c; Atkinson and Aschmann, 1993; Shu and Atkinson, 1994; Aschmann *et al.*, 1996) are correct to within $\sim \pm$20-25%, and well within the cited uncertainties of a factor of 1.5 (Atkinson *et al.*, 1992, 1995a,c; Atkinson and Aschmann, 1993; Shu and Atkinson, 1994; Aschmann *et al.*, 1996).

3. PRODUCTS OF THE GAS-PHASE REACTIONS OF O_3 WITH A SERIES OF METHYL-SUBSTITUTED ETHENES

Introduction

As noted in Sections 1 and 2 above, alkenes are important reactive components of ambient air in urban areas (Seila *et al.*, 1989; Lurmann and Main, 1992; Chameides *et al.*, 1992), accounting for ~10% of the non-methane organic compound concentration in the Los Angeles air basin and other U.S. cities (Seila *et al.*, 1989; Lurmann and Main, 1992). Because of their high reactivity with respect to ozone formation (Carter, 1994), alkenes are important in the formation of photochemical air pollution in urban areas (Chameides *et al.*, 1992). The kinetics and products of the gas-phase reaction of O_3 with alkenes have been extensively studied (Atkinson and Carter, 1984; Atkinson, 1994, 1997b) and, while the kinetics of these O_3 reactions are now reasonably well understood for a large number of alkenes (Atkinson, 1997b), there are still significant uncertainties concerning the mechanisms and products of the O_3 reactions with alkenes under atmospheric conditions (Atkinson, 1997b). As shown in Reaction Schemes 1 and 2 in Section 1 above, the gas-phase reactions of O_3 with alkenes proceed by initial addition to form a primary ozonide, which then rapidly decomposes to form, in general, two sets of carbonyl plus biradical products (Atkinson, 1997b), with the fraction stabilized depending on the total pressure (Hatakeyama *et al.*, 1984, 1986; Atkinson, 1997b). At atmospheric pressure, $O(^3P)$ atoms are not formed in any significant amount, and upper limits to the $O(^3P)$ atom formation yields are available for several alkenes (Niki *et al.*, 1984, 1987; Atkinson *et al.*, 1994a,b). However, OH radicals have been observed to be formed from the O_3 reactions with alkenes under atmospheric conditions (Paulson *et al.*, 1992a; Atkinson *et al.*, 1992, 1995a; Paulson and Seinfeld, 1992; Atkinson and Aschmann, 1993; Horie *et al.*, 1994; Shu and Atkinson, 1994; Section 2 above), and unless the OH radicals formed in the primary O_3 reaction with an alkene are scavenged the reactions systems involve both O_3 and OH radical reactions with the alkene and the measured products and their yields are not those for the O_3 reaction alone (Hakola *et al.*, 1994).

We have therefore investigated the products of the gas-phase reactions of O_3 with the methyl-substituted ethenes propene, *cis*- and *trans*-2-butene, 2-methylpropene, 2-methyl-2-butene

and 2,3-dimethyl-2-butene in the presence of sufficient concentrations of cyclohexane to scavenge >90% of the OH radicals formed.

Experimental

Experiments were carried out in the dark in three reaction chambers with differing analytical techniques. Reactions were carried out in: a 5800 liter evacuable, Teflon-coated chamber containing an *in situ* multiple reflection optical system interfaced to a Nicolet 7199 Fourier transform infrared (FT-IR) absorption spectrometer; a 7900 liter all-Teflon chamber with analysis by gas chromatography with flame ionization detection (GC-FID); and a 6500 liter all-Teflon chamber interfaced to a PE SCIEX API III MS/MS direct air sampling, atmospheric pressure ionization tandem mass spectrometer (API-MS). All three chambers are fitted with Teflon-coated fans to ensure rapid mixing of reactants during their introduction into the chamber.

Teflon Chamber Experiments with GC-FID Analyses. Reactions were carried out in a 7900 liter all-Teflon chamber at 296 ± 2 K and 740 Torr total pressure of purified air at ~5% relative humidity. The initial reactant concentrations were (in molecule cm^{-3} units): alkene, (4.72-5.73) x 10^{13}; cyclohexane, (3.6-17.5) x 10^{15}; and 4-5 additions of 50 cm^3 volume of O_3 in O_2 diluent (corresponding to an initial concentration of O_3 in the chamber of ~6 x 10^{12} molecule cm^{-3} per addition) were flushed into the chamber with a stream of N_2 gas over a 1 min period each during an experiment. The alkenes and cyclohexane were introduced into the chamber by either flushing a measured volume of the gaseous alkene (propene, *cis*- and *trans*-2-butene and 2-methylpropene) into the chamber with a stream of N_2 gas or by placing a measured volume of the liquid (cyclohexane, 2-methyl-2-butene and 2,3-dimethyl-2-butene) into a 1 liter Pyrex bulb and then flushing the contents of the bulb into the chamber with a stream of N_2. After the additions of O_3 to the chamber, the O_3 was allowed to react for ≥1 lifetime prior to collecting samples from the chamber for GC-FID analyses.

The concentrations of the alkenes and selected carbonyl products were measured during the experiments by GC-FID. The alkene reactants were quantitatively analyzed as described previously (Atkinson and Aschmann, 1993). For the analyses of the carbonyl products

acetaldehyde and acetone, 100 cm^3 volume gas samples were collected from the chamber onto Tenax-TA solid adsorbent with subsequent thermal desorption at ~225 °C onto a 30 m DB-1701 megabore column in a HP 5710 GC, initially held at 0 °C (measurements of acetone alone) or -40 °C (measurements of acetaldehyde or acetaldehyde and acetone) and then temperature programmed to 200 °C at 8 °C min^{-1}. The data from the HP 5710 GC were computer processed using an HP 3395 integrator and HP Peak 96 software. The GC-FID response factors for the reactants and products were obtained by introducing measured amounts of the chemical into the 7900 liter chamber and conducting several replicate GC-FID analyses. The chamber volume was determined by introducing a measured volume of *trans*-2-butene and determining the *trans*-2-butene concentration with a HP 5890 GC and loop/gas sampling valve injection. The alkenes were introduced into the chamber as described above, while for acetaldehyde and acetone, partial pressures of the gaseous compound were measured in a 2.03 liter Pyrex bulb using an MKS Baratron 0-100 Torr sensor, and the contents of the bulb flushed into the chamber with a stream of N_2 gas.

Evacuable Chamber Experiments with FT-IR Spectroscopic Analyses. Experiments were carried out in the 5800 liter evacuable, Teflon-coated chamber at 298 ± 2 K and 740 Torr total pressure of synthetic air (80% N_2 + 20% O_2) at <1% relative humidity. Sufficient cyclohexane was included to scavenge ≥91% (≥95% in all but one reaction involving 2,3-dimethyl-2-butene) of the OH radicals formed from the reactions of O_3 with the alkenes, and the initial reactant concentrations (in molecule cm^{-3} units) were: alkene, 2.4 x 10^{14}; and cyclohexane, (1.3-3.7) x 10^{16}; and 3-4 additions of O_3 in O_2 diluent (each addition corresponding to ~3.6 x 10^{13} molecule cm^{-3} in the chamber) were added to the chamber during an experiment. The alkenes were introduced into the chamber by flushing measured partial pressures in a 5.25 liter Pyrex bulb into the chamber with a stream of N_2 gas, and cyclohexane was introduced as described above for the 7900 liter all-Teflon chamber experiments.

The concentrations of the alkenes and reaction products were measured by FT-IR absorption spectroscopy, with 64 co-added interferograms (scans) per spectrum (1.8 min measurement time) recorded with a full width at half maximum (fwhm) resolution of 0.7 cm^{-1} and a pathlength of 62.9 m. FT-IR calibration spectra of the alkenes were obtained by

measuring partial pressures of the gaseous compound in a 5.25 liter Pyrex bulb with an MKS Baratron 0-100 Torr sensor and flushing the contents of the bulb into the 5800 liter chamber. IR reference spectra of O_3 and the observed products (except for ketene) were available from previous calibrations in this laboratory (Tuazon and Atkinson, 1990). The product spectra were analyzed by desynthesis, which consisted of successively subtracting known absorptions with the use of the calibrated reference spectra (Tuazon and Atkinson, 1990). The analyses were based on the following absorption bands of the reactant alkenes and products (peak maxima or band centers in cm^{-1}): propene, 912.3; 2-methylpropene, 890.0; *trans*-2-butene, 962.9; *cis*-2-butene, 670.6 and 975.9; 2-methyl-2-butene, 800.2; 2,3-dimethyl-2-butene, 1164.7; HCHO, 1745.8; CH_3CHO, 1746.3; $CH_3C(O)CH_3$, 1217.4; CH_3OH, 1033.5; CH_4, 1306.1; CO_2, 667.8 and 2349; CO, 2144; and ketene, 2151.8. The quantitative measurement of ketene was based on its published spectrum (Halverson and Williams, 1947), from which an absorption coefficient (base 10) of 8.5×10^{-18} cm^2 $molecule^{-1}$ for the P-branch maximum of the 2151.8 cm^{-1} band was derived.

Teflon Chamber Experiments with API-MS Analyses. Experiments with API-MS analyses were carried out in a 6500 liter Teflon chamber interfaced to a PE SCIEX API III MS/MS instrument via a 25 mm diameter x 75 cm length Pyrex tube, with a sampling flow rate of ~20 liter min^{-1}. The operation of the API-MS in the MS (scanning) and MS/MS [with collision activated dissociation (CAD)] modes has been described elsewhere (Kwok *et al.*, 1995, 1996a,b; Atkinson *et al.*, 1995d). Use of the MS/MS mode with CAD allows the "daughter ion" or "parent ion" spectrum of a given ion peak observed in the MS scanning mode to be obtained (Kwok *et al.*, 1995, 1996a,b; Atkinson *et al.*, 1995d). The positive ion mode was used in all these API-MS and API-MS/MS analyses, with protonated water hydrates ($H_3O^+(H_2O)_n$) generated by the corona discharge in the chamber diluent gas being responsible for the protonation of analytes,

$$H_3O^+(H_2O)_n + M \rightarrow MH^+(H_2O)_m + (n-m+1)H_2O \qquad (11)$$

where M is the neutral analyte of interest. Ions are drawn by an electric potential from the ion source through the sampling orifice into the mass-analyzing first quadrupole or third quadrupole.

Neutral molecules and particles are prevented from entering the orifice by a flow of high-purity nitrogen ("curtain" gas), and as a result of the declustering action of the curtain gas on the hydrated ions, the ions that are mass-analyzed are mainly protonated molecular ions ($[M+H]^+$) (Kwok *et al.*, 1995, 1996a,b; Atkinson *et al.*, 1995d).

The initial reactant concentrations (in molecule cm^{-3} units): alkene, $\sim 4.8 \times 10^{13}$; and cyclohexane, (7.6-8.4) x 10^{15}; and 2 additions of 50 cm^3 volume of O_3 in O_2 diluent (corresponding to an initial concentration of O_3 in the chamber of $\sim 6 \times 10^{12}$ molecule cm^{-3} per addition) were flushed into the chamber with a stream of N_2 gas.

Chemicals. The chemicals used (acetaldehyde, acetone, *cis*-2-butene, *trans*-2-butene, cyclohexane, 2,3-dimethyl-2-butene, 2-methyl-2-butene, 2-methylpropene and propene) were all of $\geq$99.0% stated purity. O_3 in O_2 diluent was prepared as needed using a Welsbach T-408 ozone generator with calibrated settings of voltage and flow of O_2 (99.995%, Liquid Carbonic).

Results

Carbonyl Formation Yields from GC-FID Analyses. The formation of acetaldehyde was observed from the reactions of O_3 with propene, *cis*- and *trans*-2-butene and 2-methyl-2-butene, and acetone was observed as a product from the reactions of 2-methylpropene, 2-methyl-2-butene and 2,3-dimethyl-2-butene. Representative plots of the amounts of acetaldehyde and acetone formed against the amounts of alkene reacted are shown in Figures 4 (the 2-methyl-2-butene reaction) and 5 (the 2-methylpropene and 2,3-dimethyl-2-butene reactions). The acetaldehyde and acetone formation yields obtained from least-squares analyses of the experimental data are given in Table 2. For the reaction of O_3 with 2-methyl-2-butene, acetone formation yields were determined from two independent series of experiments (with independent sets of 2-methyl-2-butene and acetone GC-FID calibration factors being determined for each series of experiments), and as shown in Figure 4 the agreement between these two sets of experiments was excellent.

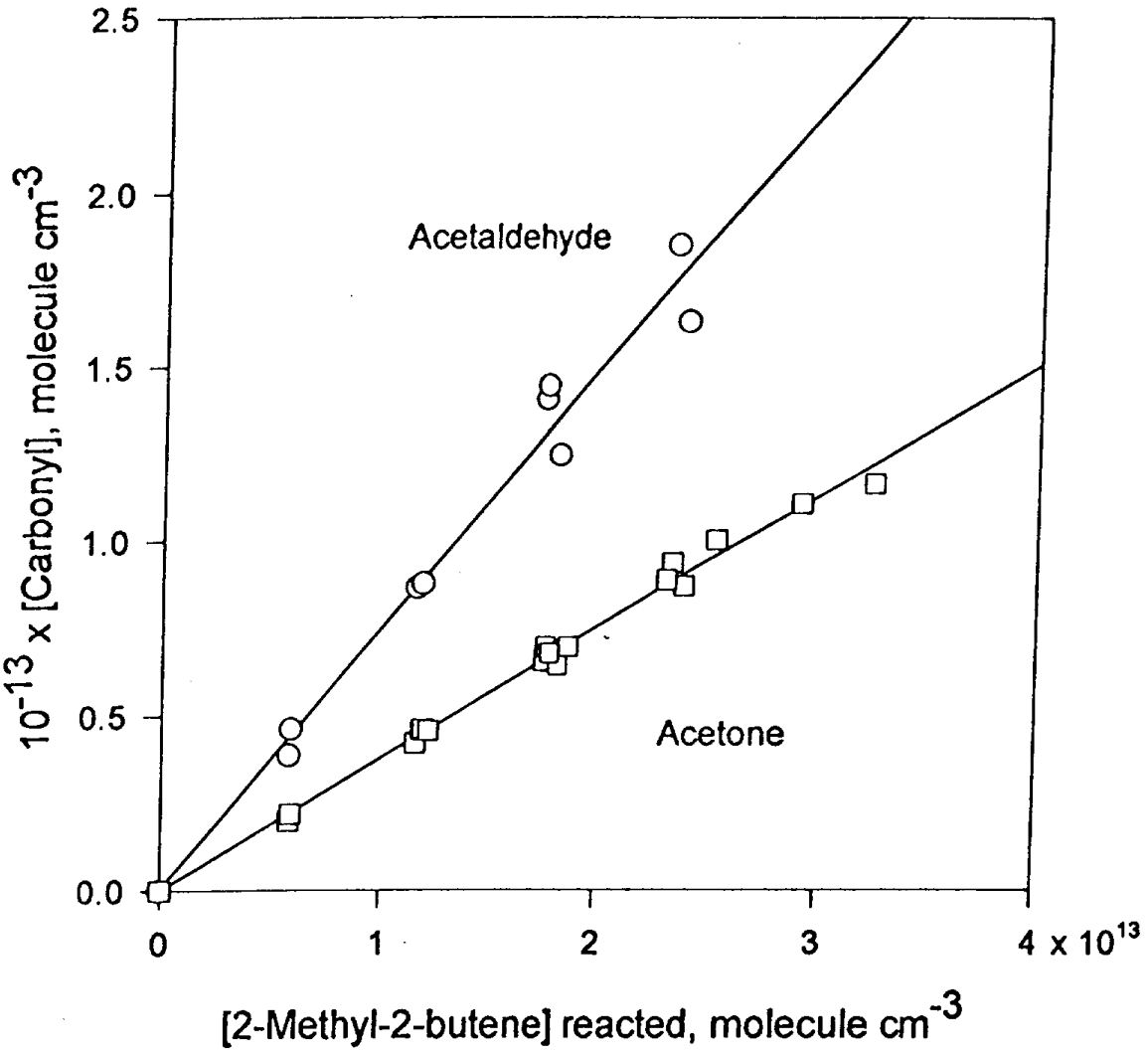

Figure 4. Plots of the amounts of acetaldehyde and acetone formed against the amounts of 2-methyl-2-butene with O_3 in the presence of sufficient cyclohexane to scavenge $\geq 95\%$ of the OH radicals formed.

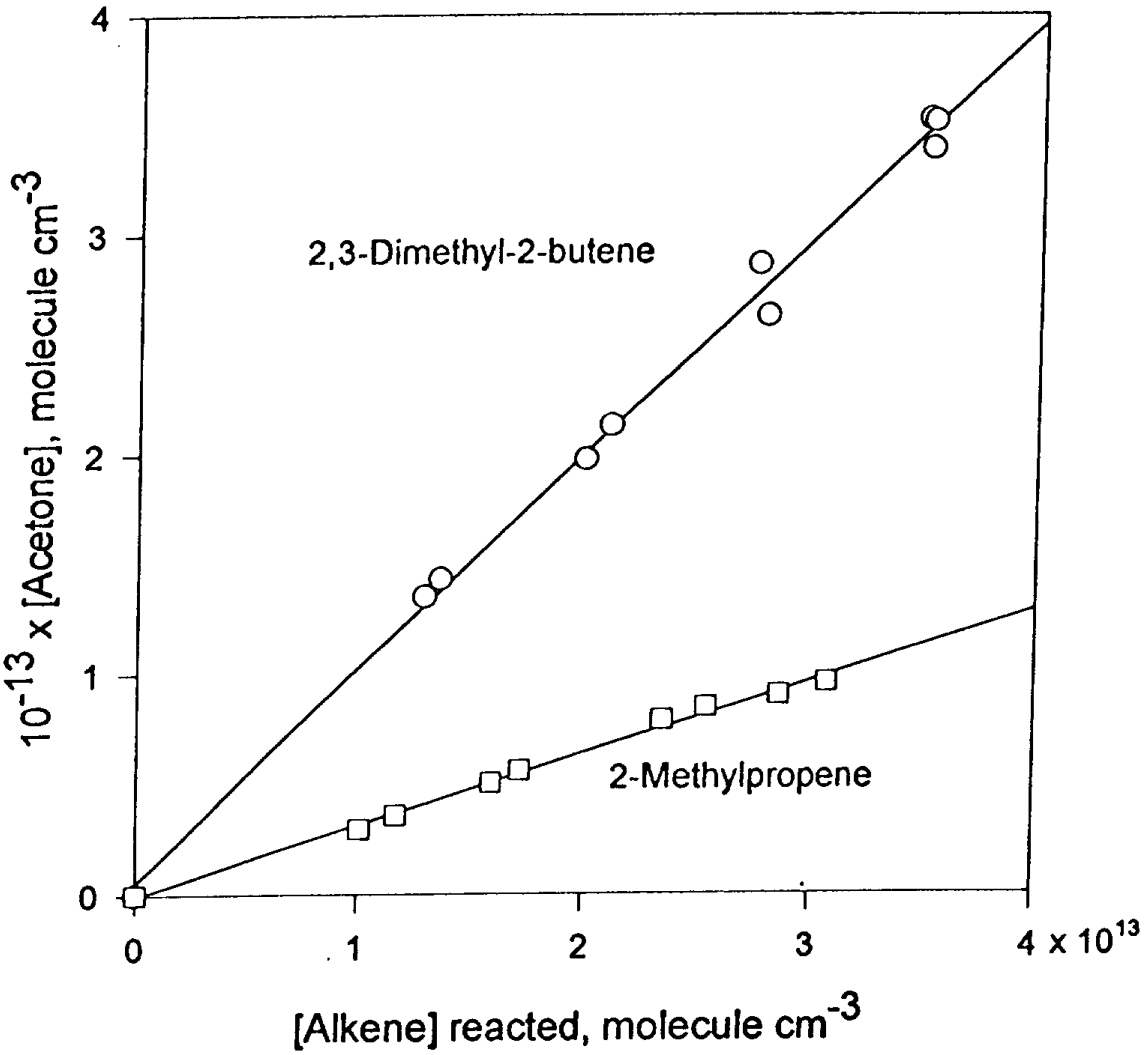

Figure 5. Plots of the amounts of acetone formed against the amounts of 2-methylpropene and 2,3-dimethyl-2-butene reacted with O_3 in the presence of sufficient cyclohexane to scavenge $\geq 95\%$ of the OH radicals formed.

Table 2. Products and their yields from the reaction of O_3 with alkenes in the presence of an OH radical scavenger at room temperature and one atmosphere of air

Alkene	Product	Formation Yield[a]	
		GC-FID	FT-IR
Propene	HCHO		0.645 ± 0.048
	acetaldehyde	0.446 ± 0.092	
	methanol		0.055 ± 0.007
	ketene		0.036 ± 0.004
	CO		0.276 ± 0.031
	CO_2		0.258 ± 0.018
	CH_4		0.096 ± 0.010
	glyoxal		0.030 ± 0.005
2-Methylpropene	HCHO		1.01 ± 0.07
	acetone	0.323 ± 0.030	0.294 ± 0.030
	methanol		0.054 ± 0.007
	CO		0.093 ± 0.011
	CO_2		0.277 ± 0.023
	CH_4		not observed

Table 2. Products and their yields from the reaction of O_3 with alkenes in the presence of an OH radical scavenger at room temperature and one atmosphere of air (continued)

Alkene	Product	Formation Yield[a]	
		GC-FID	FT-IR
cis-2-Butene	HCHO		0.161 ± 0.030
	acetaldehyde	1.19 ± 0.14	1.08 ± 0.08
	methanol		0.098 ± 0.018
	ketene		0.074 ± 0.019
	CO		0.244 ± 0.034
	CO_2		0.36 ± 0.10
	CH_4		0.190 ± 0.025
	glyoxal		0.065 ± 0.012
trans-2-Butene	HCHO		0.168 ± 0.015
	acetaldehyde	1.14 ± 0.14	1.09 ± 0.09
	methanol		0.069 ± 0.008
	ketene		0.045 ± 0.009
	CO		0.217 ± 0.026
	CO_2		0.229 ± 0.025
	CH_4		0.113 ± 0.018
	glyoxal		0.099 ± 0.014

Table 2. Products and their yields from the reaction of O_3 with alkenes in the presence of an OH radical scavenger at room temperature and one atmosphere of air (continued)

Alkene	Product	Formation Yield[a]	
		GC-FID	FT-IR
2-Methyl-2-butene	HCHO		0.317 ± 0.032
	acetaldehyde	0.745 ± 0.099	
	acetone	0.376 ± 0.032	0.339 ± 0.030
	methanol		0.061 ± 0.008
	ketene		0.016 ± 0.004
	CO		0.056 ± 0.009
	CO_2		0.249 ± 0.039
	CH_4		0.044 ± 0.007
2,3-Dimethyl-2-butene	HCHO		0.426 ± 0.081
	acetone	0.977 ± 0.086	1.14 ± 0.19
	methanol		0.055 ± 0.014
	CO_2		0.275 ± 0.040
	CH_4		not observed

[a]Uncertainties are 2 standard deviations combined with estimated overall uncertainties in the GC-FID response factors of ±5% and in the FT-IR measurement uncertainties of ±4%, apart from glyoxal (±8%) and ketene (±15% uncertainty in the literature calibration).

Products and Their Yields from FT-IR Analyses. The reactions of O_3 with propene, 2-methylpropene, *cis*-2-butene, 2-methyl-2-butene, and 2,3-dimethyl-2-butene in the presence of excess cyclohexane are illustrated by the infrared spectra presented, respectively, in Figures 6-10. As expected, the reactions of *cis*-2-butene and *trans*-2-butene with O_3 produced the same products with similar yields. The product spectra showed the presence of HCHO, methanol and CO_2 from all six alkene reactions; CO from all but the 2,3-dimethyl-2-butene reaction; methane and ketene from the propene, *cis*-2-butene, *trans*-2-butene and 2-methyl-2-butene reactions; acetone from the 2-methylpropene, 2-methyl-2-butene and 2,3-dimethyl-2-butene reactions; and acetaldehyde from the propene, *cis*- and *trans*-2-butene, and 2-methyl-2-butene reactions.

Plots of the observed product concentrations against the amounts of alkenes consumed are shown in Figures 11-16, and the measured formation yields of the products are summarized in Table 2. The interferences to the absorption bands of acetaldehyde are such that its yields from the propene and 2-methyl-2-butene reactions could not be reliably determined. The residual spectra, obtained after subtraction of the absorptions by the known species, are also depicted in Figures 6-10. In each case, a broad absorption band is found near 1740 cm^{-1} and several others in the 900-1400 cm^{-1} region. The general positions and features of the bands in this 900-1400 cm^{-1} region indicate the presence of ozonides. Thus, for example, in the case of *cis*-2-butene (and *trans*-2-butene) the peak at 1124 cm^{-1} (Figure 8) showed, on scale expansion, a Q-branch feature similar to that of the strongest band of propylene ozonide (Niki *et al.*, 1977). Similarly, for 2-methylpropene (Figure 7), 2-methyl-2-butene (Figure 9) and 2,3-dimethyl-2-butene (Figure 10), absorptions near 1070, 1230 and 1380 cm^{-1} in the residual spectrum may possibly be due to isobutene ozonide (Gravin and Schubert, 1956; Niki *et al.*, 1987).

The presence of cyclohexane oxidation products (for example, cyclohexanone) in these reaction systems interfered with the infrared analysis of the minor carbonyl products formed from the alkene, since they contribute appreciably to the overlapped band near 1740 cm^{-1}. Indeed, the absorptions of cyclohexanone itself could not be properly subtracted from the residual spectra. In the case of the *cis*-2-butene (Figure 8) and *trans*-2-butene reactions, the analysis of glyoxal as a product was made possible by its sufficiently resolved Q-branch feature at 1731 cm^{-1}. However, although methylglyoxal is a known product from the 2,3-dimethyl-2-butene reaction (Niki *et al.*, 1987) and its Q-branch at 1733 cm^{-1} was detectable in the spectrum

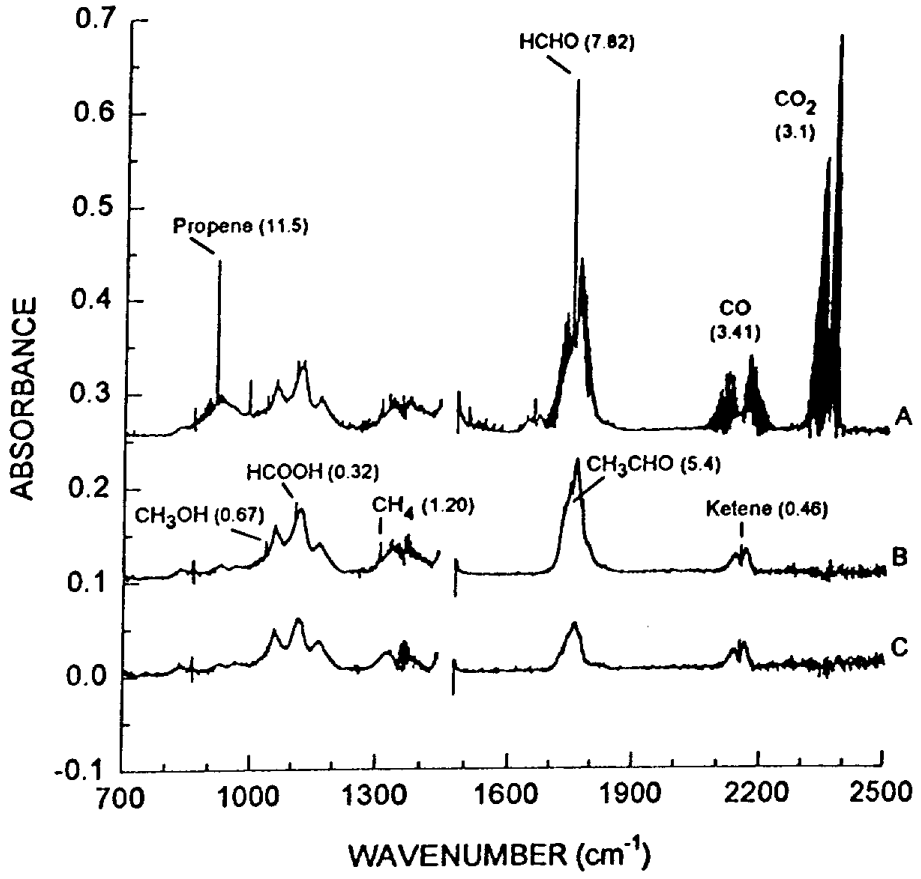

Figure 6. FT-IR spectra from the reaction of O_3 with propene in air in the presence of excess cyclohexane. (A) Reaction mixture with 51.6% of propene consumed. (B) From (A) after subtraction of absorptions by propene, HCHO, CO, and CO_2. (C) Residual spectrum after subtraction of absorptions by the known compounds, except ketene; subtraction of CH_3CHO was based on the yield measured by GC-FID. The discontinuities in the spectra represent regions severely distorted by strong absorptions of the added cyclohexane.

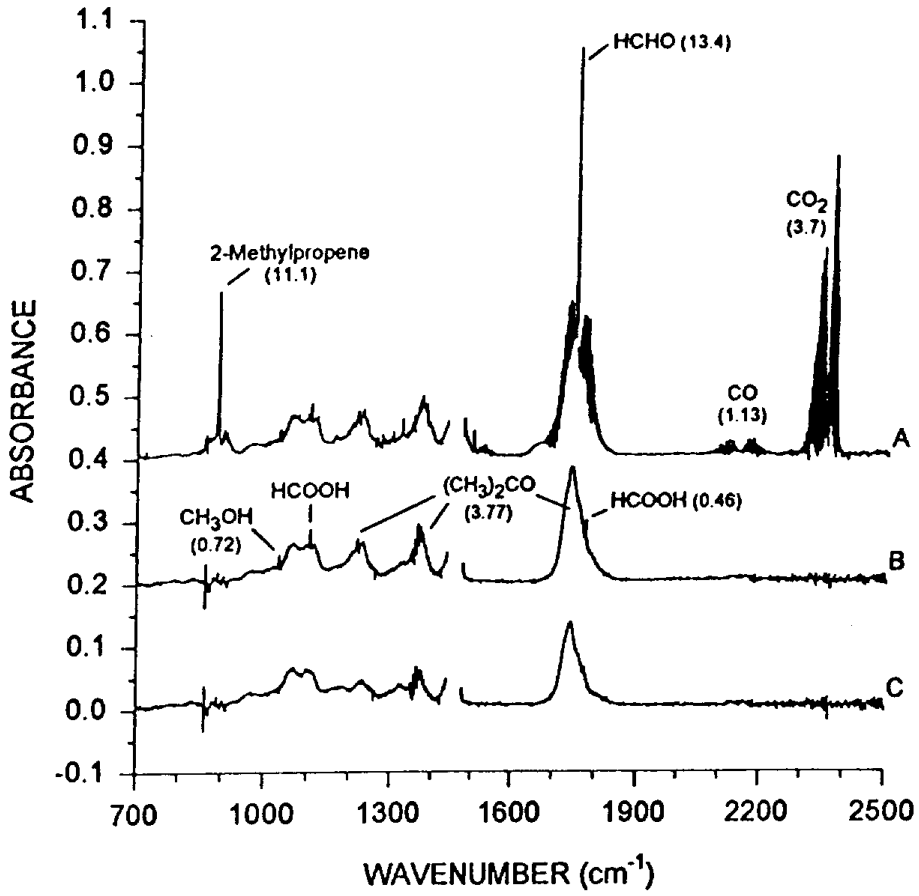

Figure 7. FT-IR spectra from the reaction of O_3 with 2-methylpropene in air in the presence of excess cyclohexane. (A) Reaction mixture with 53.9% of 2-methylpropene consumed. (B) From (A) after subtraction of absorptions by 2-methylpropene, HCHO, CO, and CO_2. (C) Residual spectrum after subtraction of absorptions by the known compounds. The discontinuities in the spectra represent regions severely distorted by strong absorptions of the added cyclohexane.

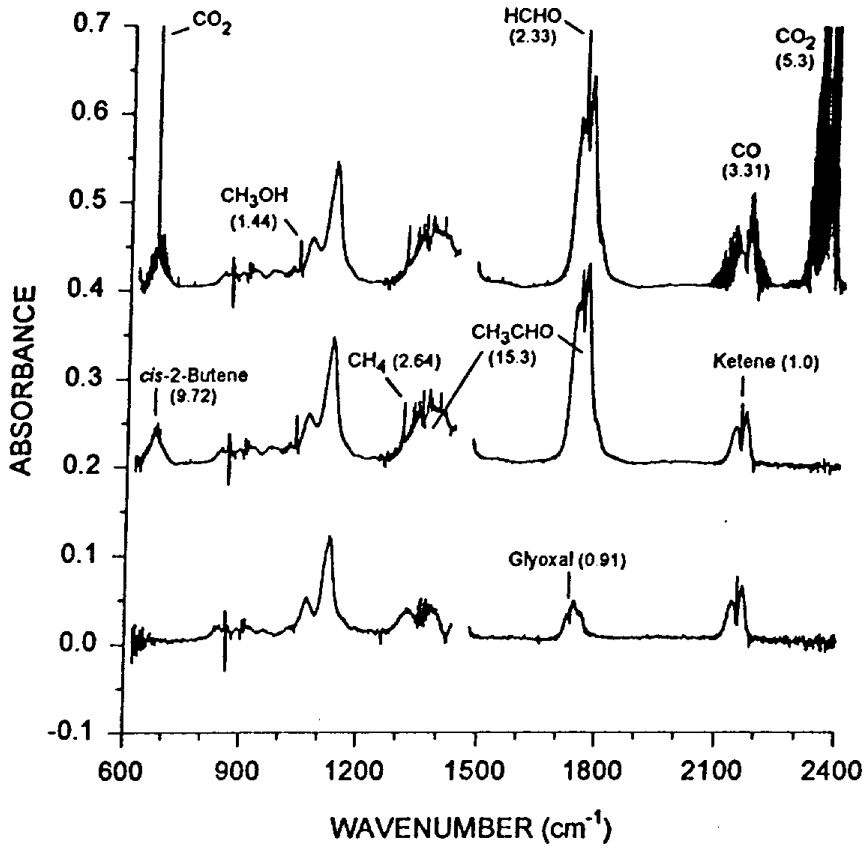

Figure 8. FT-IR spectra from the reaction of O_3 with *cis*-2-butene in air in the presence of excess cyclohexane. (A) Reaction mixture with 59.5% of *cis*-2-butene consumed. (B) From (A) after subtraction of absorptions by *cis*-2-butene, HCHO, CO, and CO_2. (C) Residual spectrum after subtraction of absorptions by the known compounds, except ketene and glyoxal. The discontinuities in the spectra represent regions severely distorted by strong absorptions of the added cyclohexane.

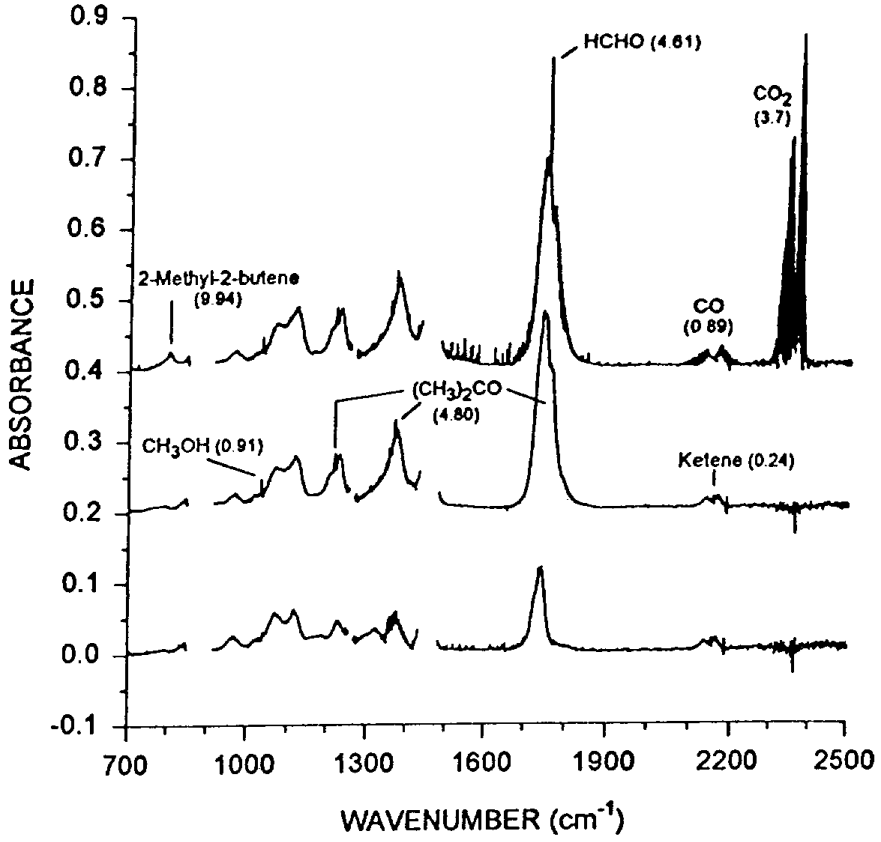

Figure 9. FT-IR spectra from the reaction of O_3 with 2-methyl-2-butene in air in the presence of excess cyclohexane. (A) Reaction mixture with 58.6% of 2-methyl-2-butene consumed. (B) From (A) after subtraction of absorptions by 2-methyl-2-butene, HCHO, CO, and CO_2. (C) Residual spectrum after subtraction of absorptions by the known compounds, except ketene; CH_3CHO absorptions was also subtracted based on the yield measured by GC-FID. The discontinuities in the spectra represent regions severely distorted by strong absorptions of the added cyclohexane.

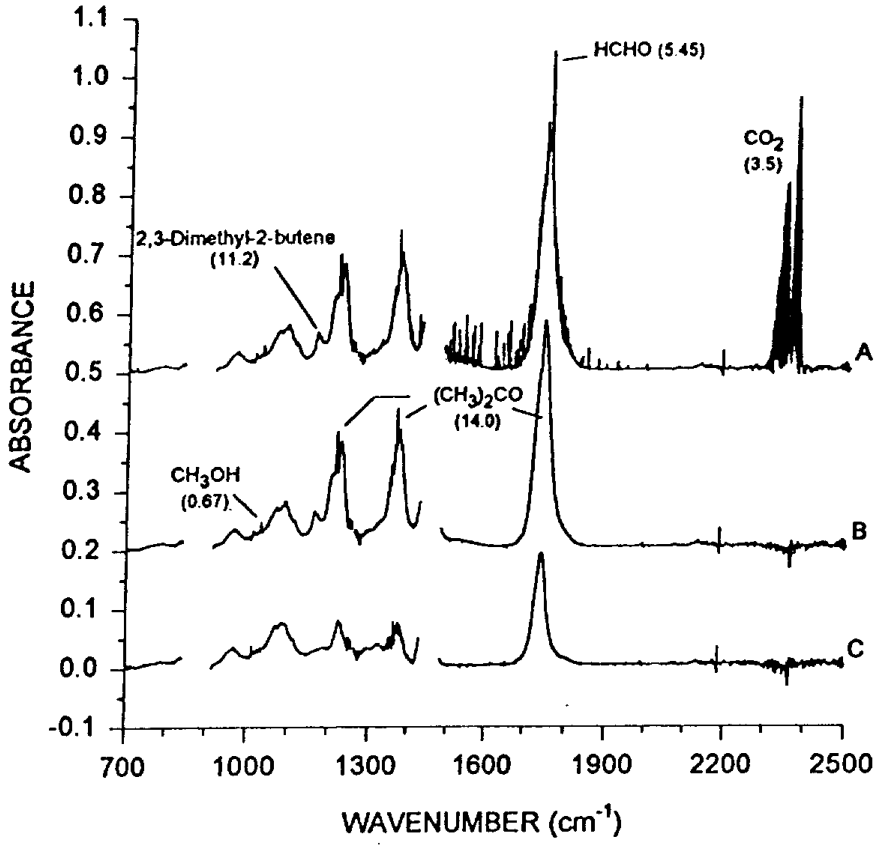

Figure 10. FT-IR spectra from the reaction of O_3 with 2,3-dimethyl-2-butene in air in the presence of excess cyclohexane. (A) Reaction mixture with 53.2% of 2,3-dimethyl-2-butene consumed. (B) From (A) after subtraction of absorptions by HCHO and CO_2. (C) Residual spectrum after subtraction of absorptions by the known compounds. The discontinuities in the spectra represent regions severely distorted by strong absorptions of the added cyclohexane.

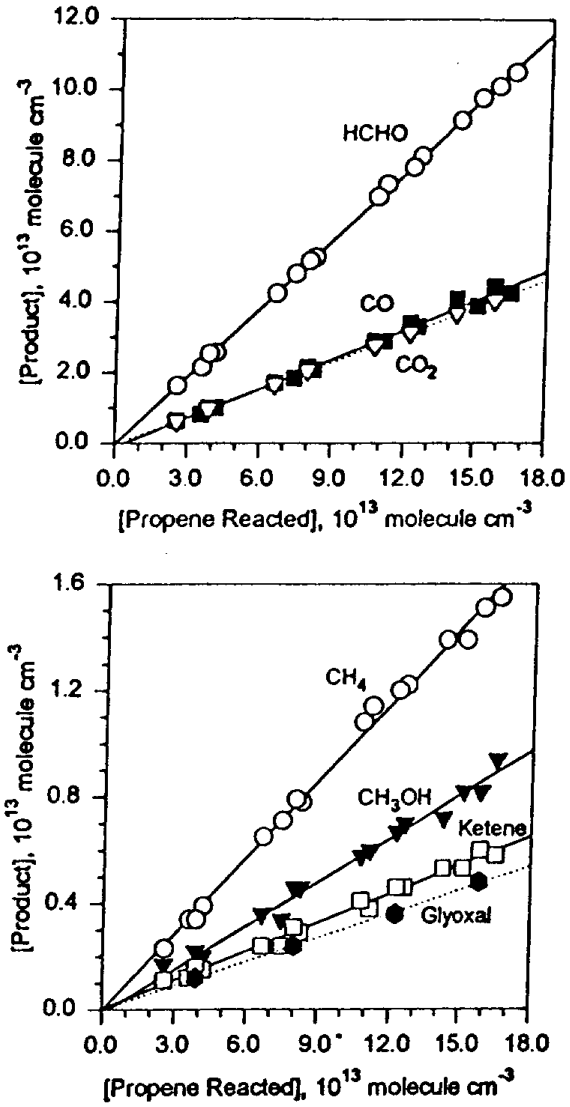

Figure 11. Plots of the amounts of products formed against the amounts of propene reacted with O_3 in the presence of sufficient cyclohexane to scavenge $\geq 95\%$ of the OH radicals formed. Data from two separate experiments are combined in each plot (except for CO_2 and glyoxal where data from one experiment were excluded because of background interference).

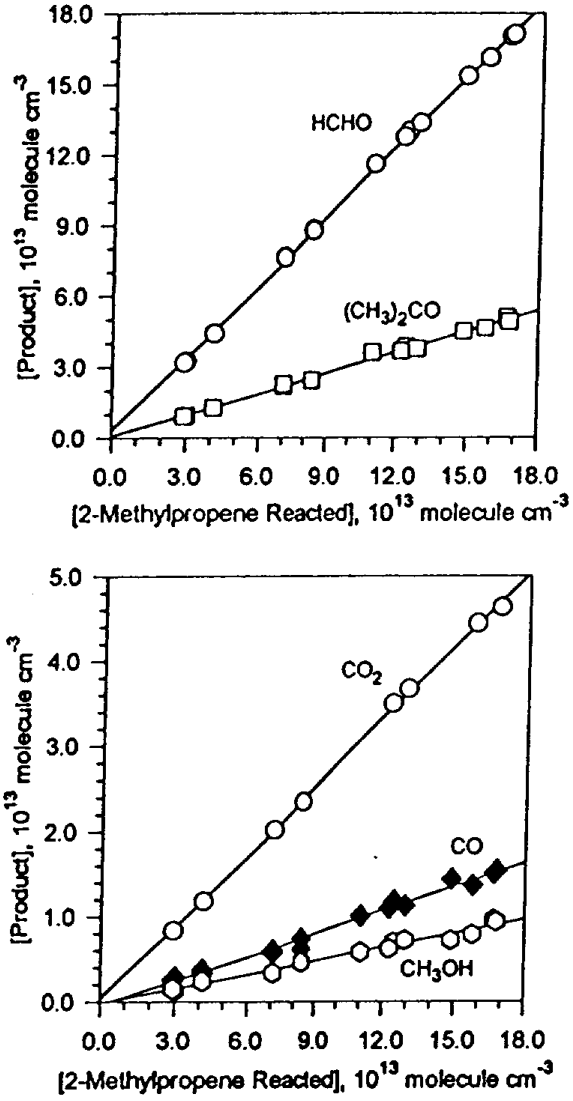

Figure 12. Plots of the amounts of products formed against the amounts of 2-methylpropene reacted with O_3 in the presence of sufficient cyclohexane to scavenge $\geq 95\%$ of the OH radicals formed. Data from two separate experiments are combined in each plot.

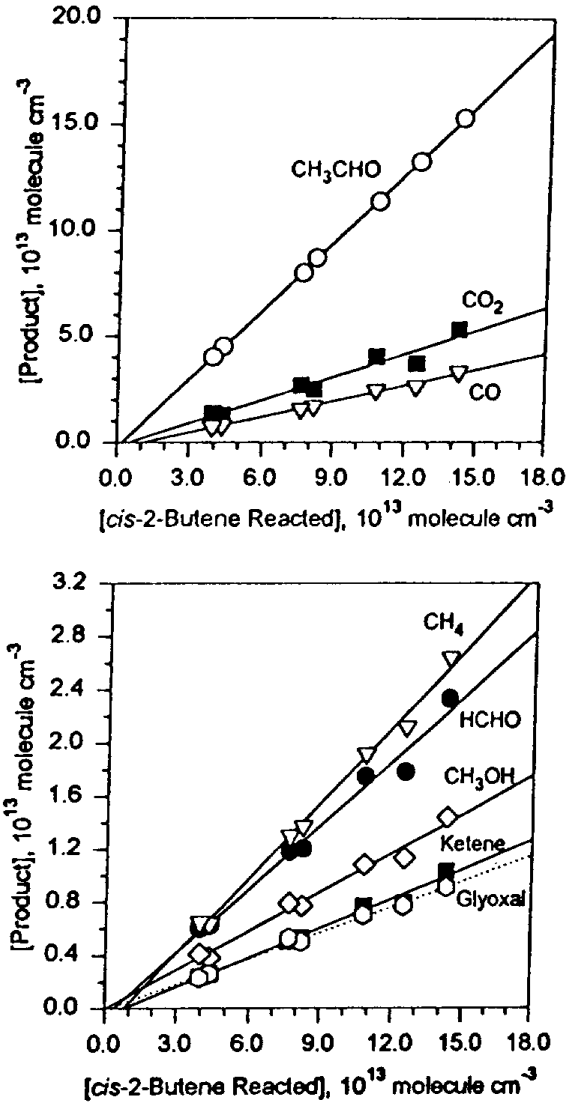

Figure 13. Plots of the amounts of products formed against the amounts of *cis*-2-butene reacted with O_3 in the presence of sufficient cyclohexane to scavenge $\geq 95\%$ of the OH radicals formed. Data from two separate experiments are combined in each plot.

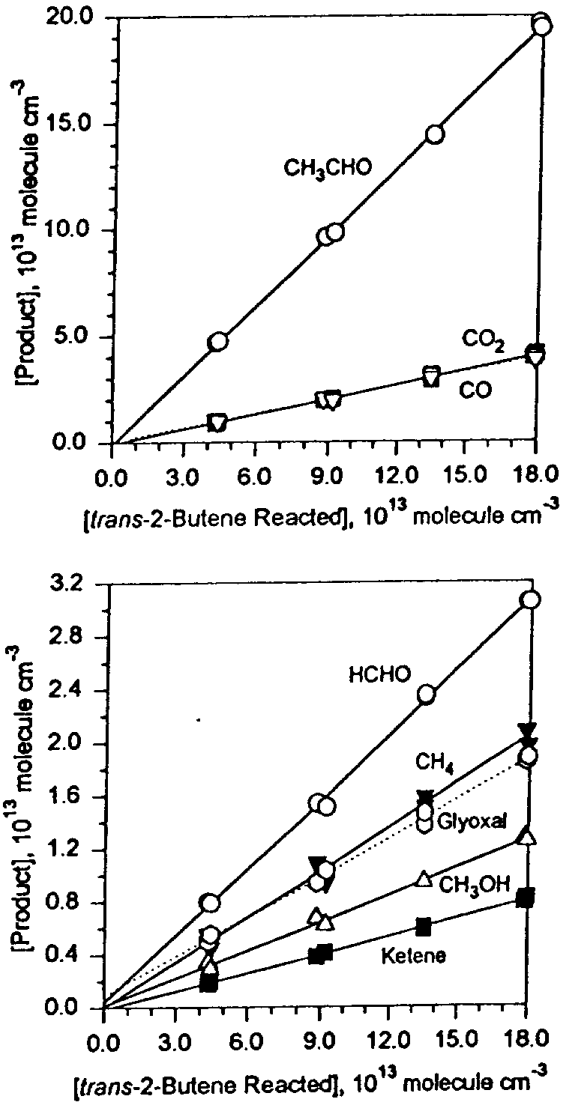

Figure 14. Plots of the amounts of products formed against the amounts of *trans*-2-butene reacted with O_3 in the presence of sufficient cyclohexane to scavenge $\geq 95\%$ of the OH radicals formed. Data from two separate experiments are combined in each plot.

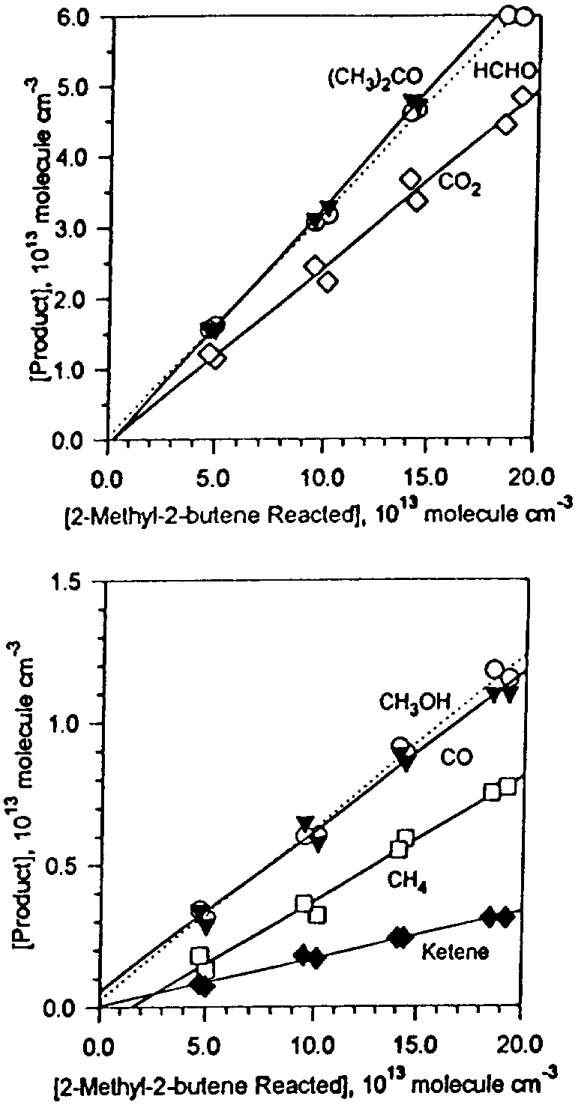

Figure 15. Plots of the amounts of products formed against the amounts of 2-methyl-2-butene reacted with O_3 in the presence of sufficient cyclohexane to scavenge $\geq 95\%$ of the OH radicals formed. Data from two separate experiments are combined in each plot.

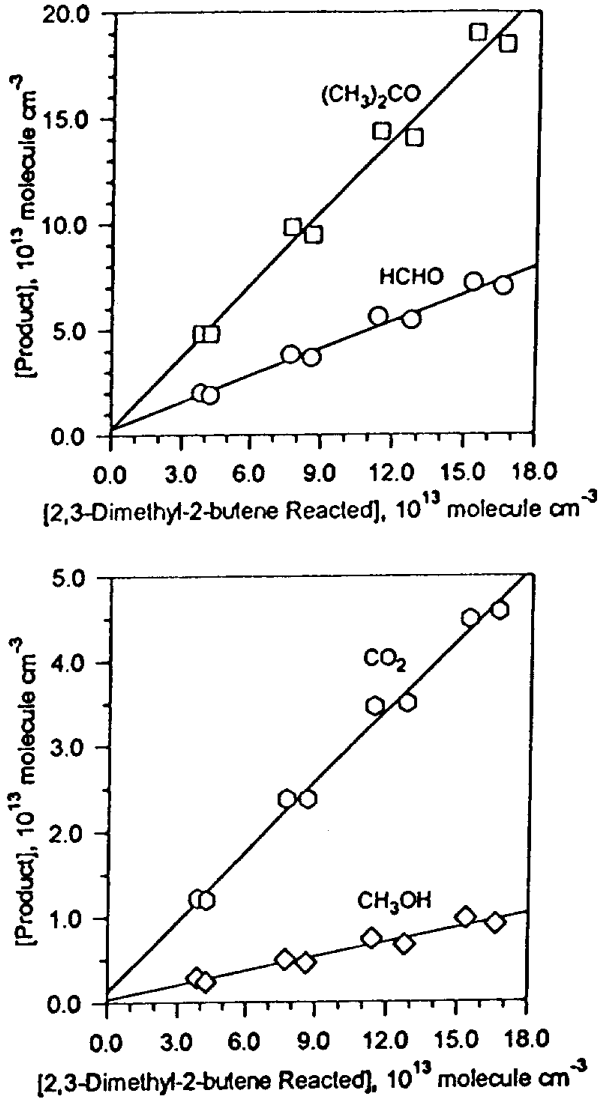

Figure 16. Plots of the amounts of products formed against the amounts of 2,3-dimethyl-2-butene reacted with O_3 in the presence of sufficient cyclohexane to scavenge $\geq 95\%$ of the OH radicals formed. Data from two separate experiments are combined in each plot.

in Figure 10 upon scale expansion, methylglyoxal could not be reliably quantified due to its severe overlap with the absorption features of cyclohexanone at 1735 cm^{-1} and with those of hydroxyacetone, another known product of the 2,3-dimethyl-2-butene reaction (Niki *et al.*, 1987), whose C=O stretch lies at 1740 cm^{-1} and whose formation in the present experiments is suggested only by a discernible Q-branch at 1107 cm^{-1}. Moreover, Niki *et al.* (1987) suggested that for the reaction of O_3 with 2,3-dimethyl-2-butene, tentatively identified products $CH_3C(O)CH_2OOH$ and $(CH_3)_2C(OH)C(CH_3)_2OOH$ also contributed to the absorptions near 1740 cm^{-1} and the 900-1400 cm^{-1} region.

Products Observed from API-MS and API-MS/MS Analyses. Because of the formation of OH radicals from the reactions of O_3 with alkenes (Niki *et al.*, 1987; Paulson *et al.*, 1992a; Atkinson *et al.*, 1992, 1995a; Paulson and Seinfeld, 1992; Atkinson and Aschmann, 1993; Horie *et al.*, 1994; Shu and Atkinson, 1994; Section 2 above) and the need to scavenge the OH radicals to ascertain the products formed from the O_3 reactions alone, the products formed include the products of the OH radical reaction with cyclohexane in the absence of NO. These additional products complicate the analyses, and particularly analyses using API-MS, because of the relatively high yields of cyclohexanone plus cyclohexanol together with the presence of the other, not well understood, products formed from the OH radical with cyclohexane in the absence of NO (Atkinson *et al.*, 1992; Atkinson and Aschmann, 1993; Rowley *et al.*, 1991; Aschmann *et al.*, 1997).

For the six alkene reactions studied, in all cases the API-MS spectra of reacted O_3 - alkene - cyclohexane (in excess) - air mixtures showed the presence of ion peaks at 83, 99, 101, 115, 117, 119, 197 and 199 u. The ion peaks at 99, 117 and 197 u are the $[M+H]^+$, $[M+H+M_2O]^+$ and $[M_2+H]^+$ ions of M = cyclohexanone, and those at 83, 119 and 199 u are the $[M+H-H_2O]^+$, $[M+H]^+$ and $[cyclohexanone+M+H]^+$ ions of M = cyclohexanol, with cyclohexanone and cyclohexanol being known products of the OH radical-initiated reaction of cyclohexane in the absence of NO (Atkinson *et al.*, 1992; Atkinson and Aschmann, 1993). The ion peak at 115 u is probably the $[M+H]^+$ ion of M = $CHO(CH_2)_4CHO$ formed from the reactions of the $CHO(CH_2)_4CH_2O\dot{O}$ peroxy radical with other peroxy radicals (including with another $CHO(CH_2)_4CH_2O\dot{O}$ radical), with the $CHO(CH_2)_4CH_2O\dot{O}$ peroxy radical being formed

by O_2 addition to the $CHO(CH_2)_4\dot{C}H_2$ radical formed from decomposition of the cyclohexyoxy radical (Aschmann *et al.*, 1997). Furthermore, weak ion peaks at 113 u were also observed which could be the $[M+H-H_2O]^+$ ions of M = $CHO(CH_2)_4CH_2OH$ also formed from the reactions of the $CHO(CH_2)_4CH_2O\dot{O}$ peroxy radical with organic peroxy radicals.

The remaining ion peaks observed from these reactions included significant or dominant ion peaks at 45 u from the propene reaction, at 59, 117 and 157 u from the 2-methylpropene reaction, at 45 and 89 u from the *trans*-2-butene reaction, at 45 u from the *cis*-2-butene reaction, at 45, 59, 117 and 157 u from the 2-methyl-2-butene reaction, and at 59, 117, 157 and 159 from the 2,3-dimethyl-2-butene reaction. API-MS/MS "daughter" and "parent" ion CAD spectra of these ions indicated that the 45 and 89 u ion peaks were the $[M+H]^+$ and $[M_2+H]^+$ peaks of M = acetaldehyde; and that the 59, 117, 157 and 159 u ion peaks were the $[M+H]^+$, $[M_2+H]^+$, [M+cyclohexanone+H]$^+$ and [M+cyclohexanol+H]$^+$ peaks of M = acetone.

Discussion

Table 2 shows that the formation yields of acetone measured by GC and by FT-IR absorption spectroscopy from the 2-methylpropene, 2-methyl-2-butene and 2,3-dimethyl-2-butene reactions are in excellent agreement, and similarly for the yields of acetaldehyde from the *cis*- and *trans*-2-butene reactions, with the agreement between the two independent sets of analyses being within 13%. The formation yields of the "primary" carbonyls from the present work are compared to the literature data of Niki *et al.* (1987) and Grosjean *et al.* (1996a), obtained in the presence of an OH radical scavenger, in Table 3. Again, the agreement between the various studies is seen to be good, especially for the 2-methylpropene and 2,3-dimethyl-2-butene reactions. While the primary carbonyl formation yields of Grosjean *et al.* (1996a) for the propene and 2-methyl-2-butene reactions are respectively 15-20% higher and 10-20% lower than our present yields, the yields are almost certainly within the combined overall experimental uncertainties.

The sum of the primary carbonyls determined in this work are 1.09 for propene, 1.30-1.33 for 2-methylpropene, 1.08-1.19 for *cis*-2-butene, 1.09-1.14 for *trans*-2-butene, 1.08-1.12 for 2-methyl-2-butene and 0.98-1.14 for 2,3-dimethyl-2-butene. The formation yields of the "primary" carbonyls HCHO and CH_3CHO from the propene reaction are approximately equal

Table 3. Formation yields of the "primary" carbonyls from the gas-phase reactions of O_3 with a series of methyl-substituted ethenes at room temperature and atmospheric pressure of air in the presence of an OH radical scavenger

Alkene	Primary carbonyl	Formation yield	Reference
Propene	HCHO	0.780 ± 0.015	Grosjean *et al.* (1996a)
		0.645 ± 0.048[a]	This work
	CH_3CHO	0.520 ± 0.026	Grosjean *et al.* (1996a)
		0.446 ± 0.092[b]	This work
2-Methylpropene	HCHO	0.950 ± 0.098	Grosjean *et al.* (1996a)
		1.01 ± 0.07[a]	This work
	$CH_3C(O)CH_3$	0.340 ± 0.031	Grosjean *et al.* (1996a)
		0.323 ± 0.030[b]	This work
		0.294 ± 0.030[a]	This work
2-Methyl-2-butene	CH_3CHO	0.685 ± 0.019	Grosjean *et al.* (1996a)
		0.745 ± 0.099[b]	This work
	$CH_3C(O)CH_3$	0.302 ± 0.006	Grosjean *et al.* (1996a)
		0.376 ± 0.032[b]	This work
		0.339 ± 0.030[a]	This work

Table 3. Formation yields of the "primary" carbonyls from the gas-phase reactions of O_3 with a series of methyl-substituted ethenes at room temperature and atmospheric pressure of air in the presence of an OH radical scavenger (continued)

Alkene	Primary carbonyl	Formation yield	Reference
2,3-Dimethyl-	$CH_3C(O)CH_3$	1.02 ± 0.13	Niki *et al.* (1987)
2-butene		1.006 ± 0.049	Grosjean *et al.* (1996a)
		0.997 ± 0.086[b]	This work
		1.14 ± 0.19[a]	This work

[a]FT-IR measurement.
[b]GC-FID measurement.

(using the CH_3CHO yield and assuming a sum of the two primary carbonyls of unity), while the formation of the disubstituted biradical $[(CH_3)_2\dot{C}O\dot{O}]^*$ (plus HCHO or CH_3CHO) from the 2-methylpropene and 2-methyl-2-butene reactions is preferred (Table 2). Our present observations concerning the relative importance of the two sets of (carbonyl plus biradical) from alkenes of structure $RCH=CH_2$, $R_1R_2C=CH_2$ and $R_1CH=CR_2R_3$ are in general agreement with previous literature data of Atkinson *et al.* (1995a), Grosjean and Grosjean (1996a,b,c,d) and Grosjean *et al.* (1996a,b) for some 33 alkenes (Atkinson, 1997b). Hence apart from the 2-methylpropene reaction, the sum of the primary carbonyls is 1.1 ± 0.1. In the case of the 2-methylpropene reaction, it appears that HCHO is also formed from decomposition of the $[(CH_3)_2\dot{C}O\dot{O}]^*$ biradical in addition to "direct" HCHO formation from decomposition of the primary ozonide, as also observed by Grosjean *et al.* (1996a). Formation of HCHO from subsequent reactions of the $[(CH_3)_2\dot{C}O\dot{O}]^*$ biradical is further indicated by the observation of significant HCHO formation from the 2-methyl-2-butene and 2,3-dimethyl-2-butene reactions (Table 2). Formation of HCHO in significant yield was also observed by Niki *et al.* (1987) from the 2,3-dimethyl-2-butene reaction and by Grosjean *et al.* (1996a) from the 2-methyl-2-butene and 2,3-dimethyl-2-butene reactions [with yields of 0.246 ± 0.020 (Grosjean *et al.*, 1996a) and 0.288 ± 0.023 (Grosjean *et al.*, 1996a), respectively]. The 2-methyl-2-butene and 2,3-dimethyl-2-butene reactions both involve formation of the $[(CH_3)_2\dot{C}O\dot{O}]^*$ biradical, with the 2,3-dimethyl-2-butene reaction forming only the $[(CH_3)_2\dot{C}O\dot{O}]^*$ biradical. The expected reactions of the $[(CH_3)_2\dot{C}O\dot{O}]^*$ biradical include (Niki *et al.*, 1987; Atkinson, 1997b)

$$[(CH_3)_2\dot{C}O\dot{O}]^* + M \rightarrow (CH_3)_2\dot{C}O\dot{O} + M \quad (12)$$

$$[(CH_3)_2\dot{C}O\dot{O}]^* \rightarrow [CH_3C(OOH)=CH_2]^* \rightarrow OH + CH_3C(O)\dot{C}H_2 \quad (13)$$

followed by reactions of the $CH_3C(O)\dot{C}H_2$ radical (Atkinson, 1994, 1997b)

$$CH_3C(O)\dot{C}H_2 + O_2 \rightarrow CH_3C(O)CH_2O\dot{O} \quad (14)$$

$$CH_3C(O)CH_2O\dot{O} + HO_2 \rightarrow CH_3C(O)CH_2OOH + O_2 \quad (15)$$

$$CH_3C(O)CH_2O\dot{O} + R\dot{O}_2 \rightarrow \alpha\ CH_3C(O)CH_2OH + (1-\alpha)\ CH_3C(O)CHO + R\dot{O}_2\ \text{products} + O_2 \quad (16)$$

$$CH_3C(O)CH_2O\dot{O} + R\dot{O}_2 \rightarrow CH_3C(O)CH_2\dot{O} + R\dot{O} + O_2 \quad (17)$$

$$CH_3C(O)CH_2\dot{O} \rightarrow CH_3\dot{C}O + HCHO \quad (18)$$

Methylglyoxal and hydroxyacetone have been previously observed as products from the 2,3-dimethyl-2-butene reaction (Niki *et al.*, 1987; Grosjean *et al.*, 1996a), and methylglyoxal has been observed from the 2-methylpropene and 2-methyl-2-butene reactions (Grosjean *et al.*, 1996a). The subsequent reactions of the $CH_3\dot{C}O$ radical lead to the formation of acetyl peroxy and methyl peroxy radicals and hence to $CH_3C(O)OH$, $CH_3C(O)OOH$, CH_3OH, and HCHO (Atkinson, 1994, 1997b).

Methane and ketene were only observed as products from the alkenes giving rise to a $[CH_3\dot{C}HO\dot{O}]^*$ biradical (propene, *cis*- and *trans*-2-butene and 2-methyl-2-butene), indicating that the reactions involved are

$$[CH_3\dot{C}HO\dot{O}]^* \rightarrow CH_4 + CO_2 \quad (19)$$

and

$$[CH_3\dot{C}HO\dot{O}]^* \rightarrow CH_2CO + H_2O \quad (20)$$

Our methane formation yield from the *cis*-2-butene reaction of 0.183 ± 0.012 is in reasonable agreement with the yield of 0.14 measured by Niki *et al.* (1987).

The potential reactions of the $[\dot{C}H_2O\dot{O}]^*$ and $[CH_3\dot{C}HO\dot{O}]^*$ biradicals are (Atkinson, 1994, 1997b)

$$[\dot{C}H_2O\dot{O}]^* + M \rightarrow \dot{C}H_2O\dot{O} + M \quad (21a)$$

$$[\dot{C}H_2O\dot{O}]^* \rightarrow CO_2 + H_2 \quad (21b)$$

$$[\dot{C}H_2O\dot{O}]^* \rightarrow CO + H_2O \quad (21c)$$

$$[\dot{C}H_2O\dot{O}]^* \rightarrow CO_2 + 2\,H \quad (21d)$$

$$[\dot{C}H_2O\dot{O}]^* \rightarrow H\dot{C}O + OH \quad (21e)$$

and

$$[CH_3\dot{C}HO\dot{O}]^* + M \rightarrow CH_3\dot{C}HO\dot{O} + M \quad (22a)$$

$$[CH_3\dot{C}HO\dot{O}]^* \rightarrow \dot{C}H_3 + CO + OH \text{ (or } CH_3\dot{C}O + OH \text{ or } HC(O)\dot{C}H_2 + OH) \quad (22b)$$

$$[CH_3\dot{C}HO\dot{O}]^* \rightarrow \dot{C}H_3 + CO_2 + H \quad (22c)$$

$$[CH_3\dot{C}HO\dot{O}]^* \rightarrow H\dot{C}O + CH_3\dot{O} \quad (22d)$$

$$[CH_3\dot{C}HO\dot{O}]^* \rightarrow CH_4 + CO_2 \quad (22e)$$

$$[CH_3\dot{C}HO\dot{O}]^* \rightarrow CH_3OH + CO \quad (22f)$$

$$[CH_3\dot{C}HO\dot{O}]^* \rightarrow CH_2CO + H_2O \quad (22g)$$

and these reactions can account for the observed products (Table 1) and for the formation of OH radicals (Atkinson and Aschmann, 1993). In particular, our data for the *cis*- and *trans*-2-butene reactions, together with our previously measured OH radical formation yields (Atkinson and Aschmann, 1993), suggest that for the $[CH_3\dot{C}HO\dot{O}]^*$ biradical, pathways (a), (b), (e) and (g) account for 0.18, 0.41, 0.18 and 0.07, respectively, for *cis*-2-butene and 0.18, 0.64, 0.11 and 0.05, respectively, for *trans*-2-butene, with these reaction pathways for the *trans*-2-butene reaction accounting for essentially 100% of the $[CH_3\dot{C}HO\dot{O}]^*$ reactions. The products formed from the subsequent reactions of the thermalized biradicals, such as the $CH_3\dot{C}HO\dot{O}$ biradical formed from the 2-butenes, are not fully understood at the present time.

4. PRODUCTS OF THE GAS-PHASE REACTIONS OF A SERIES OF METHYL-SUBSTITUTED ETHENES WITH THE OH RADICAL

Introduction

As noted in Section 3 above, alkenes are a significant component of ambient air in urban areas and in the atmosphere they react with OH radicals, NO_3 radicals and O_3 (Atkinson, 1994, 1997b), with the daytime OH radical reaction often dominating as the alkene removal process (Atkinson, 1988; Blake *et al.*, 1993). The kinetics and products of the gas-phase reaction of OH radicals with alkenes have been studied previously (Atkinson, 1989, 1994, 1997b). However, while the kinetics of these OH radical reactions are now reasonably well understood for a large number of alkenes (Atkinson, 1997b), only for a few simple acyclic alkenes have product studies been conducted at room temperature and atmospheric pressure of air (Niki *et al.*, 1978, 1981; Atkinson *et al.*, 1985, 1995b; Tuazon and Atkinson, 1990; Paulson *et al.*, 1992b; Paulson and Seinfeld, 1992; Miyoshi *et al.*, 1994; Hakola *et al.*, 1993, 1994; Kwok *et al.*, 1995, 1996a; Atkinson, 1997b).

The gas-phase reactions of the OH radical with alkenes proceed mainly by initial addition of the OH radical to the >C=C< bond(s) to form a β-hydroxyalkyl radical (Atkinson, 1997b), which in the troposphere then rapidly and solely adds O_2 to form the β-hydroxyalkyl peroxy radical. In the presence of NO, the β-hydroxyalkyl peroxy radical reacts with NO to form either the β-hydroxynitrate or the β-hydroxyalkoxy radical plus NO_2 (Atkinson, 1997b),

$$CH_3CH_2CH(OH)CH_2O\dot{O} + NO \xrightarrow{M} CH_3CH_2CH(OH)CH_2ONO_2 \quad (23a)$$

$$CH_3CH_2CH(OH)CH_2O\dot{O} + NO \rightarrow CH_3CH_2CH(OH)CH_2\dot{O} + NO_2 \quad (23b)$$

while in the absence of NO (or at low NO concentrations), the β-hydroxyalkyl peroxy radicals are expected to react with HO_2 radicals and with organic peroxy radicals (including the self-reaction) (Atkinson, 1997b).

$$CH_3CH_2CH(OH)CH_2O\dot{O} + HO_2 \rightarrow CH_3CH_2CH(OH)CH_2OOH + O_2 \quad (24)$$

$$\rightarrow CH_3CH(OH)CH_2OH + CH_3CH(OH)CHO + R\dot{O}_2 \text{ products} + O_2 \quad (25a)$$

$$CH_3CH_2CH(OH)CH_2O\dot{O} + R\dot{O}_2 \rightarrow CH_3CH(OH)CH_2\dot{O} + R\dot{O} + O_2 \quad (25b)$$

The β-hydroxyalkoxy radicals formed from the reactions of the β-hydroxyalkyl peroxy radicals with NO and with $R\dot{O}_2$ radicals can then react with O_2, decompose or, for $\geq C_4$ side chains, isomerize via a 6-member transition state, as shown, for example, in Reaction Scheme (3) in Section 1. The α-hydroxyalkyl radicals react rapidly with O_2 to form the carbonyl (Atkinson, 1994, 1997b).

$$CH_3CH_2\dot{C}HOH + O_2 \rightarrow CH_3CH_2CHO + HO_2 \quad (26)$$

The alkoxy radical ($\dot{O}CH_2CH_2CH(OH)CH_2OH$) formed subsequent to the isomerization reaction is predicted to undergo a further isomerization to form the polyfunctional product $HOCH_2CH_2CH(OH)CHO$ (Atkinson, 1997a,b; Kwok *et al.*, 1996a).

Previous studies have shown that at room temperature and atmospheric pressure of air the $HOCH_2CH_2\dot{O}$ radical formed from OH radical addition to ethene reacts with O_2 and decomposes (Niki *et al.*, 1981), while the β-hydroxyalkoxy radicals formed from propene, 1-butene and *trans*-2-butene predominantly decompose (Niki *et al.*, 1978; Atkinson *et al.*, 1985). However, the carbonyl products observed and quantified from the OH radical reactions with isoprene (Tuazon and Atkinson, 1990; Paulson *et al.*, 1992b; Miyoshi *et al.*, 1994), the C_5-C_8 1-alkenes (Paulson and Seinfeld, 1992; Atkinson *et al.*, 1995b) and a series of $C_{10}H_{16}$ monoterpenes (Hakola *et al.*, 1993, 1994) indicate that decomposition of the intermediate β-hydroxyalkoxy radicals is not the sole process and that other reaction pathways, including isomerization (Kwok *et al.*, 1996a; Atkinson, 1997a), must be occurring. Indeed, the recent study of Kwok *et al.* (1996a), employing atmospheric pressure ionization mass spectrometry to study the products of the OH radical-initiated reactions of 1-butene through 1-octene, observed formation of C_n-dihydroxycarbonyls from the C_n-1-alkene reactions, direct evidence for the occurrence of isomerization of the β-hydroxyalkoxy radicals involved. Atkinson (1997a) has used the literature product data for the alkanes and alkenes to propose methods for the

calculation of the reaction rates of alkoxy and β-hydroxyalkoxy radicals under tropospheric conditions, and these estimation methods predict that decomposition of the β-hydroxyalkoxy radicals will dominate over their reaction with O_2 at around room temperature and atmospheric pressure of air (Atkinson, 1997a).

In this work, we have used gas chromatography, *in situ* Fourier transform infrared (FT-IR) absorption spectroscopy, and direct air sampling, atmospheric pressure ionization tandem mass spectrometry (API-MS) to investigate the products formed from the reactions of the OH radical with the methyl-substituted ethenes propene, 2-methylpropene, *cis*- and *trans*-2-butene, 2-methyl-2-butene and 2,3-dimethyl-2-butene at room temperature and atmospheric pressure of air.

Experimental

Experiments were carried out in three reaction chambers with differing analytical techniques. Reactions were carried out in: a 5800 liter evacuable, Teflon-coated chamber containing an *in situ* multiple reflection optical system interfaced to a Nicolet 7199 Fourier transform infrared (FT-IR) absorption spectrometer and with irradiation provided by a 24-kW xenon arc filtered through a 0.25 in. thick Pyrex pane (to remove wavelengths <300 nm); a 7900 liter Teflon chamber with analysis by gas chromatography with flame ionization detection (GC-FID) and irradiation provided by two parallel banks of blacklamps; and a 6500 liter Teflon chamber interfaced to a PE SCIEX API III MS/MS direct air sampling, atmospheric pressure ionization tandem mass spectrometer (API-MS), again with irradiation provided by two parallel banks of blacklamps. All three chambers are fitted with Teflon-coated fans to ensure rapid mixing of reactants during their introduction into the chamber.

Hydroxyl radicals were generated in the presence of NO by the photolysis of methyl nitrite (CH_3ONO) or ethyl nitrite (C_2H_5ONO) in air at wavelengths >300 nm (Atkinson *et al.*, 1981, 1995b; Tuazon and Atkinson, 1990):

$$RCH_2ONO + h\nu \rightarrow RCH_2\dot{O} + NO \qquad (27)$$

$$RCH_2\dot{O} + O_2 \rightarrow RCHO + HO_2 \qquad (28)$$

$$HO_2 + NO \rightarrow OH + NO_2 \quad (29)$$

where R = H or CH_3. NO was added to the reactant mixtures to avoid the formation of O_3, and hence of NO_3 radicals (Atkinson *et al.*, 1981). Experiments were carried out in the 7900 liter Teflon chamber for the GC-FID measurement of the formation yields of carbonyls other than HCHO (Atkinson *et al.*, 1995b; Section 3 above) and in the 5800 liter evacuable, Teflon-coated chamber for FT-IR absorption spectroscopic determination of the HCHO (and other carbonyl) formation yields (Atkinson *et al.*, 1995b; Section 3 above). Because HCHO is the primary photolytic product of methyl nitrite (see above), the photolysis of ethyl nitrite in air was used as the OH radical source for the determination of HCHO formation yields in the 5800 liter evacuable chamber (Tuazon and Atkinson, 1990; Atkinson *et al.*, 1995b). In the 6500 liter and 7900 liter Teflon chambers with analyses by GC-FID and API-MS, OH radicals were generated by the photolysis of CH_3ONO in air. Additional experiments were carried out in the 6500 liter Teflon chamber with API-MS analyses in which OH radicals were generated in the absence of NO from the reaction of O_3 with the alkene being studied (Atkinson *et al.*, 1992; Atkinson and Aschmann, 1993).

Teflon Chamber with Analysis by GC-FID. For the experiments carried out in the 7900 liter Teflon chamber, the initial reactant concentrations (in molecule cm^{-3} units) were: CH_3ONO, (1.85-2.25) x 10^{14}; NO, (1.95-2.30) x 10^{14}; and alkene, (2.28-2.50) x 10^{13}. Irradiations were carried out at 20% of the maximum light intensity for 1-6 mins. The concentrations of the alkenes and the carbonyl (apart from HCHO) products were measured during the experiments by gas chromatography with flame ionization detection (GC-FID) as described in Section 3.

Evacuable Chamber with Analysis by FT-IR Absorption Spectroscopy. The initial concentrations of the alkenes, methyl or ethyl nitrite, and NO in the experiments using FT-IR absorption spectroscopic analyses in the 5800 liter evacuable chamber were (2.4-4.8) x 10^{14} molecule cm^{-3}, 2.4 x 10^{14} molecule cm^{-3}, and (1.8-2.4) x 10^{14} molecule cm^{-3}, respectively. 0.5-1.0 min intermittent irradiations were carried out, with FT-IR spectroscopic and GC-FID analyses during the dark periods. The alkenes were introduced into the chamber by flushing measured partial

pressures in a 5.25 liter Pyrex bulb into the chamber with a stream of N_2 gas. The concentrations of alkenes and selected products were measured by FT-IR absorption spectroscopy, with 64 co-added interferograms (scans) per spectrum (1.8 min measurement time) recorded with a full width at half maximum (fwhm) resolution of 0.7 cm^{-1} and a pathlength of 62.9 m.

FT-IR absorptions of the alkenes were obtained by measuring known partial pressures of the gaseous compound into a 5.25 liter Pyrex bulb with an MKS Baratron 0-100 Torr sensor and flushing the contents of the bulb into the 5800 liter chamber with FT-IR detection of the authentic compound. IR reference spectra of the products measured were available from previous IR calibrations in this laboratory (see also Section 3 above).

Teflon Chamber with Analysis by API-MS. Experiments with API-MS analyses were carried out in a 6500 liter Teflon chamber which was interfaced to a PE SCIEX API III MS/MS instrument via a 25 mm diameter x 75 cm length Pyrex tube, with a sampling flow rate of ~20 liter min^{-1}. The operation of the API-MS in the MS (scanning) and MS/MS [with collision activated dissociation (CAD)] modes has been described elsewhere (Atkinson *et al.*, 1995d; Kwok *et al.*, 1995, 1996a,b). Use of the MS/MS mode with CAD allows the "daughter ion" or "parent ion" spectrum of a given ion peak observed in the MS scanning mode to be obtained (Atkinson *et al.*, 1995d; Kwok *et al.*, 1995, 1996a,b). The positive ion mode was used in all these API-MS and API-MS/MS analyses, with protonated water hydrates ($H_3O^+(H_2O)_n$) generated by the corona discharge in the chamber diluent gas being responsible for the protonation of analytes,

$$H_3O^+(H_2O)_n + M \rightarrow MH^+(H_2O)_m + (n - m + 1)H_2O \qquad (30)$$

where M is the neutral analyte of interest. Ions are drawn by an electric potential from the ion source through the sampling orifice into the mass-analyzing first quadrupole or third quadrupole. Neutral molecules and particles are prevented from entering the orifice by a flow of high-purity nitrogen ("curtain" gas), and as a result of the declustering action of the curtain gas on the hydrated ions, the ions that are mass-analyzed are mainly protonated molecular ions ($[M+H]^+$) (Atkinson *et al.*, 1995d; Kwok *et al.*, 1995, 1996a,b).

For reactions of 2-methylpropene, *cis*-2-butene, 2-methyl-2-butene and 2,3-dimethyl-2-butene carried out in the presence of NO, OH radicals were generated by the photolysis of methyl nitrite. The initial concentrations of CH_3ONO, NO and alkene were $\sim 4.8 \times 10^{13}$ molecule cm^{-3} each, and irradiations were carried out for 1-2 min at 20% of the maximum light intensity. For reaction carried out in the absence of initially added NO, OH radicals were generated by the dark reaction of O_3 with the alkene (Atkinson *et al.*, 1992; Atkinson and Aschmann, 1993), with the initial concentration of the alkene being $\sim 4.8 \times 10^{13}$ molecule cm^{-3} and with 2 additions of 50 cm^3 volume of O_3 in O_2 diluent (each addition corresponding to an initial concentration of O_3 in the chamber of $\sim 6 \times 10^{12}$ molecule cm^{-3}) being made to the chamber. The alkenes studied in these experiments also included propene and *trans*-2-butene.

Chemicals. The chemicals used (acetaldehyde, acetone, *cis*-2-butene, *trans*-2-butene, 2,3-dimethyl-2-butene, 2-methyl-2-butene, 2-methylpropene and propene) were all of $\geq 99.0\%$ stated purity. Methyl nitrite was prepared as described by Taylor *et al.* (1980) while ethyl nitrite was distilled from a commercial 15% solution by weight of C_2H_5ONO in ethanol (Aldrich Chemical Company), and both nitrites were stored at 77 K under vacuum.

Results

Reactions in the Presence of NO

Teflon Chamber with GC-FID Analyses. GC-FID analyses showed the formation of acetone from the OH radical-initiated reactions of 2-methylpropene, 2-methyl-2-butene and 2,3-dimethyl-2-butene and of acetaldehyde from the reactions of *cis*-2-butene and 2-methyl-2-butene. Because the carbonyl products react with the OH radical (Atkinson, 1989, 1994), the secondary reactions of the OH radical with the products were taken into account to determine the product formation yields. These secondary reactions were taken into account as described previously by Atkinson *et al.* (1982), using the recommended OH radical reaction rate constants for the alkenes and carbonyl products (Atkinson, 1989, 1994, 1997b), with the corrections for secondary reactions being $< 15\%$ for acetaldehyde and $< 0.03\%$ for acetone. Figure 17 shows representative plots of the amounts of acetone formed against the amounts of 2-methyl-2-butene and 2,3-dimethyl-2-butene reacted, and the formation yields obtained from least-squares analyses of the experimental

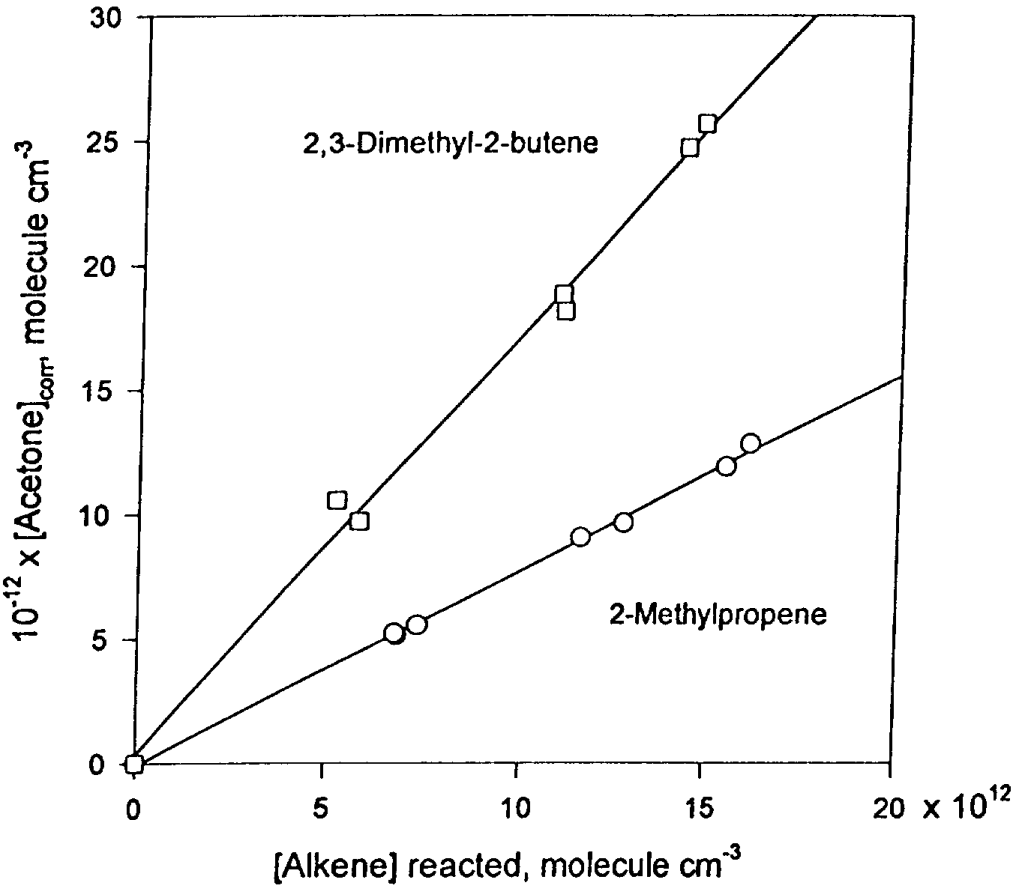

Figure 17. Plots of the amounts of acetone formed, corrected for reaction with the OH radical, against the amounts of 2-methyl-2-butene and 2,3-dimethyl-2-butene reacted with the OH radical in the presence of NO.

data are given in Table 4. Two independent sets of experiments were carried out to measure the acetone formation yield from the 2-methyl-2-butene reaction, and the agreement between the two measured acetone formation yields was excellent (Table 4).

Evacuable Chamber with Analyses by FT-IR Spectroscopy. Products from the gas-phase reactions of the OH radical with 2-methylpropene, *cis*-2-butene, 2-methyl-2-butene and 2,3-dimethyl-2-butene in the presence of NO have been identified and quantified by *in situ* FT-IR absorption spectroscopy. Figures 18-21 show FT-IR spectra of reactants and products from the CH_3ONO - NO - alkene - air irradiations. The products observed and their measured formation yields from these FT-IR absorption spectroscopy analyses are given in Table 4, where the measured concentrations of HCHO, CH_3CHO and $CH_3C(O)CH_3$ were again corrected for secondary reactions (see above). The corrections for secondary reactions were $<5\%$ for HCHO and CH_3CHO, and were negligible for acetone. Plots of the amounts of products formed, corrected for secondary reactions, against the amounts of alkene reacted are shown in Figures 22-25. We have previously shown that any contribution to HCHO formation from the secondary reactions of CH_3CHO generated from the photolysis of ethyl nitrite is minor ($<4\%$ formation yield) in irradiated C_2H_5ONO - NO - 1-alkene - air mixtures (Atkinson *et al.*, 1995b), and the formation of HCHO from ethyl nitrite chemistry in the present experiments would be even less because of the higher reactivity of the alkenes studied here (Atkinson, 1994, 1997b).

The residual spectra after subtraction of known components (Figures 18-21) showed weak but distinct set of absorption bands near 855, 1300, and 1650 cm^{-1}, which are characteristic of the $-ONO_2$ groups. These bands were assigned to hydroxynitrates, although the low signal-to-noise ratio near the 3600 cm^{-1} region did not allow the presence of O-H stretch absorption bands to be observed. These hydroxynitrates are expected to be formed during the reactions of the β-hydroxyalkyl peroxy radicals with NO (Atkinson, 1994, 1997b). The approximate yields of the hydroxynitrates (Table 4) were calculated using an average absorption coefficient for the $-ONO_2$ absorption band at $\sim$1300 cm^{-1} previously derived for analogous compounds (Tuazon and Atkinson, 1990). In the case of the 2-methyl-2-butene reaction, the formation of a minor carbonyl product is also clearly indicated by the occurrence of a band at 1736 cm^{-1} (Figure 20D).

Table 4. Products and their formation yields observed from the reactions of the OH radical with alkenes in the presence of NO at 296 ± 2 K and 740 Torr total pressure of air

Alkene	Product	Formation yield	
		GC-FID[a]	FT-IR[b]
2-Methylpropene	acetone	0.783 ± 0.062	0.892 ± 0.069
	formaldehyde		0.903 ± 0.101
	hydroxynitrate		~0.09
cis-2-Butene	acetaldehyde	1.85 ± 0.25	1.57 ± 0.13
	hydroxynitrate		~0.06
2-Methyl-2-butene	acetaldehyde	0.975 ± 0.100	0.824 ± 0.090
	acetone	0.917 ± 0.092[c]	0.802 ± 0.060
		0.878 ± 0.065[c]	
		0.896 ± 0.079[d]	
	hydroxynitrate		~0.13

Table 4. Products and their formation yields observed from the reactions of the OH radical with alkenes in the presence of NO at 296 ± 2 K and 740 Torr total pressure of air (continued)

Alkene	Product	Formation yield	
		GC-FID[a]	FT-IR[b]
2,3-Dimethyl-2-butene	acetone	1.70 ± 0.17	1.61 ± 0.18
	hydroxynitrate		~0.07

[a]Indicated errors are two least-squares standard deviations combined with estimated overall uncertainties in the GC-FID response factors for the alkene and carbonyl products of ±5% each.
[b]Indicated errors for the FT-IR data are two least-squares standard deviations combined with the errors arising from the measurement uncertainties of ±4% for the alkenes and products.
[c]Independent sets of experiments, each with measured GC-FID calibration factors.
[d]For combined data sets.

Teflon Chamber with Analyses by API-MS. Experiments were carried out using direct air sampling atmospheric pressure ionization tandem mass spectrometry (API-MS) for analysis of the products formed from the reactions of the OH radical with 2-methylpropene, *cis*-2-butene, 2-methyl-2-butene and 2,3-dimethyl-2-butene in the presence of NO, with OH radicals being generated by the photolysis of methyl nitrite.

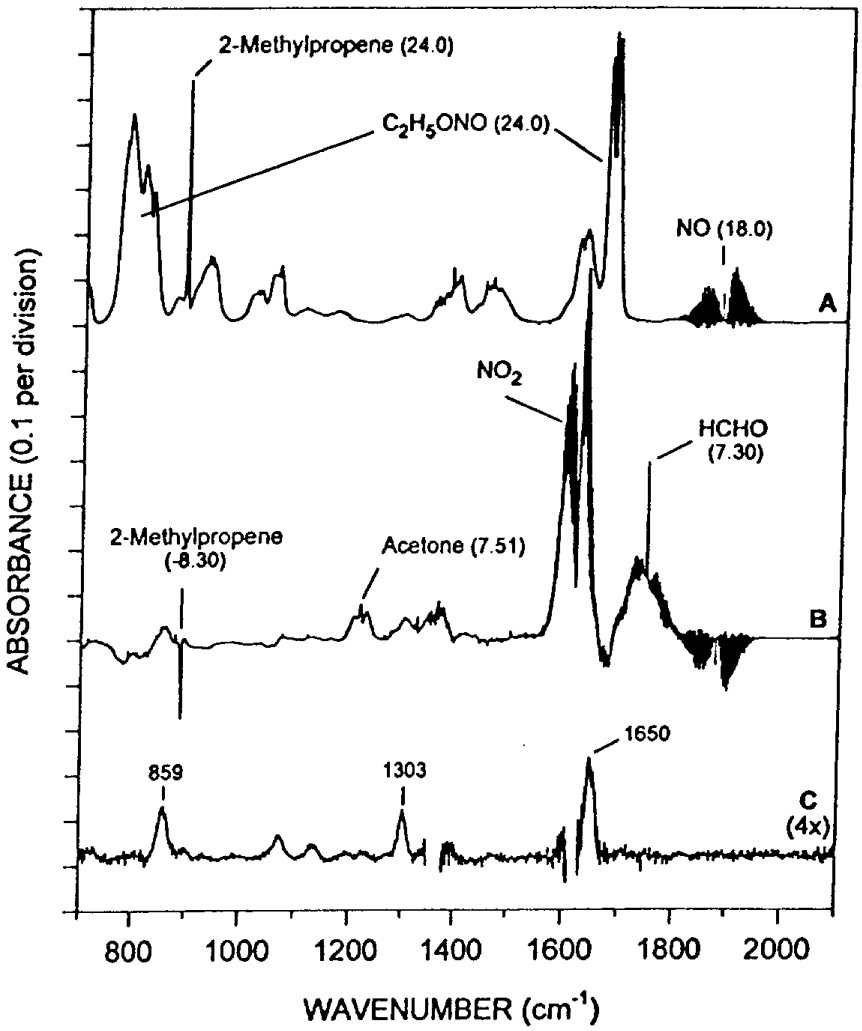

Figure 18. Infrared spectrum from a 2-methylpropene - CH_3CH_2ONO - NO irradiation experiment. (A) Initial reactant mixture. (B) Difference spectrum: spectrum of mixture after 3.25 min of photolysis minus that of reaction mixture prior to irradiation. (C) Residual spectrum. [Gaps in the ~1625 cm^{-1} and ~1350 cm^{-1} regions are due to distortions by the strong absorptions, respectively, of the NO_2 formed and the NO_3^- accumulated on the KBr window.] Values in parentheses are concentrations in units of 10^{13} molecule cm^{-3}.

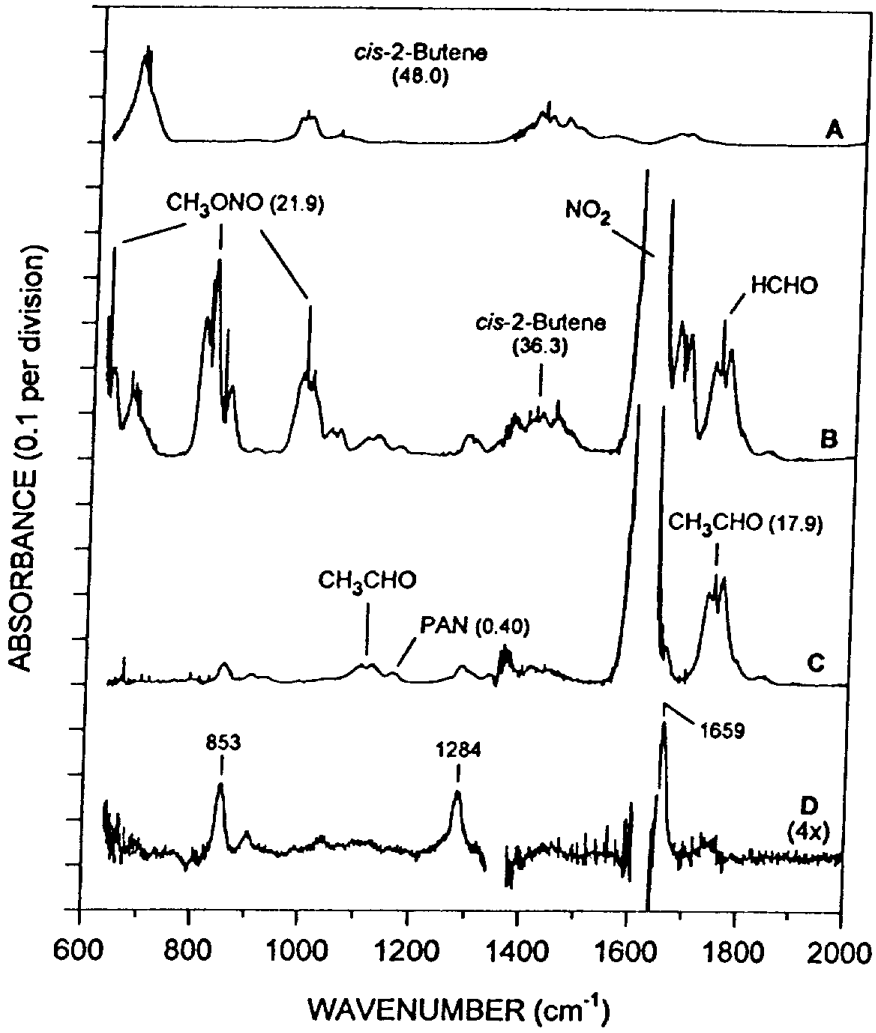

Figure 19. Infrared spectra from a *cis*-2-butene - CH_3ONO - NO irradiation experiment. (A) Initial alkene. (B) Mixture after 3.5 min of irradiation. (C) Product spectrum from (B). (D) Residual spectrum. [Gaps in the ~ 1625 cm^{-1} and ~ 1350 cm^{-1} regions are due to distortions by the strong absorptions, respectively, of the NO_2 formed and the NO_3^- accumulated on the KBr window.] Values in parentheses are concentrations in units of 10^{13} molecule cm^{-3}.

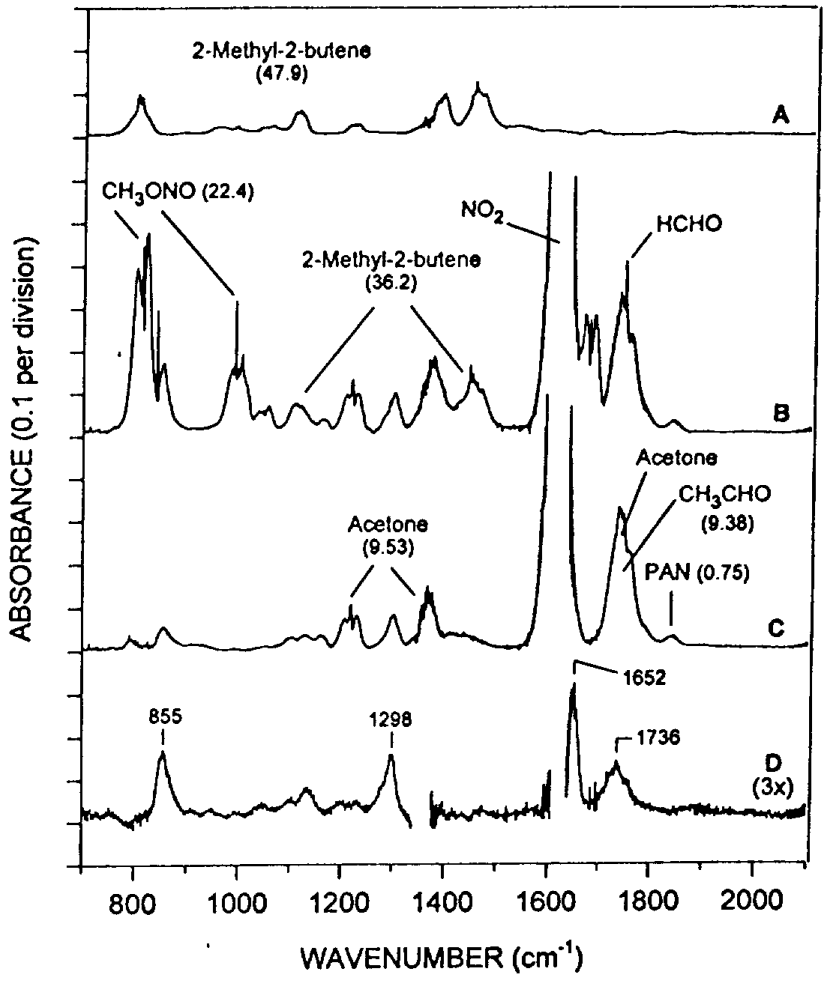

Figure 20. Infrared spectra from a 2-methyl-2-butene - CH_3ONO - NO irradiation experiment. (A) Initial alkene. (B) Mixture after 3.0 min of irradiation. (C) Product spectrum from (B). (D) Residual spectrum. [Gaps in the ~1625 cm^{-1} and ~1350 cm^{-1} regions are due to distortions by the strong absorptions, respectively, of the NO_2 formed and the NO_3^- accumulated on the KBr window.] Values in parentheses are concentrations in units of 10^{13} molecule cm^{-3}.

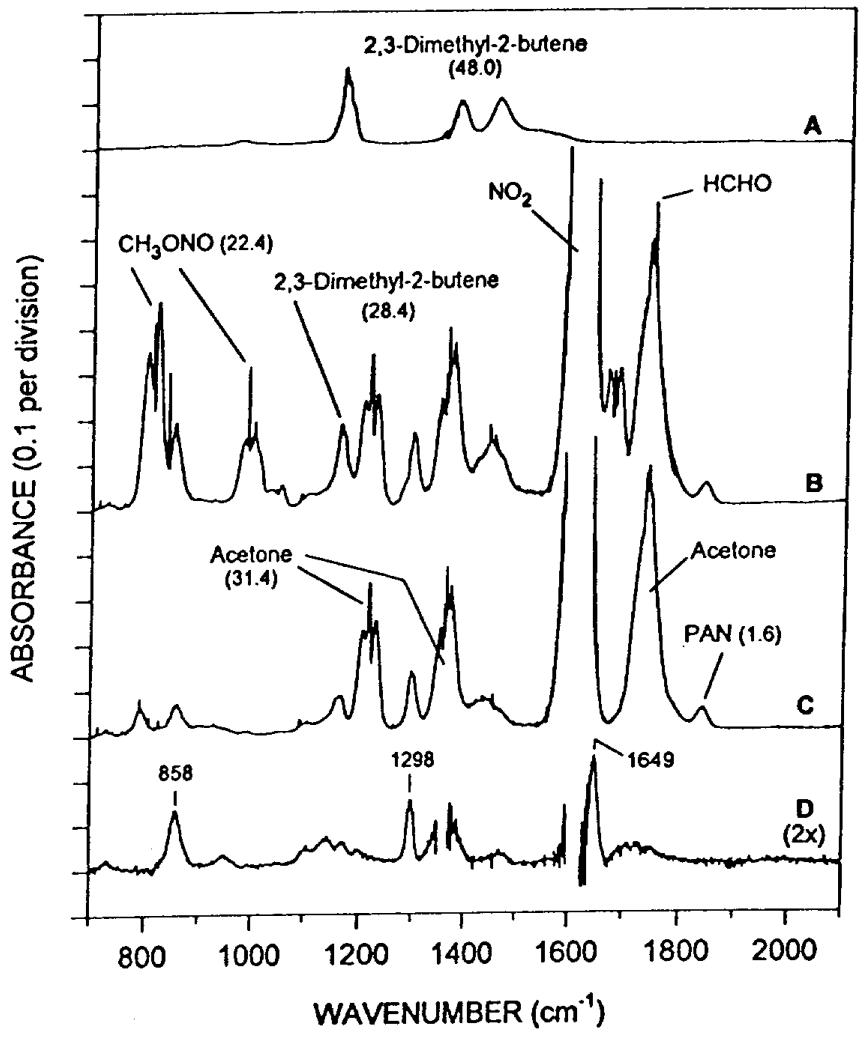

Figure 21. Infrared spectra from a 2,3-dimethyl-2-butene - CH_3ONO - NO irradiation experiment. (A) Initial alkene. (B) Mixture after 2.7 min of irradiation. (C) Product spectrum from (B). (D) Residual spectrum. [Gaps in the ~1625 cm^{-1} and ~1350 cm^{-1} regions are due to distortions by the strong absorptions, respectively, of the NO_2 formed and the NO_3^- accumulated on the KBr window.] Values in parentheses are concentrations in units of 10^{13} molecule cm^{-3}.

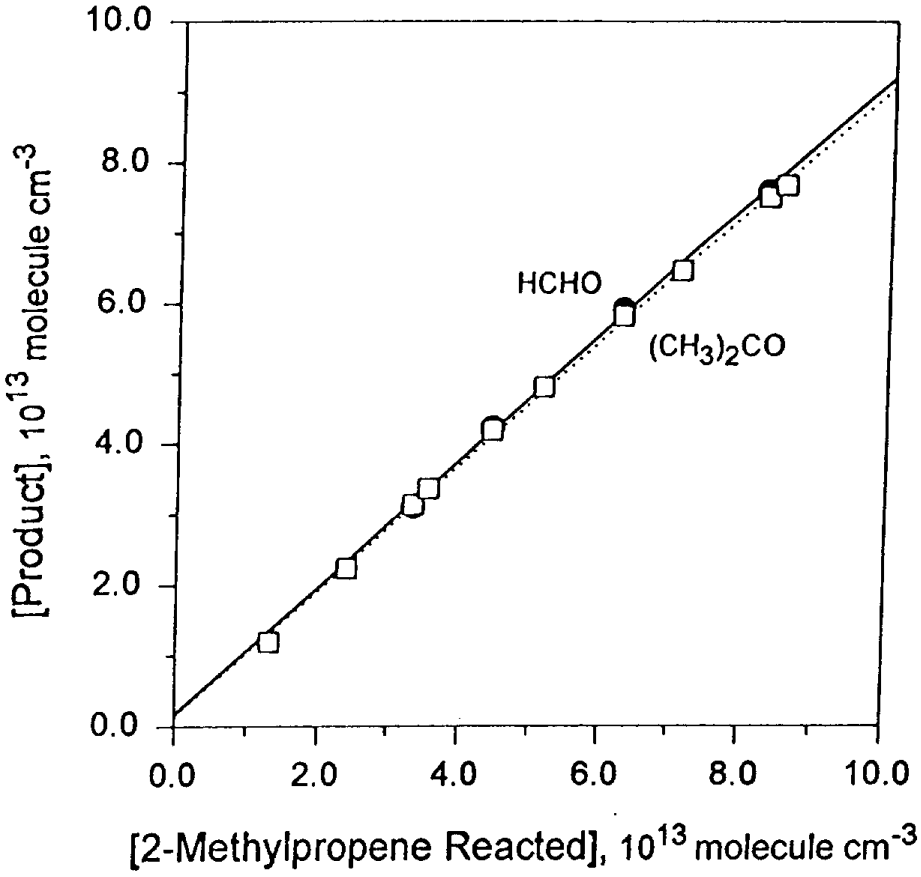

Figure 22. Plots of the amounts of HCHO and acetone formed, corrected for reaction with the OH radical, against the amounts of 2-methylpropene reacted with the OH radical in irradiated CH_3ONO (or C_2H_5ONO) - NO - 2-methylpropene - air mixtures. The HCHO data are from an experiment using ethyl nitrite as the OH radical precursor.

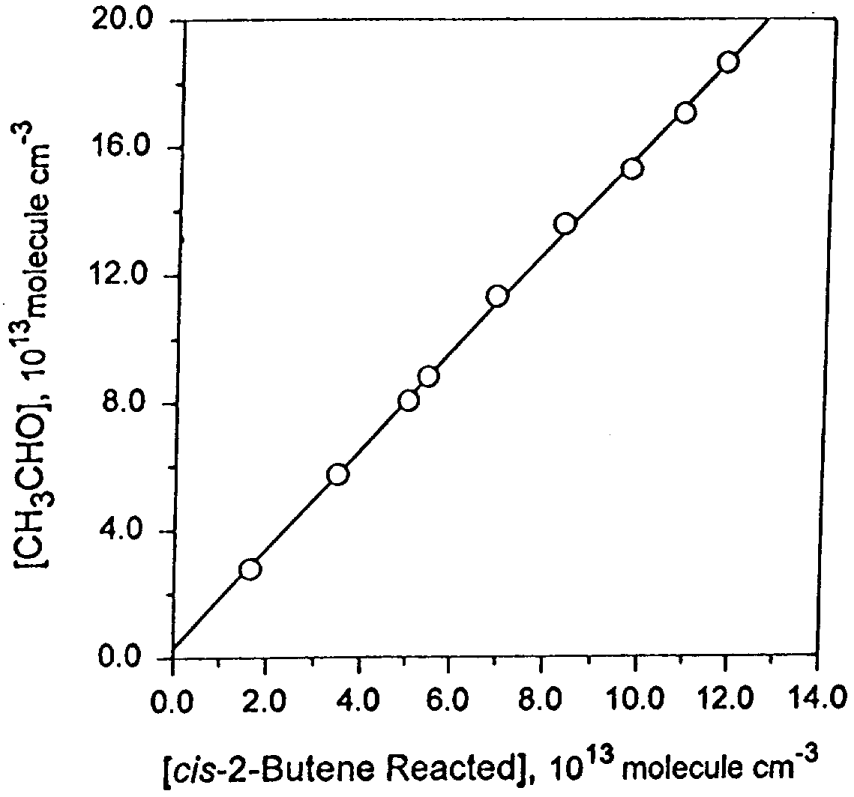

Figure 23. Plots of the amounts of CH_3CHO formed, corrected for reaction with the OH radical, against the amounts of *cis*-2-butene reacted with the OH radical in irradiated CH_3ONO - NO - *cis*-2-butene - air mixtures.

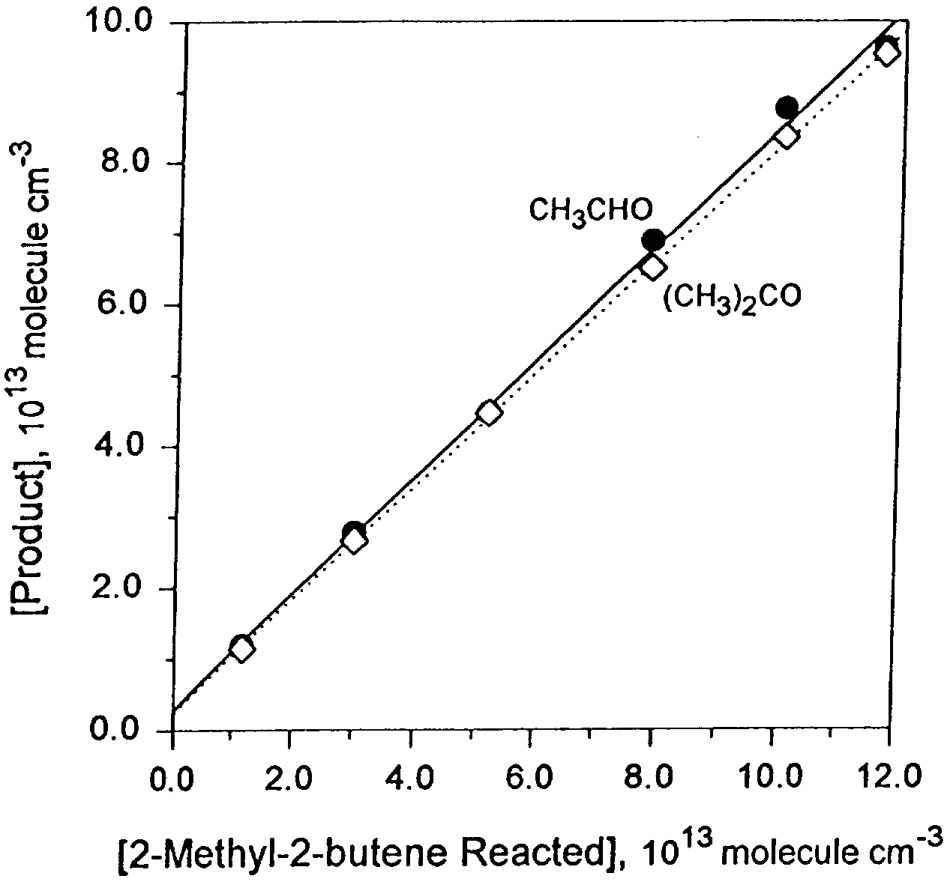

Figure 24. Plots of the amounts of CH_3CHO and $CH_3C(O)CH_3$ formed, corrected for reaction with the OH radical, against the amounts of 2-methyl-2-butene reacted with the OH radical in irradiated CH_3ONO - NO - 2-methyl-2-butene - air mixtures.

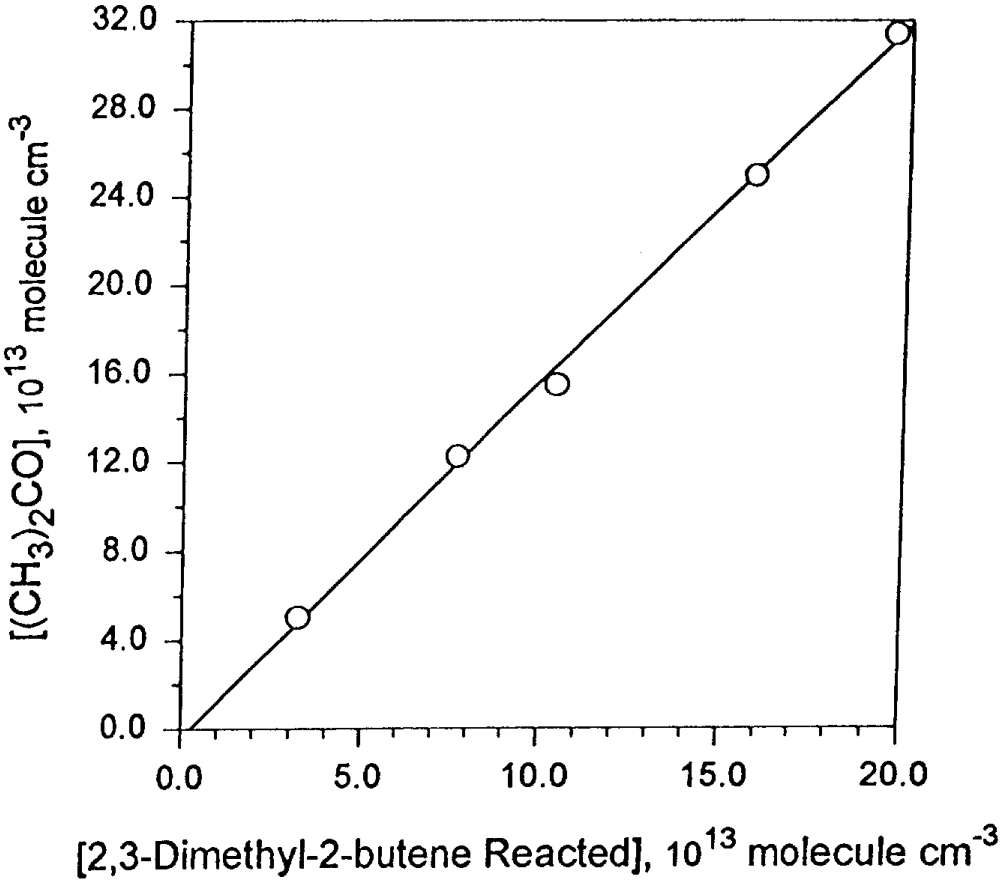

Figure 25. Plots of the amounts of $CH_3C(O)CH_3$ formed, corrected for reaction with the OH radical, against the amounts of 2,3-dimethyl-2-butene reacted with the OH radical in irradiated CH_3ONO - NO - 2,3-dimethyl-2-butene - air mixtures.

API-MS analyses of irradiated CH_3ONO - NO - 2-methylpropene - air mixtures showed the presence of two strong product ion peaks at 59 and 117 u, with much weaker ion peaks at 77, 135 and 193 u. The 59 u ion peak is attributed to $[M+H]^+$ of acetone, and this assignment was consistent with the API-MS/MS analyses. API-MS/MS daughter ion and parent ion spectra showed that the 117 u ion peak was the $[M_2+H]^+$ dimer peak of acetone, and showed that the remaining peaks were water cluster peaks of acetone (at 77 u), of the acetone dimer ion (at 135 u) and of the acetone trimer (at 193 u), with an API-MS/MS daughter ion spectrum of the 193 u ion peak showing a water loss fragment at 175 u (with the 175 u peak being $[(acetone)_3+H]^+$). No evidence was observed for the formation of a hydroxynitrate (although these are generally seldom observed with positive ion API-MS under our experimental conditions) nor of the hydroxycarbonyl $(CH_3)_2C(OH)CHO$ formed from reaction of the intermediate β-hydroxyalkoxy radical, $(CH_3)_2C(OH)CH_2O$, with O_2.

API-MS analyses of irradiated CH_3ONO - NO - *cis*-2-butene - air mixtures showed the presence of ion peaks not present in the pre-reaction spectra at 45 (attributed to $[M+H]^+$ of acetaldehyde), 63, 81, 87, 89, 136, 154 and 180 u. API-MS/MS daughter ion spectra of the 136 u ion peak showed strong fragment ions at 46 and 73 u, with the 46 u fragment being attributed to $[NO_2]^+$ and the 73 u ion peak being a loss of HNO_3. API-MS/MS parent ion spectra of the 45 u and 136 u ion peaks both showed the presence of a 180 u ion peak, attributed to an $[acetaldehyde+135+H]^+$ dimer ion, and with the parent ion spectrum of the 136 u ion peak showing ion peaks at 154 u ($+H_2O$), 172 ($+2H_2O$) and 198 u ($[180+H_2O]^+$) in addition to the 180 u ion peak. An API-MS/MS daughter ion spectrum of the 180 u ion peak showed the presence of a strong 136 u fragment and its fragments at 46 and 73 u, while a daughter ion spectrum of the 198 u ion peak showed fragments at 180 u and the same ions as observed from the 180 u ion, suggesting that the 198 u ion peak was a water cluster of the 180 u ion. The 136 u ion peak is therefore attributed to the $[M+H]^+$ ion of the β-hydroxynitrate $CH_3CH(OH)CH(ONO_2)CH_3$. The 89 u ion peak was shown to be the dimer ion of acetaldehyde and the 63 and 81 u ion peaks to be water cluster ions of acetaldehyde $[acetaldehyde+H_2O+H]^+$ and $[acetaldehyde+2H_2O+H]^+$. Although the 89 u ion peak could have been the $[M+H]^+$ ion of $CH_3CH(OH)C(O)CH_3$ (formed from reaction of the intermediate β-hydroxyalkoxy radical

$CH_3CH(OH)CH(O)CH_3$ with O_2), the lack of a strong $[M+H-H_2O]^+$ ion peak at 71 u indicates that this product was of minor or negligible importance.

API-MS analyses of irradiated CH_3ONO - NO - 2-methyl-2-butene - air mixtures showed the presence of significant ion peaks at 59, 77, 87 and 117 u, together with weaker ion peaks at 85, 103 and 145 u. The 59 u product ion peak is attributed to the $[M+H]^+$ ion of acetone (consistent with the API-MS/MS spectrum of the 59 u ion). API-MS/MS daughter ion spectra of the 117 u ion peak and API-MS/MS parent ion spectra of the 59 u ion peak showed that the 117 u ion peak was the dimer $[M_2+H]^+$ of acetone and indicated that the 77 u ion peak was a water cluster peak of the $[acetone+H]^+$ ion, that the 103 u ion peak was a heterodimer of acetone and acetaldehyde $[acetone+acetaldehyde+H]^+$ and that the 85 u ion peak was $[acetone+acetaldehyde+H-H_2O]^+$. In particular, the API-MS/MS daughter ion spectrum of the 103 u ion peak showed a strong 59 u fragment (in addition to weaker fragment ions at 85, 47, 45, 43 and 19 u), whereas an API-MS/MS spectrum of an authentic sample of 3-hydroxy-3-methyl-2-butanone (the hydroxycarbonyl which would be formed from the reaction of the intermediate β-hydroxyalkoxy radical with O_2) showed strong fragment ions at 85 and 57 u together with weaker fragment ions at 43, 41 and 29 u. These API-MS/MS spectra show that the 103 u ion peak in the reacted mixture was not due to 3-hydroxy-3-methyl-2-butanone and no evidence for the formation of this potential product was obtained [note also the API-MS/MS spectra of the 103 u ion peak observed in the O_3 reaction with 2-methyl-2-butene in the absence of an OH radical scavenger showed the presence of a strong 57 u fragment ion, consistent with the expected formation of 3-hydroxy-3-methyl-2-butanone from the OH radical-initiated reaction of 2-methyl-2-butene in the absence of NO; see below]. The API-MS/MS daughter ion spectrum of the 87 u product ion peak showed strong fragment ions at 69 ($-H_2O$), 45, 43 and 41 u, while the parent ion spectrum showed a dimer ion at 173 u (corresponding to $[M_2+H]^+$ for M = 86 u) and a heterodimer $[acetone+M+H]^+$ at 145 u, together with peaks at 208, 236 and 299 u. The peak at 299 u could be the homodimer of the β-hydroxynitrate(s) $CH_3CH(OH)C(ONO_2)(CH_3)_2$ and/or $(CH_3)_2C(OH)CH(ONO_2)CH_3$, with the 208 u ion peak being a heterodimer [β-hydroxynitrate+acetone+H]$^+$ and the 236 u ion peak being a fragment ion ($-HNO_3$) of the 299 u homodimer peak. We interpret these API-MS data concerning the products of the OH radical-initiated reaction of 2-methyl-2-butene as showing the formation of

acetaldehyde, acetone and a hydroxynitrate, presumably the β-hydroxynitrate $CH_3CH(OH)C(ONO_2)(CH_3)_2$ and/or $(CH_3)_2C(OH)CH(ONO_2)CH_3$. Moreover, decomposition of the β-hydroxynitrate(s) in the chamber or in the ionization region of the API-MS instrument led, by loss of nitric acid, to a product with a molecular weight of 86, probably $CH_3CH(OH)C(CH_3)=CH_2$ or $(CH_3)_2C(OH)CH=CH_2$.

API-MS and API-MS/MS analyses of irradiated CH_3ONO - NO - 2,3-dimethyl-2-butene - air mixtures showed the presence of two strong ion peaks at 59 and 117 u, with weaker ion peaks at 83, 99, 101, 159, 201 and 217 u. The 59 u ion peak is attributed to the $[M+H]^+$ ion of acetone, consistent with API-MS/MS analyses, and API-MS/MS spectra parent ion spectra of the 59 u ion peak and daughter ion spectra of the 117 u ion peak showed that the 117 u ion peak was the $[M_2+H]^+$ dimer peak of acetone and that the 99 u ion peak was $[(acetone)_2+H-H_2O]^+$. API-MS/MS spectra showed that the 159, 201 and 217 u ion peaks were $[100+58+H]^+$, $[100+100+H]^+$ and $[100+117]^+$, respectively, indicating a product of molecular weight 100 u. API-MS/MS spectra of the 101 u ion peak showed a strong fragment at 83 u due to loss of H_2O, and we tentatively ascribe the 100 u product as $(CH_3)_2C(OH)C(CH_3)=CH_2$ arising from decomposition of the β-hydroxynitrate $(CH_3)_2C(OH)C(ONO_2)(CH_3)_2$, either in the chamber or in the ionization region of the API-MS instrument. This behavior is analogous to the 2-methyl-2-butene reaction discussed above. The 99 u ion peak observed in the API-MS analyses appears to be due to loss of H_2 from the 101 u ion peak and a loss of H_2O from the $[(acetone)_2+H]^+$ dimer ion peak.

Reactions in the Absence of NO

Experiments were carried out using API-MS for analysis of the products formed from the reactions of the OH radical with 2-methylpropene, *cis*-2-butene, 2-methyl-2-butene and 2,3-dimethyl-2-butene in the absence of NO, with OH radicals being generated from the dark reaction of O_3 with the alkene being studied.

API-MS and API-MS/MS spectra of the products of reacted O_3 - propene - air mixtures showed the presence of significant ion peaks at 45, 75, 77, 93, 111, 139, 169, 185, 231 and 277 u. The 45 u ion peak is attributed to the $[M+H]^+$ ion of acetaldehyde. API-MS/MS daughter ion and parent ion spectra of ion peaks at 75, 77 and 93 u indicated that the reaction products

were mainly those of molecular weight 44, 74, 76 and 93 u. Thus, the API-MS/MS parent ion spectrum of the 75 u ion peak ($[74+H]^+$) showed peaks at 93 u ($[74+H_2O+H]^+$), 119 u ($[74+44+H]^+$), 149 u ($[74+74+H]^+$), 151 u ($[74+76+H]^+$), and 167 u ($[74+92+H]^+$); the API-MS/MS parent ion spectrum of the 77 u ion peak ($[76+H]^+$) showed peaks at 95 u ($[76+H_2O+H]^+$), 151 u ($[76+74+H]^+$), 153 u ($[76+76+H]^+$), and 169 u ($[76+92+H]^+$); and the API-MS/MS parent ion spectrum of the 93 u ion peak ($[92+H]^+$) showed peaks at 111 u ($[92+H_2O+H]^+$), 169 u ($[92+76+H]^+$) and 185 u ($[92+92+H]^+$).

API-MS and API-MS/MS spectra of the products of reacted O_3 - 2-methylpropene - air mixtures showed the presence of significant ion peaks at 59, 75, 77, 89, 91, 105, 107, 117, 149, 165, 181, 197 and 213 u. The 59 u ion peak is attributed to the $[M+H]^+$ ion of acetone, and API-MS/MS daughter parent spectrum of the 59 u ion peak indicated that the 117 u ion peak was a proponated acetone dimer, $[(acetone)_2+H]^+$, ion. API-MS/MS daughter ion and parent ion spectra of ion peaks at 89, 91 and 107 u indicated that the reaction products were mainly those of molecular weight 58, 88, 90 and 106 u. Thus, the API-MS/MS parent ion spectrum of the 107 u ion peak ($[106+H]^+$) showed peaks at 125 u ($[106+H_2O+H]^+$), 165 u ($[106+58+H]^+$), 197 u ($[106+90+H]^+$) and 213 u ($[106+106+H]^+$), and the API-MS/MS parent ion spectrum of the 91 u ion peak ($[90+H]^+$) showed peaks at 163 u ($[90+90+H-H_2O]^+$), 181 u ($[90+90+H]^+$) and 197 u ($[90+106+H]^+$). The API-MS/MS parent ion spectrum of the 89 u ion peak ($[88+H]^+$) showed peaks at 91 u ($90+H-H_2]^+$), 107 u ($[88+H_2O+H]^+$ or $[106+H-H_2O]^+$), 179 u ($[88+90+H]^+$) and 197 u ($[88+90+H+ H_2O]^+$); however, the observation of ion peaks in the parent ion spectrum at 91, 107 and 213 u suggest that the 89 u ion peak was also a fragment of the 107 u and 91 u ion peaks.

API-MS and API-MS/MS spectra of the products of reacted O_3 - *cis*-2-butene - air mixtures showed the presence of significant ion peaks at 45, 89, 107, 117, 151, 179, 195, 197 and 213 u. The 45 u ion peak is attributed to the $[M+H]^+$ ion of acetaldehyde, and API-MS/MS daughter ion and parent ion spectra of ion peaks at 89, 91 and 107 u and API-MS/MS daughter ion spectra of the 195 u ion peak indicated that the reaction products were mainly those of molecular weight 44, 88, 90 and 106 u. Thus, the API-MS/MS parent ion spectrum of the 107 u ion peak ($[106+H]^+$) showed peaks at 151 u ($[106+44+H]^+$), 195 u ($[106+88+H]^+$), 197 u ($[106+90+H]^+$) and 213 u ($[106+106+H]^+$), the API-MS/MS parent ion spectrum of

the 91 u ion peak ($[90+H]^+$) showed peaks at 109 u ($[90+H_2O+H]^+$), 179 (weak) ($[90+88+H]^+$), 181 u ($[90+90+H]^+$) and 197 u ($[90+106+H]^+$), and the API-MS/MS parent ion spectrum of the 89 u ion peak ($[88+H]^+$) showed peaks at 107 u ($[88+H_2O+H]^+$), 133 u ($[88+44+H]^+$), 177 u ($[88+88+H]^+$), 179 ($[88+90+H]^+$) and 195 u ($[88+106+H]^+$). Very similar data were obtained for the analogous *trans*-2-butene reaction.

API-MS and API-MS/MS spectra of the products of reacted O_3 - 2-methyl-2-butene - air mixtures showed the presence of ion peaks at 45, 59, 85, 87, 103, 105, 117, 147, 177, 179, 225 and 241 u. The 45 u and 59 u ion peaks are attributed to the $[M+H]^+$ ions of acetaldehyde and acetone, respectively, with the 89 u and 117 u ion peaks being attributed to the protonated homodimers of acetaldehyde and acetone, respectively. In addition to the formation of acetaldehyde and acetone as products, API-MS/MS daughter ion and parent ion spectra of ion peaks at 103 u, 105 u and 121 u indicated the presence of products of molecular weight 102 (3-hydroxy-3-methyl-2-butanone), 104 (2-methyl-2,3-butanediol) and 120 u [$(CH_3)_2C(OH)CH(OOH)CH_3$ and/or $(CH_3)_2C(OOH)CH(OH)CH_3$]. For example, the API-MS/MS parent ion spectrum of the 103 u ion peak showed ions at 121 u ($102+H_2O+H]^+$, 147 u ($[102+44+H]^+$) and 161 u ($[102+58+H]^+$); the API-MS/MS parent ion spectrum of the 105 u ion peak showed ions at 163 u ($[104+58+H]^+$), 209 u ($[104+104+H]^+$) and 225 u ($[104+120+H]^+$; and the API-MS/MS parent ion spectrum of the 121 u ion peak showed ions at 179 u ($[120+58+H]^+$), 225 u ($[120+104+H]^+$), 241 u ($[120+120+H]^+$, 267 u ($[120+102+44+H]^+$) and 281 u ($[120+102+58+H]^+$).

API-MS and API-MS/MS spectra of the products of reacted O_3 - 2,3-dimethyl-2-butene - air mixtures showed the presence of ion peaks at 59, 99, 101, 117, 147, 159, 193, 210, 235, 253, and 269 u. The 59 u ion peak was attributed to the $[M+H]^+$ ion of acetone, with the 117 u ion peak being attributed to the protonated homodimer of acetone. In addition to the formation of acetone as a product, API-MS/MS daughter ion and parent ion spectra of ion peaks at 119 u and 135 u were carried out together with API-MS/MS daughter ion or parent ion spectra of the 101, 117, 201 and 253 u ions. These API-MS/MS spectra indicated the presence of products of molecular weight 118 and 134 u (in addition to acetone). API-MS/MS daughter ion spectra showed that the 101 and 117 u ion peaks were strong fragment ions ($-H_2O$) of the 119 and 135 u ion peaks, respectively. The API-MS/MS parent ion spectrum of the 119 u ion peak showed

ions at 237 u ($118+118+H]^+$, 253 u ($[118+134+H]^+$) and 271 u ($[118+134+H_2O+H]^+$), and the API-MS/MS parent ion spectrum of the 135 u ion peak showed ions at 253 u ($[134+118+H]^+$) and 269 u ($[134+134+H]^+$).

Discussion

Reactions in the Presence of NO

The GC-FID and FT-IR spectroscopic product formation yield data given in Table 4 and the qualitative API-MS data all show that the dominant products of the gas-phase reactions of the OH radical with 2-methylpropene, *cis*-2-butene, 2-methyl-2-butene and 2,3-dimethyl-2-butene in the presence of NO are the two carbonyls arising from decomposition of the intermediate β-hydroxyalkoxy radical(s) and β-hydroxynitrates formed in the reaction of the β-hydroxyalkyl peroxy radicals with NO. Formation of organic nitrates from the reactions of the OH radical with *cis*-2-butene and 2,3-dimethyl-2-butene in the presence of NO has been reported previously by Muthuramu *et al.* (1993) and Niki *et al.* (1987), respectively. Muthuramu *et al.* (1993) reported the formation of the β-hydroxynitrate $CH_3CH(OH)CH(ONO_2)CH_3$ from the reaction of the $CH_3CH(OH)CH(O\dot{O})CH_3$ radical with NO in a 3.7 $\pm$ 0.9% yield, while Niki *et al.* (1987) reported a yield of an organic nitrate, presumed to be $(CH_3)_2C(OH)C(ONO_2)(CH_3)_2$, of 15% of the overall reaction products from the OH radical-initiated reaction of 2,3-dimethyl-2-butene in the presence of NO. Our present semi-quantitative FT-IR data for the formation of hydroxynitrates from the *cis*-2-butene and 2,3-dimethyl-2-butene reactions are reasonably consistent with these data of Muthuramu *et al.* (1993) and Niki *et al.* (1987). Only for the 2,3-dimethyl-2-butene reaction has carbonyl data previously been obtained, and Niki *et al.* (1987) reported an acetone yield of 1.7 $\pm$ 0.1 for this reaction, in excellent agreement with both our GC-FID and FT-IR data (Table 4).

The major discrepancy between the GC-FID analyses and the FT-IR absorption spectroscopic analyses arises for the 2-methylpropene reaction, where the GC-FID quantification of acetone is 12% lower than the FT-IR data. For all four reactions, hydroxynitrate formation from the β-hydroxyalkyl peroxy radical + NO reaction accounts for ~10% of the overall products observed, with decomposition of the β-hydroxyalkoxy radical dominating over the alternative isomerization and O_2 reaction and leading to the formation of the carbonyls expected

from >C=C< bond cleavage in ~90% yield each. These experimental data are consistent with the estimated rates of decomposition and reaction with O_2 of the intermediate β-hydroxyalkoxy radicals (Atkinson, 1997a,b) [isomerization via a 6-member transition state is not possible for any of the intermediate β-hydroxyalkoxy radicals formed in these reactions]. In particular, the API-MS analyses showed no evidence for the formation of the hydroxycarbonyls which would be formed from reaction of the intermediate β-hydroxyalkoxy radicals with O_2. It could not be established in the present work whether the product of the 2-methyl-2-butene reaction with the 1736 cm^{-1} absorption band (Figure 20D) was due to the presumably stable hydroxyketone $(CH_3)_2C(OH)C(O)CH_3$, or not.

Reactions in the Absence of NO

The products suggested by the API-MS and API-MS/MS analyses are listed in Table 5. These are those expected from the general reaction sequence (taking the 2-methyl-2-butene reaction as an example):

$$(CH_3)_2C(OH)CH(O\dot{O})CH_3 + RO_2 \rightarrow \begin{cases} (CH_3)_2C(OH)CH(\dot{O})CH_3 + R\dot{O} + O_2 & (31a) \\ (CH_3)_2C(OH)C(O)CH_3 + (CH_3)_2C(OH)C(OH)CH_3 + R\dot{O}_2 \text{ products} + O_2 & (31b) \end{cases}$$

$$(CH_3)_2C(OH)CH(O\dot{O})CH_3 + HO_2 \rightarrow (CH_3)_2C(OH)CH(OOH)CH_3 + O_2 \quad (32)$$

followed by the decomposition reaction of the β-hydroxyalkoxy radicals to lead to the same carbonyls as observed from the reactions in the presence of NO (see above) [acetaldehyde plus acetone for the 2-methyl-2-butene reaction].

Table 5. Products formed from the gas-phase reactions of the OH radical with methyl-substituted ethenes in the absence of NO, as observed by API-MS and API-MS/MS analyses

Alkene	MW product	Tentative identification
Propene	44	CH_3CHO
	74	$CH_3C(O)CH_2OH$, $CH_3CH(OH)CHO$
	76	$CH_3CH(OH)CH_2OH$
	92	$CH_3CH(OOH)CH_2OH$, $CH_3CH(OH)CH_2OOH$
2-Methylpropene	58	$CH_3C(O)CH_3$
	88	$(CH_3)_2C(OH)CHO$
	90	$(CH_3)_2C(OH)CH_2OH$
	106	$(CH_3)_2C(OOH)CH_2OH$, $(CH_3)_2C(OH)CH_2OOH$
cis-, *trans*-2-Butene	44	CH_3CHO
	88	$CH_3CH(OH)C(O)CH_3$
	90	$CH_3CH(OH)CH(OH)CH_3$
	106	$CH_3CH(OOH)CH(OH)CH_3$

Table 5. Products formed from the gas-phase reactions of the OH radical with methyl-substituted ethenes in the absence of NO, as observed by API-MS and API-MS/MS analyses (continued)

Alkene	MW product	Tentative identification
2-Methyl-2-butene	44	CH_3CHO
	58	$CH_3C(O)CH_3$
	102	$(CH_3)_2C(OH)C(O)CH_3$
	104	$(CH_3)_2C(OH)CH(OH)CH_3$
	120	$(CH_3)_2C(OOH)CH(OH)CH_3$, $(CH_3)_2C(OH)CH(OOH)CH_3$
2,3-Dimethyl-2-butene	58	$CH_3C(O)CH_3$
	118	$(CH_3)_2C(OH)C(OH)(CH_3)_2$
	134	$(CH_3)_2C(OOH)C(OH)(CH_3)_2$

5. PRODUCTS OF THE GAS-PHASE OH AND NO_3 RADICAL-INITIATED REACTIONS OF NAPHTHALENE

Introduction

Naphthalene is the simplest polycyclic aromatic hydrocarbon (PAH), and the most abundant PAH in polluted urban areas (Arey *et al.*, 1987, 1989). Previous studies have shown that in the gas phase naphthalene reacts with OH radicals and NO_3 radicals by initial addition of these radicals to the aromatic rings (Atkinson, 1989, 1991; Atkinson *et al.*, 1990, 1994c; Atkinson and Arey, 1994). No gas-phase reaction of naphthalene with O_3 has been observed (Atkinson and Carter, 1984; Atkinson, 1994). The gas-phase OH radical and NO_3 radical reactions have been shown to proceed by initial addition to the aromatic rings to form hydroxycyclohexadienyl- and nitrooxycyclohexadienyl-type radicals, which can back-decompose to the reactants or react with NO_2 or O_2 to yield products (Lorenz and Zellner, 1983; Atkinson, 1989, 1991; Atkinson *et al.*, 1990, 1994c; Koch *et al.*, 1994), where X = OH or ONO_2 (Reaction Scheme 5).

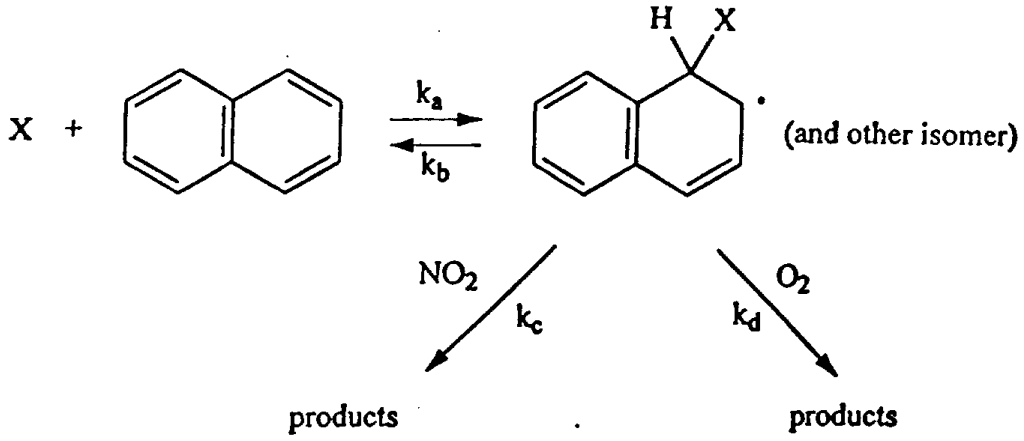

Reaction Scheme 5

In the troposphere the OH-naphthalene adduct is sufficiently thermally stable that its removal reactions are with NO_2 and/or O_2 (Lorenz and Zellner, 1983; Atkinson, 1989; Koch *et al.*, 1994). However, at room temperature the NO_3-naphthalene adduct decomposes rapidly in competition with its reactions with NO_2 and O_2 (Atkinson *et al.*, 1990, 1994c; Atkinson, 1991), and we have recently shown that $k_d/k_c < 4 \times 10^{-7}$ at room temperature and atmospheric pressure (Atkinson *et al.*, 1994c). The loss processes of naphthalene in the troposphere are therefore with the OH radical and the NO_3 radical (Atkinson and Arey, 1994), with the naphthalene lifetimes due to these reactions being given by $(2.2 \times 10^{-11}\ [OH])^{-1}$ (Atkinson, 1989) and $(3.6 \times 10^{-28}[NO_3][NO_2])^{-1}$ for NO_2 concentrations $\geq 2 \times 10^{12}$ molecule cm^{-3} (Atkinson, 1991), respectively, with the OH radical reaction being expected to dominate under most conditions (Arey *et al.*, 1989; Atkinson and Arey, 1994).

Previous product studies of the gas-phase OH radical-initiated reaction of naphthalene (Pitts *et al.*, 1985; Atkinson *et al.*, 1987; Bunce and Zhu, 1994; Lane and Tang, 1994) have shown that the OH radical reaction in the presence of NO_x leads to the formation of nitronaphthalenes (Atkinson *et al.*, 1987), naphthols (Atkinson *et al.*, 1987) and a number of ring-opened products (Bunce and Zhu, 1994; Lane and Tang, 1994), with measured formation yields of the nitronaphthalenes and naphthols of $\sim 0.6\%$ and $\sim 10\%$, respectively (Atkinson *et al.*, 1987). The NO_3 radical-initiated reaction has been shown to form 1- and 2-nitronaphthalene in $\sim 16\%$ and $\sim 7\%$ yields, respectively (Pitts *et al.*, 1985; Atkinson *et al.*, 1987).

Clearly, a large fraction of the products from these atmospherically-important reactions of naphthalene have not been identified or quantified to date. In this work, we have used gas chromatographic (GC) techniques together with *in situ* direct air sampling, atmospheric pressure ionization tandem mass spectroscopy (API-MS) to investigate the products of the gas-phase reactions of OH radicals and NO_3 radicals with naphthalene in the presence of NO_x.

Experimental

Experiments were carried out in 6500-7900 liter all-Teflon chambers equipped with two parallel banks of blacklamps at 296 ± 2 K and 740 Torr total pressure of purified air at a relative humidity of $\sim 5\%$. Two series of experiments were carried out with analyses by GC with flame ionization (GC-FID), mass spectrometric (GC-MS) or Fourier transform infrared

(GC-FTIR) detection and by API-MS, respectively, and these two sets of experiments used different reactant concentrations. Naphthalene was introduced into both chambers by flushing a Pyrex tube packed with solid naphthalene with a stream of N_2 gas at a flow rate of ~2 liter min^{-1} for ~45 mins. The NO and initial NO_2 concentrations during these experiments were monitored using a Thermo Environmental Instruments, Inc., Model 42 chemiluminescence NO-NO_2-NO_x analyzer (7900 liter chamber with GC analyses) or a Columbia Scientific Industries CSI 1600 oxides of nitrogen analyzer (6500 liter chamber with API-MS analyses). For both series of experiments, OH radicals were generated by the photolysis of methyl nitrite (CH_3ONO) in air at wavelengths >300 nm (Atkinson *et al.*, 1981), and NO was added to the reactant mixtures to suppress the formation of O_3 and hence NO_3 radicals (Atkinson *et al.*, 1981). For both series of experiments, NO_3 radicals were generated from the thermal decomposition of N_2O_5 (Atkinson *et al.*, 1984),

$$N_2O_5 \rightarrow NO_3 + NO_2 \qquad (33)$$

and NO_2 was added to the reactant mixtures to ensure that the NO_3-naphthalene adduct reacted only with NO_2 [reaction (c)] and to minimize reactions of naphthalene with species other than NO_3 radicals (Atkinson *et al.*, 1987).

Reactions with Gas Chromatographic Analyses. Reactions were carried out in a 7900 liter all-Teflon chamber. For the OH radical-initiated reactions, the initial reactant concentrations (in molecule cm^{-3} units) were: CH_3ONO, (0.41-2.16) x 10^{14}; NO, ~2.4 x 10^{14}; naphthalene, (1.99-2.18) x 10^{13}; and 1,4-dichlorobenzene (as an internal standard; see below), (1.83-2.17) x 10^{13}. Irradiations were carried out at 20% of the maximum light intensity for 5-10 min for the experiments with initial CH_3ONO concentrations of (2.13-2.16) x 10^{14} molecule cm^{-3}, and 5-20 min for the experiment with the lower initial CH_3ONO concentration of 4.1 x 10^{13} molecule cm^{-3}. For the NO_3 radical-initiated reactions, the initial reactant concentrations (in molecule cm^{-3} units) were: NO_2, (4.06-4.25) x 10^{13}; naphthalene, (1.89-1.95) x 10^{13}; and 1,4-dichlorobenzene (an internal standard), (1.65-2.17) x 10^{13}. One addition of N_2O_5, corresponding

to an initial concentration in the chamber of (1.68-2.02) x 10^{13} molecule cm^{-3}, was made to the chamber during these experiments.

During both the OH radical- and NO_3 radical-initiated experiments, naphthalene and 1,4-dichlorobenzene were analyzed by collecting 100 cm^3 volume gas samples from the chamber onto Tenax-TA solid adsorbent, with subsequent thermal desorption at ~225 °C onto a 60 m DB-5MS megabore column in a Hewlett Packard (HP) 5890 GC, initially held at 0 °C and then temperature programmed to 160 °C at 20 °C min^{-1} and then to 250 °C at 10 °C min^{-1}. Larger volume (~ 15 liter) gas samples were collected onto Tenax-TA solid adsorbent at ~0.45 liter min^{-1} for the quantification of naphthalene, 1,4-dichlorobenzene and reaction products, with subsequent elution with 1 m*l* of diethyl ether. The eluate volume was reduced to ~500 μl, as measured with a 500 μl syringe, and a 2 μl aliquot was analyzed by GC-FID on a 60 m DB-5MS column (0.25 mm ID, 25 μm film thickness) in an HP 5890 GC, held at 40 °C and then temperature programmed to 120 °C at 20 °C min^{-1} and then to 280 °C at 6 °C min^{-1}. Replicate injections using the same temperature program and GC column type were carried out using an HP 5890 GC interfaced to an HP 5970 mass selective detector operated in the scanning mode to confirm the identities assigned to the product peaks. GC-FID response factors were measured using authentic standards when available, or were estimated using the calculated Effective Carbon Numbers (ECN) (Scanlon and Willis, 1985). Several tentative product identifications were made based on structural information from GC-MS analyses with both electron impact and chemical ionization and on GC-FTIR analyses.

Reactions with API-MS Analyses. Reactions of naphthalene and naphthalene-d_8 with OH radicals and NO_3 radicals in the presence of NO_x were carried out in a 6500 liter all-Teflon chamber interfaced to a PE SCIEX API III MS/MS direct air sampling, atmospheric pressure ionization tandem mass spectrometer (API-MS). For the OH radical-initiated reactions, the initial CH_3ONO, NO and naphthalene concentrations were equal at either ~1.2 x 10^{13} molecule cm^{-3} or ~1.2 x 10^{14} molecule cm^{-3}, and irradiations were carried out at 20% of the maximum light intensity for 2-6 min (lower concentration experiments) or at the maximum light intensity for 1.5-2.5 min (higher concentration experiments). For the NO_3 radical-initiated reactions, the initial naphthalene and NO_2 concentrations were equal at (1.2-12) x 10^{13} molecule cm^{-3}, and

typically one addition of N_2O_5 (corresponding to initial N_2O_5 concentrations in the chamber of (0.28-17) x 10^{13} molecule cm^{-3}) was made to the chamber during an experiment.

The 6500 liter Teflon chamber was interfaced to a PE SCIEX API III MS/MS instrument via a 25 mm diameter x 75 cm length Pyrex tube, with a sampling flow rate of ~20 liter min^{-1}. The operation of the API-MS in the MS (scanning) and MS/MS [with collision activated dissociation (CAD)] modes has been described elsewhere (Kwok *et al.*, 1995, 1996a,b; Atkinson *et al.*, 1995d). Use of the MS/MS mode with CAD allows the "daughter ion" or "parent ion" spectrum of a given ion peak observed in the MS scanning mode to be obtained (Kwok *et al.*, 1995, 1996a,b). The positive ion mode was used in all these API-MS and API-MS/MS analyses, with protonated water hydrates ($H_3O^+(H_2O)_n$) generated by the corona discharge in the chamber diluent gas being responsible for the protonation of analytes,

$$H_3O^+(H_2O)_n + M \rightarrow MH^+(H_2O)_m + (n - m + 1)H_2O \quad (34)$$

where M is the neutral analyte of interest. Ions are drawn by an electric potential from the ion source through the sampling orifice into the mass-analyzing first quadrupole or third quadrupole. Neutral molecules and particles are prevented from entering the orifice by a flow of high-purity nitrogen ("curtain" gas), and as a result of the declustering action of the curtain gas on the hydrated ions, the ions that are mass-analyzed are mainly protonated molecular ions ($[M+H]^+$).

Gas samples were also collected onto Tenax-TA solid adsorbent for analyses by GC-FID and GC-MS, using the procedures described above.

Chemicals. The chemicals used, and their stated purities, were: 1,4-dichlorobenzene (99+%), naphthalene (98%), naphthalene-d_8 (98+%), 1-nitronaphthalene (99%), 2-nitronaphthalene (98%), 1-naphthol (99+%), 2-naphthol (99%), 1,4-naphthoquinone (97%), 2-nitro-1-naphthol (99%), Aldrich Chemical Company; and 1-nitro-2-naphthol (purity not stated), TCI America.

2-Formyl-*trans*-cinnamaldehyde was synthesized from the ozonation of naphthalene in solution, using the methods described by Bailey and Erikson (1961). 2-Formyl-*trans*-cinnamaldehyde was purified from the reaction mixture by normal-phase high performance liquid chromatography (HPLC) with elution by 97% CH_2Cl_2/3% CH_3CN (both HPLC grade, Fisher

Scientific) using a semi-preparative silica column (5 μm, 25 cm length x 10 mm id). After HPLC fractionation, the fractions containing 2-formyl-*trans*-cinnamaldehyde were combined and evaporated to ~0.5 m*l* volume. The sample was then solvent exchanged into $CDCl_3$ using a procedure similar to that described by Hakola *et al.* (1993). After being dissolved in 0.5 liter of HPLC-grade water (Fisher Scientific), the sample was applied to a prewetted 500 mg C_{18} SPE column (Burdick and Jackson). The water remaining on the column was removed with a gentle stream of N_2 gas and the sample eluted off the column with ~700 μ*l* of $CDCl_3$. ^1H NMR and COSY spectra were obtained using a GE 300 MHz NMR spectrometer.

Methyl nitrite and N_2O_5 were prepared and stored as described previously (Atkinson *et al.*, 1981, 1984), and NO_2 was prepared as needed by reacting NO with an excess concentration of O_2.

Results

OH Radical Reaction. Shown in Figure 26 is a chromatogram typical of those resulting from GC-FID analyses of products from irradiated CH_3ONO - NO -naphthalene - air mixtures sampled on Tenax-TA solid adsorbent and eluted with diethyl ether. Similar chromatograms of reaction products resulted from OH radical-initiated reactions of naphthalene-d_8. A total of 16 product peaks are labeled in Figure 26 and the following products were identified by GC-MS and quantified by GC-FID utilizing authentic standards: 1,4-naphthoquinone, 1-naphthol, 2-naphthol, 1-nitronaphthalene, 1-hydroxy-2-nitronaphthalene and 2-hydroxy-1-nitronaphthalene. Because it was not resolved from a product of m.w. 176, 2-nitronaphthalene was quantified by GC-MS utilizing the area of its molecular ion peak. 2-Formylbenzaldehyde and phthalic anhydride were identified by matching their MS and FTIR spectra with available libraries (EPA/NIH, 1980; Pouchert, 1989; EPA, 1990) and quantified based on their ECN.

API-MS positive ion spectra of irradiated CH_3ONO - NO - naphthalene - air and CH_3ONO - NO - naphthalene-d_8 - air mixtures are shown in Figure 27 (top) and 27 (bottom), respectively. Based on GC-MS analyses and confirmed by API-MS and API-MS/MS spectra of authentic standards of 1,4-naphthoquinone, 1-naphthol, 1-nitronaphthalene and 1-hydroxy-2-nitronaphthalene, product ion peaks observed from the naphthalene reaction were attributed

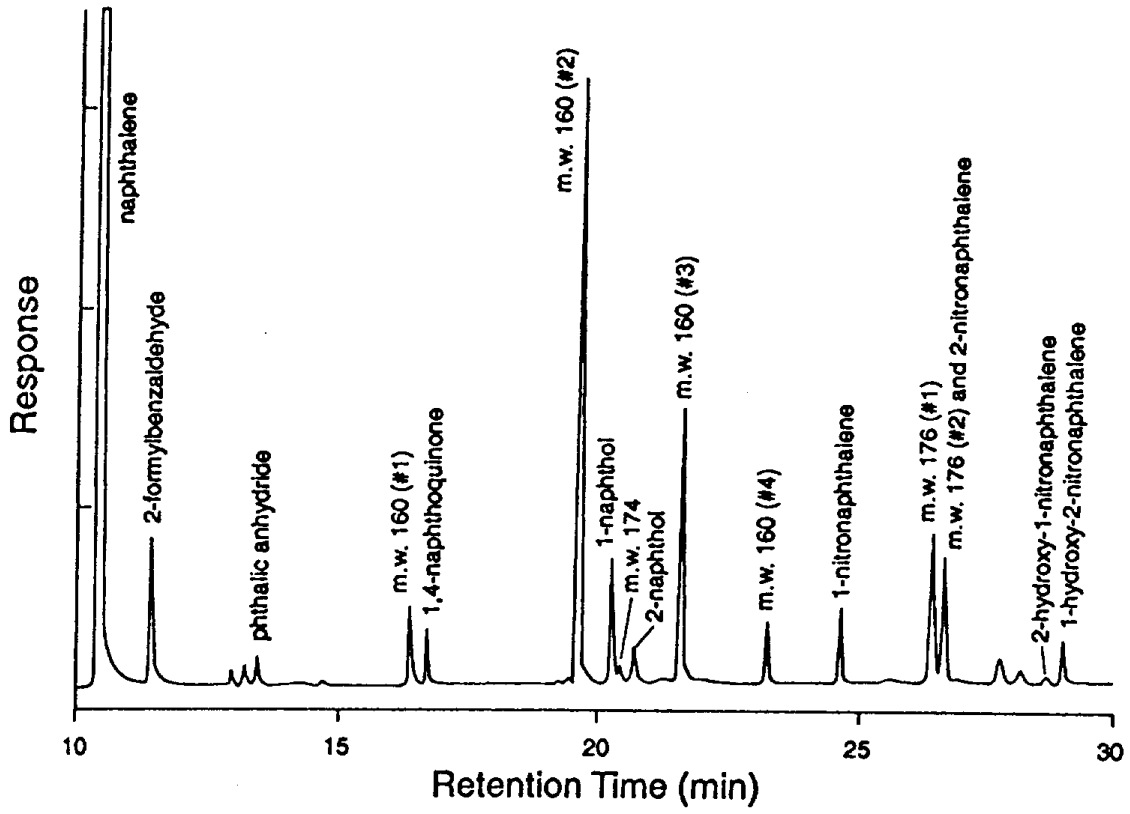

Figure 26. GC-FID chromatogram of the diethyl ether eluate of a sample collected on Tenax solid adsorbent from the gas-phase OH radical-initiated reaction of naphthalene.

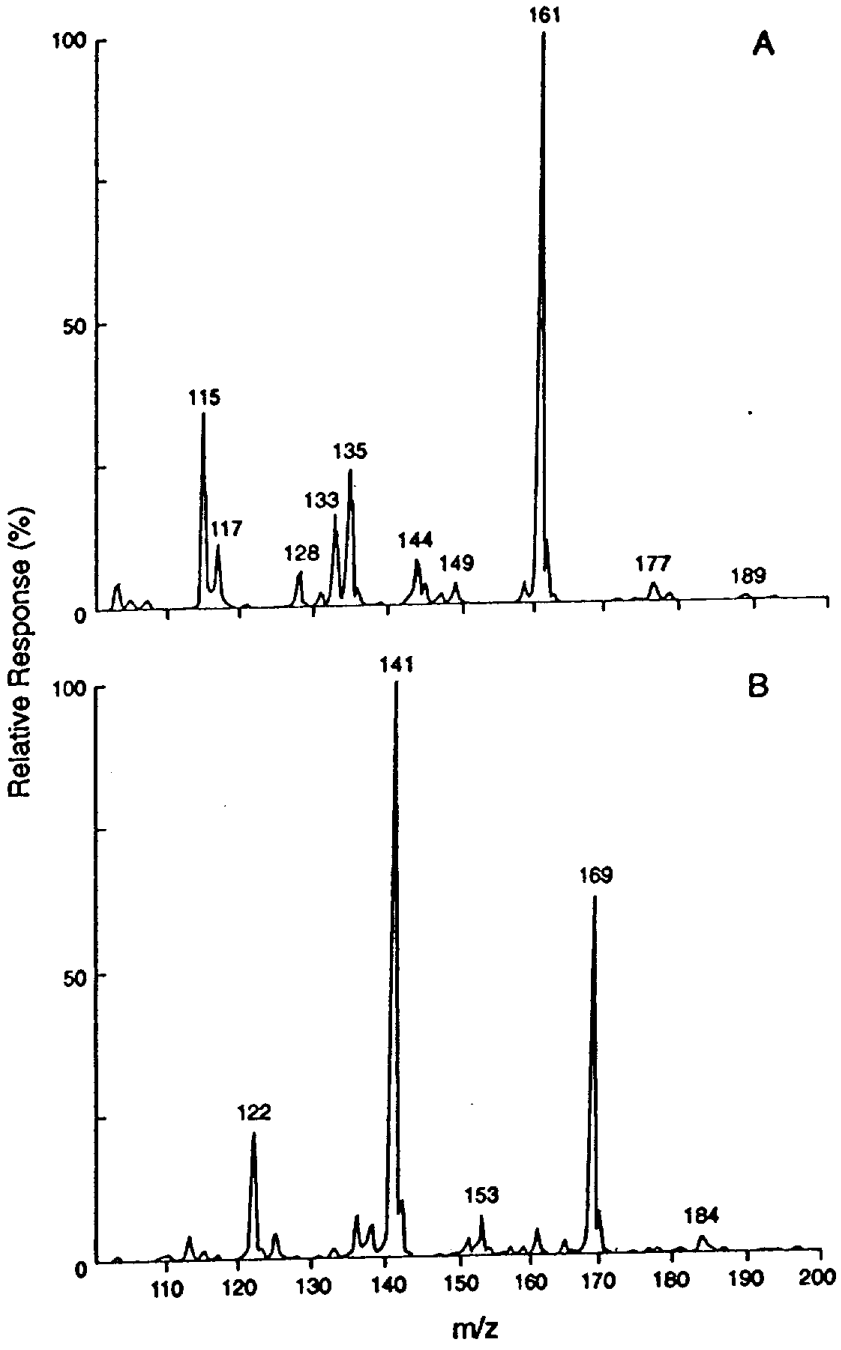

Figure 27. API-MS spectra of irradiated CH_3ONO - NO - naphthalene - air (A) and CH_3ONO - NO - naphthalene-d_8 - air (B) mixtures.

to: 135 u, $[M+H]^+$ of 2-formylbenzaldehyde; 144 u, $[M]^+$ of naphthol(s); 149 u, $[M+H]^+$ of phthalic anhydride; 159 u, $[M+H]^+$ of 1,4-naphthoquinone; and 189 u, $[M]^+$ of hydroxynitronaphthalene(s). Corresponding ion peaks were observed from the naphthalene-d_8 reaction at 141 u ($[M+H]^+$ of 2-formylbenzaldehyde-d_6) [this ion peak is also a fragment ion, see below], 151 u ($[M]^+$ of naphthols-d_7), 153 u ($[M+H]^+$ of phthalic anhydride-d_4) and 165 u ($[M+H]^+$ of 1,4-naphthoquinone-d_6).

At least seven additional products were observed in the GC analyses. Four of these products, two of which were formed in relatively high yield (see below), are labelled m.w. 160 (#1), (#2), (#3) and (#4) in Figure 26 and their EI mass spectra were all very similar with base peaks at m/z 131 and significant fragment ion peaks at m/z 103 and m/z 77. Only the fourth peak to elute showed a small molecular ion at m/z 160, but chemical ionization MS showed that all four products were of molecular weight 160 u from the naphthalene reaction and 168 u from the naphthalene-d_8 reaction. GC-FTIR analyses of the naphthalene reaction products indicated the presence of aldehydic -CHO group(s) in m.w. 160 peaks #1, #2 and #3 by the presence of absorption bands at 2715 and 2816 cm^{-1}, 2731 and 2834 cm^{-1}, and 2733 and 2817 cm^{-1}, respectively, and C=O stretch bands at 1740 and 1789 (doublet) cm^{-1}, 1706 cm^{-1}, and 1713 cm^{-1}, respectively. The molecular weight 160 peak #4 showed only the presence of a C=O stretch band at 1762 cm^{-1} and no evidence for aldehydic C-H stretch bands in the 2700-2850 cm^{-1} region.

API-MS and API-MS/MS spectra of the naphthalene and naphthalene-d_8 reactions also showed the presence of a dominant product ion peak at 161 and 169 u, respectively (Figure 27). API-MS/MS CAD spectra of these 161 and 169 u ion peaks from the naphthalene and naphthalene-d_8 reactions, respectively, are shown in Figure 28, and both spectra show losses from the $[M+H]^+$ parent ion of CO, CO_2 and $2CO_2$. The naphthalene reaction product also shows losses of H_2O and $CO+H_2O$, while the naphthalene-d_8 product shows corresponding losses of HDO and CO+HDO and $CO+D_2O$.

Based on an excellent match of their GC retention times and mass spectra, a product isolated from the ozonation of naphthalene in solution was determined to be identical to the m.w. 160 peak #3 of the OH radical-initiated reaction of naphthalene. Sufficient compound was isolated from the solution ozonation to allow its identification by ^1H NMR spectroscopy as

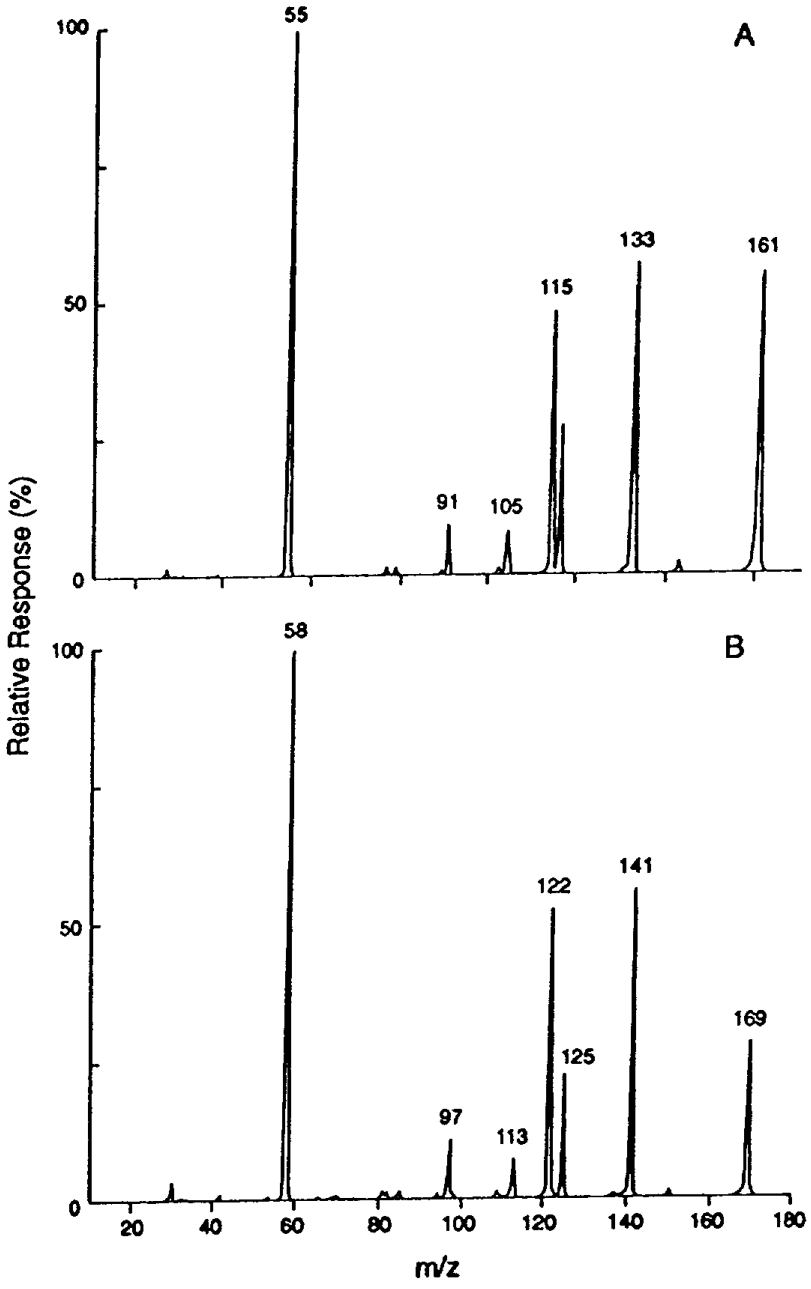

Figure 28. API-MS/MS collision induced dissociation (CAD) spectra of the 161 u (A) and 169 u (B) ion peaks observed in the OH radical-initiated reaction of naphthalene and naphthalene-d_8, respectively.

2-formyl-*trans*-cinnamaldehyde (I). The ^{1}H NMR data for this compound is presented in Table 6 along with NMR data for *trans*-cinnamaldehyde (II). Note the similarity in the chemical shifts for the aldehydic and vinylic protons H_A and H_B between I and II. The effect of the second aldehyde group is clearly seen in the downfield shifts of both H_C and H_D and the second aldehydic proton is observed as a singlet at 10.23 ppm.

The chromatographic behavior of the m.w. 160 products #2 and #3 and the close correspondence of the MS and IR spectra of these two products leads to the tentative identification of product #2 as 2-formyl-*cis*-cinnamaldehyde. Both 2-formyl-*cis*-cinnamaldehyde and 2-formyl-*trans*-cinnamaldehyde have been reported to be formed in liquid-phase ozonolysis with naphthalene (Larson *et al.*, 1986; Marley *et al.*, 1987), with 2-formyl-*cis*-cinnamaldehyde photoisomerizing to 2-formyl-*trans*-cinnamaldehyde (Larson *et al.*, 1986).

The other significant product observed in the GC analyses had a highest mass peak in the EI GC-MS analyses of 176 u from the naphthalene reaction and 183 u from the naphthalene-d_8 reaction, respectively. API-MS and API-MS/MS spectra of the naphthalene and naphthalene-d_8 reactions showed ion peaks at 177 and 184 u, respectively, consistent with the GC-MS analyses, and indicating the presence of seven non-exchangeable H atoms and one exchangeable H atom. The exchangeable H is assumed to be associated with an -OH group which has undergone rapid -OD to -OH exchange in the chamber, as observed previously (Kwok *et al.*, 1995, 1996a,b; Atkinson *et al.*, 1995d). The API-MS/MS spectrum of the 177 u ion peak from the naphthalene reaction showed fragment ions resulting from losses of H_2O, CO, $CO+H_2O$, 2CO and $2CO+H_2O$. The IR spectrum of this product from GC-FTIR analyses showed absorption bands at 3615 cm^{-1} (attributed to an -OH stretch) and 1712 cm^{-1} (attributed to a C=O stretch), but no evidence for an aldehydic C-H stretch in the 2700-2850 cm^{-1} region. These data imply the presence of C=O groups and the presence of an -OH group(s) and suggest that this product contains hydroxy, epoxide and ketone-carbonyl groups.

In general, the observed products can also react with the OH radical during the reactions, and hence these secondary reactions of the various products with the OH radical need to be taken into account. While OH radical reaction rate constants have been measured for 1,4-naphthoquinone and 1- and 2-nitronaphthalene (Atkinson, 1989), rate constants are not available for the other products observed. Rate constants for these other products were either estimated

Table 6. ^{1}H NMR chemical shifts, multiplicities, and coupling constants for 2-formyl-*trans*-cinnamaldehyde (I) and *trans*-cinnamaldehyde (II) in $CDCl_3$, GE 300 MHz NMR

I

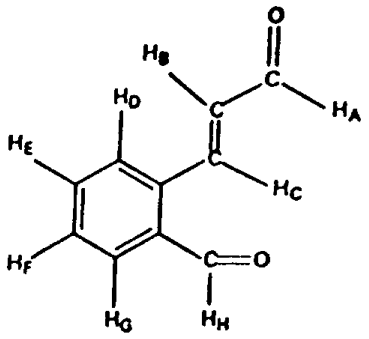

II

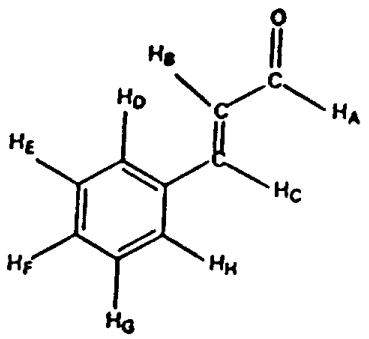

Proton	Chemical shift (ppm)	Proton	Chemical shift (ppm)
H_A	9.82 (d,1H)	H_A	9.72 (d,1H)
H_B	6.68 (dd,1H)	H_B	6.73 (dd,1H)
H_C	8.58 (d,1H)	H_C	7.49 (d,1H)
H_D,H_E,H_F	7.65-7.73 (m,3H)	H_D,H_E,H_F,H_G,H_H	7.42-7.60 (m,5H)
H_G	7.88-7.92 (m,1H)		
H_H	10.23 (s,1H)		
COSY shows coupling between:		COSY shows coupling between:	
	H_A and H_B (J=7.9 Hz)		H_A and H_B (J=7.5 Hz)
	H_B and H_C (J=15.6 Hz)		H_B and H_C (J=16.0 Hz)

from the chemical structures of the products (Kwok and Atkinson, 1995) or based on linearizing plots of the amounts of product formed against the amounts of naphthalene reacted. For example, Figure 29 shows plots of the amounts of 1,4-naphthoquinone and the molecular weight 176 product formed, corrected for reaction with the OH radical, against the amounts of naphthalene reacted. The product formation yields obtained from least-squares analyses of such plots are given in Table 7, and the rate constants used for the reactions of the OH radical with these products are noted in the footnotes to Table 7.

Figure 30 shows the time-concentration behavior of 2-formyl-*cis*-cinnamaldehyde and 2-formyl-*trans*-cinnamaldehyde. The observed behavior suggests that either: (A) the 2-formyl-*cis*-cinnamaldehyde is formed in relatively high yield and that this isomer reacts rapidly, while the *trans* isomer is formed in lower yield but is much less reactive; (B) that 2-formyl-*trans*-cinnamaldehyde is formed from the *cis*-isomer (by photolysis) and that the measured time-concentration profile of the *trans*-isomer is due to its formation from the *cis*-isomer and loss by reaction and/or photolysis; or (C) that the *cis*- and *trans*- isomers are interconverted by photolysis during the experiments and possibly also during the sampling and analysis procedures (note the anti-correlation between the concentrations of the *cis*- and *trans*- isomers at the greatest extent of reaction for the "high-OH" experiments in Figure 30) and that these two isomers are lost by reaction with the OH radical and/or photolysis. As shown in Figure 30, the observed behavior of the *cis*-isomer is consistent with a formation yield of $\sim$0.33 and predominant loss by photolysis, while assuming case (A), the formation yield of the *trans*-isomer is $\sim$9% with a much lower loss rate by photolysis and OH radical reaction than the *cis*-isomer. It is expected that the rate constants for reaction of the OH radical with 2-formyl-*cis*-cinnamaldehyde and 2-formyl-*trans*-cinnamaldehyde should be similar at $\sim$(5-7) x 10^{-11} cm^3 $molecule^{-1}$ s^{-1} at room temperature (Kwok and Atkinson, 1995; Smith *et al.*, 1996), and assumption (A) does not appear tenable. Calculations showed that the assumption that the *cis*-isomer photoisomerizes to the *trans*-isomer [assumption (B)] is consistent with the data, but the amount of *trans*-isomer calculated to be formed from the "high-OH" experiments is marginally enough to fit the observed *trans*-isomer concentration data and necessitates that the *trans*-isomer can only react or photolyze slowly. With assumption (C), the sum of the *cis*- and *trans*- isomers are reasonably consistent with a formation yield of $\sim$0.35 and a rate constant for reaction with the OH radical

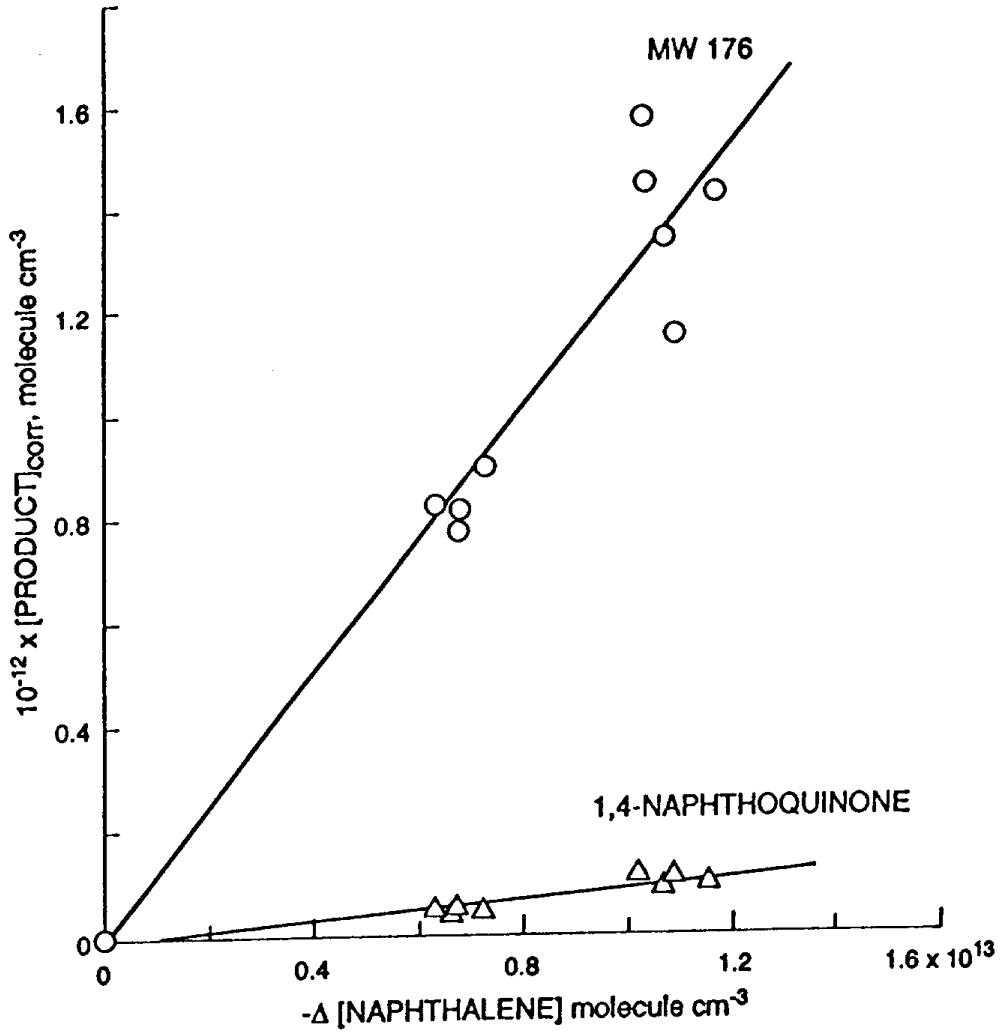

Figure 29. Plots of the amounts of the molecular weight 176 products and 1,4-naphthoquinone against the amounts of naphthalene reacted with the OH radical. The measured concentrations of the two products were corrected for reaction with the OH radical as noted in the text and footnotes d and j of Table 7.

Table 7. Products observed, and their formation yields, from the gas-phase OH radical- and NO_3 radical-initiated reactions of naphthalene

Product	Formation yield from reaction with[a]	
	OH radical	NO_3 radical
2-Formylbenzaldehyde	~0.027[b]	
Phthalic anhydride	~0.03[c]	
1,4-Naphthoquinone	0.010 ± 0.003[d]	0.019 ± 0.011[d]
MW 160 #1	0.014 ± 0.003[e]	
2-Formyl-cinnamaldehyde (*cis-* + *trans-*)	$0.35^{+0.010}_{-0.05}$ [f]	
MW 160 #4	0.015 ± 0.003[e]	
1-Naphthol	0.029 ± 0.015[g]	observed[k]
2-Naphthol	0.038 ± 0.011[g]	observed[k]
1-Nitronaphthalene	0.012 ± 0.009[d]	0.244 ± 0.065[d]
2-Nitronaphthalene	0.013 ± 0.011[d]	0.110 ± 0.036[d]
1-Hydroxy-2-nitronaphthalene	0.011 ± 0.011[h]	0.015 ± 0.019[e,l]
2-Hydroxy-1-nitronaphthalene	0.012 ± 0.014[e,l]	
MW 174	~0.05[i]	
MW 176	0.13 ± 0.03[j]	
Total	~0.67 ± 0.11	≥0.40[m]

[a] Indicated uncertainties are two least-squares standard deviations of the data, unless noted otherwise, and do not include uncertainties in the GC-FID response factors for naphthalene and the products [estimated to be $\pm$ ~(5-10)%].

[b] Expected to be a secondary product formed from reaction of 2-formyl-cinnamaldehyde with the OH radical (see text).

[c] May be a secondary product.

[d] Corrected for secondary reactions using the literature OH or NO_3 radical reaction rate constants (Atkinson, 1989, 1991).

[e] Data showed no evidence for reaction of the product with the OH radical, and hence no correction for secondary reaction was made.

[f] See text. Uncertainties are estimated.

[g] Corrected for secondary reactions with the OH radical using a rate constant of 1×10^{-10} cm^3 molecule^{-1} s^{-1}. Data suggested that 1-naphthol reacted more rapidly, and use of a rate constant for reaction with the OH radical of 2×10^{-10} cm^3 molecule^{-1} s^{-1} resulted in a yield of 0.067 $\pm$ 0.022. Data suggest that 2-naphthol may react slower, and hence the cited formation yield may be high.

[h] Corrected for secondary reaction with the OH radical using a rate constant of 2.5×10^{-11} cm^3 molecule^{-1} s^{-1}. May be a secondary product formed from 1-naphthol.

[i] Tentatively identified as 2,3-epoxy-1,4-naphthoquinone. No correction made for secondary reactions with the OH radical.

[j] Data indicate reaction with the OH radical, and a rate constant of 5.0×10^{-11} cm^3 molecule^{-1} s^{-1} has been used (which linearizes the plot of amount formed, corrected for reaction, against the amount of naphthalene reacted).

[k] Concentrations too low to quantify.

[l] No correction made for secondary reaction.

[m] Because of the expected high reactivity of 1- and 2-naphthol towards NO_3 radicals (with reaction rates relative to that of naphthalene of ~50-500 for the NO_2 concentrations used), significant amounts of the reaction products could have proceeded via the initial formation of 1- and 2-naphthol.

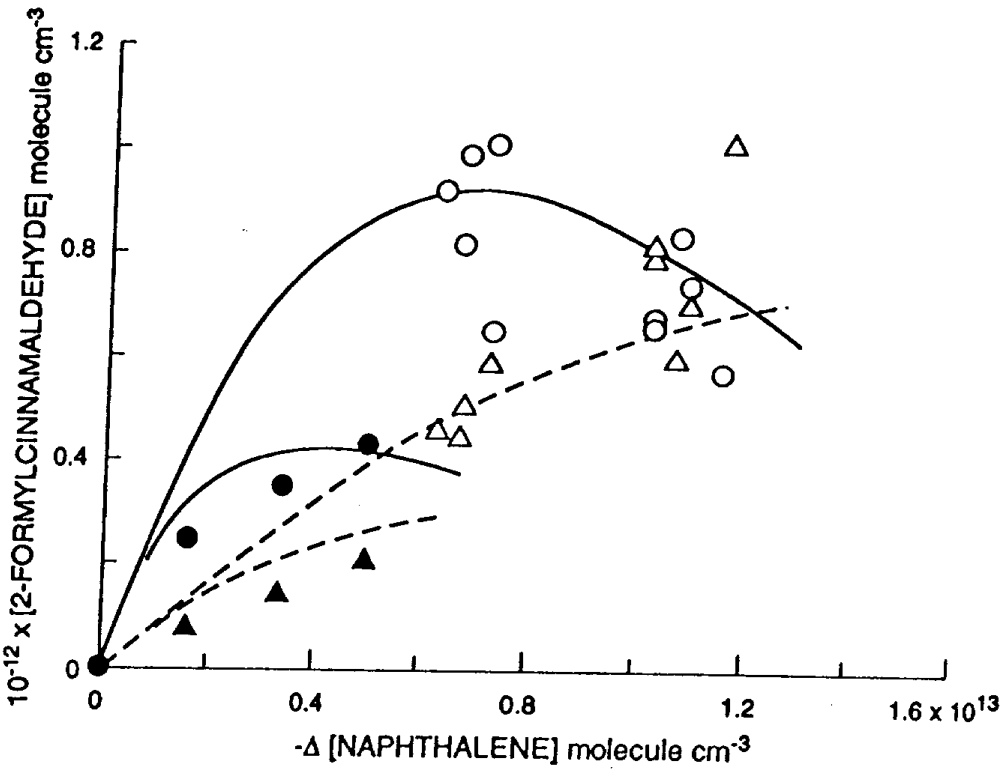

Figure 30. Plots of the measured amount of 2-formyl-*cis*-cinnamaldehyde (○, ●) and 2-formyl-*trans*-cinnamaldehyde (Δ, ▲) against the amounts of naphthalene reacted with the OH radical. The open symbols are for the experiments carried out with a CH_3ONO concentration of (2.13-2.16) x 10^{14} molecule cm^{-3} and the filled symbols are for the experiment carried out with a CH_3ONO concentration of 4.1 x 10^{13} molecule cm^{-3}. The solid lines are for a molar yield of the 2-formyl-*cis*-cinnamaldehyde of 0.33, a rate constant for reaction with the OH radical of 6.5 x 10^{-11} cm^3 molecule^{-1} s^{-1} and a photolysis rate of 0.146 min^{-1}. The dashed lines are for a molar yield of the 2-formyl-*trans*-cinnamaldehyde of 0.09, a rate constant for reaction with the OH radical of 5.4 x 10^{-12} cm^3 molecule^{-1} s^{-1} and a photolysis rate of 0.055 min^{-1}.

of $\sim 4 \times 10^{-11}$ cm^3 molecule^{-1} s^{-1} [reasonably consistent with expectations (Kwok and Atkinson, 1995; Smith *et al.*, 1996)] and removal by photolysis at a rate of 0.045 min^{-1} for the light intensity and spectral distribution conditions used here (Figure 31) [increasing the OH radical reaction rate constant to 5.4×10^{-11} cm^3 molecule^{-1} s^{-1} increases the formation yield of the two isomers to ~ 0.40, with a similar data quality as shown in Figure 31]. Clearly, studies of the rates and products of photolysis and reaction with the OH radical of both 2-formyl-*cis*-cinnamaldehyde and 2-formyl-*trans*-cinnamaldehyde are needed before the precise interactions between these naphthalene reaction products and assumptions (A) through (C) can be elucidated. However, it is equally clear that the formation yield of 2-formylcinnamaldehyde from the OH radical reaction with naphthalene in the presence of NO is ~ 0.35.

By analogy with the observed formation of benzaldehyde from the reaction of cinnamaldehyde with the OH radical (Smith *et al.*, 1996), 2-formylbenzaldehyde is expected to be formed from the OH radical reaction with 2-formylcinnamaldehyde and hence is viewed as a second-generation product; the same may be the case for phthalic anhydride and 1-hydroxy-2-nitronaphthalene (Table 7). Reaction Scheme 6 shows the reaction pathways leading to the formation of the majority of the products observed, which account for $\sim 67\%$ of the overall reaction products. The only previous product study which reported quantitative product formation yields was that previously carried out in this laboratory (Atkinson *et al.*, 1987). The formation yields obtained in that study (Atkinson *et al.*, 1987) were: 1-nitronaphthalene, 0.0032 $\pm$ 0.0028; 2-nitronaphthalene, 0.0027 $\pm$ 0.0034; 1-naphthol, 0.071 $\pm$ 0.043; and 2-naphthol, 0.042 $\pm$ 0.025 (with the measured naphthol concentrations being corrected for secondary reactions using the same estimated rate constant of 1×10^{-10} cm^3 molecule^{-1} s^{-1} as used here in Table 7). The present data (Table 7) are in reasonable agreement with our previously measured yields, especially considering the low formation yields of these products and the expected dominance of secondary reactions for the naphthols.

NO_3 Radical Reaction. GC-FID analyses of reacted NO_3 - NO_2 - N_2O_5 - naphthalene (and naphthalene-d_8) - air mixtures yielded chromatograms such as that shown in Figure 32. From matching of the GC retention times, mass spectra and IR spectra with those of authentic standards, concurrent GC-MS and GC-FTIR analyses of the naphthalene and naphthalene-d_8

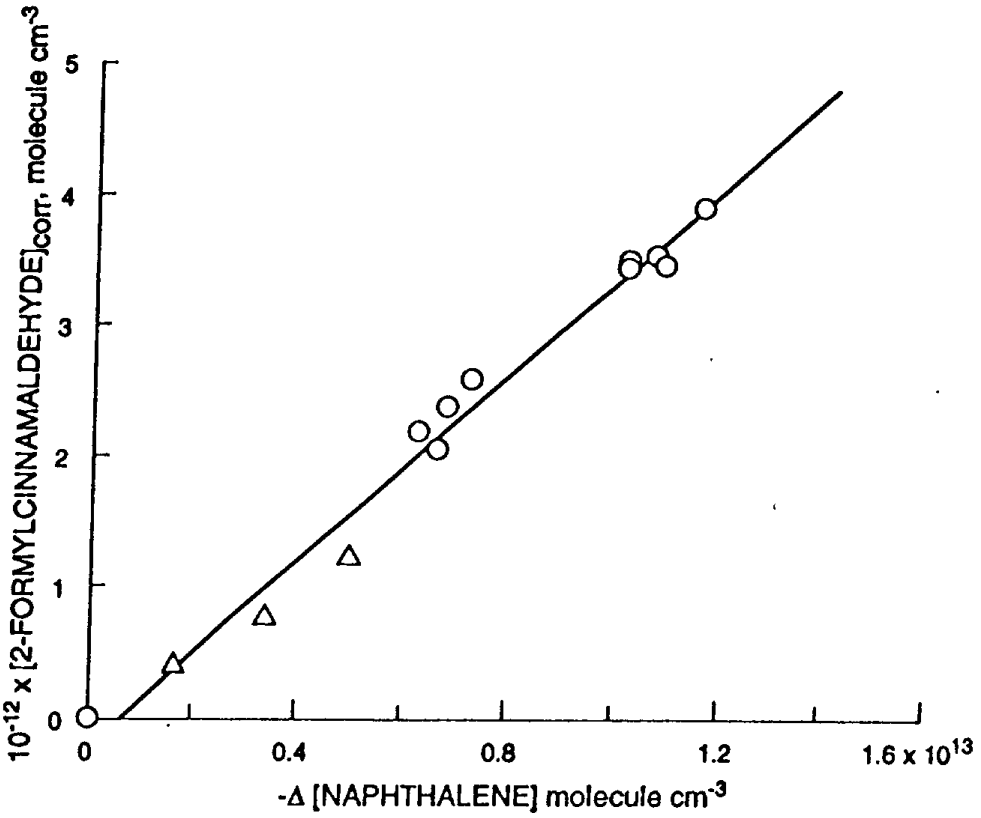

Figure 31. Plots of the amounts of 2-formylcinnamaldehyde (*cis* + *trans*) against the amounts of naphthalene reacted with the OH radical. O - experiments carried out with a CH_3ONO concentration of (2.13-2.16) x 10^{14} molecule cm^{-3}; Δ - experiment carried out with a CH_3ONO concentration of 4.1 x 10^{13} molecule cm^{-3}. The measured concentrations have been corrected for reaction with the OH radical with a rate constant of 4.1 x 10^{-11} cm^3 molecule^{-1} s^{-1} and for removal by photolysis at a rate of 0.045 min^{-1} under the experimental conditions used.

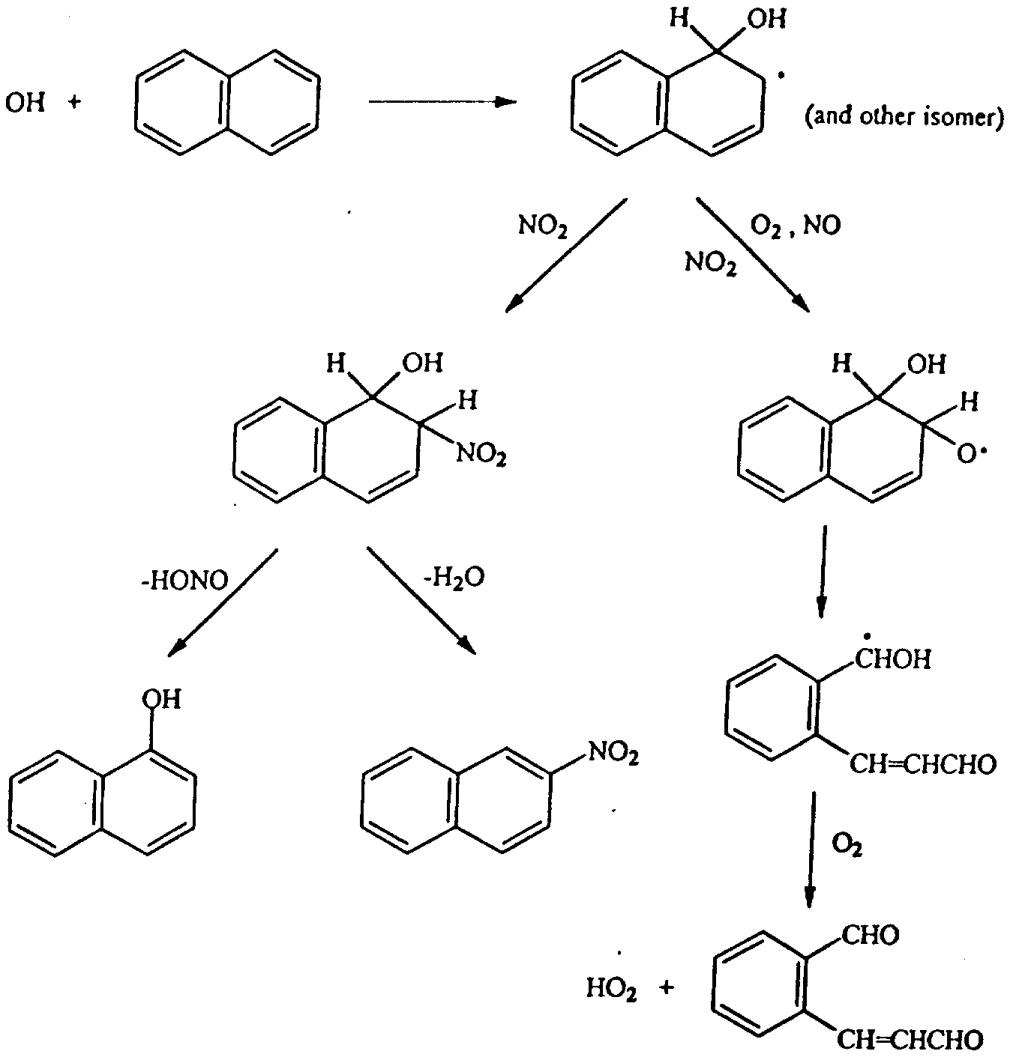

Reaction Scheme 6

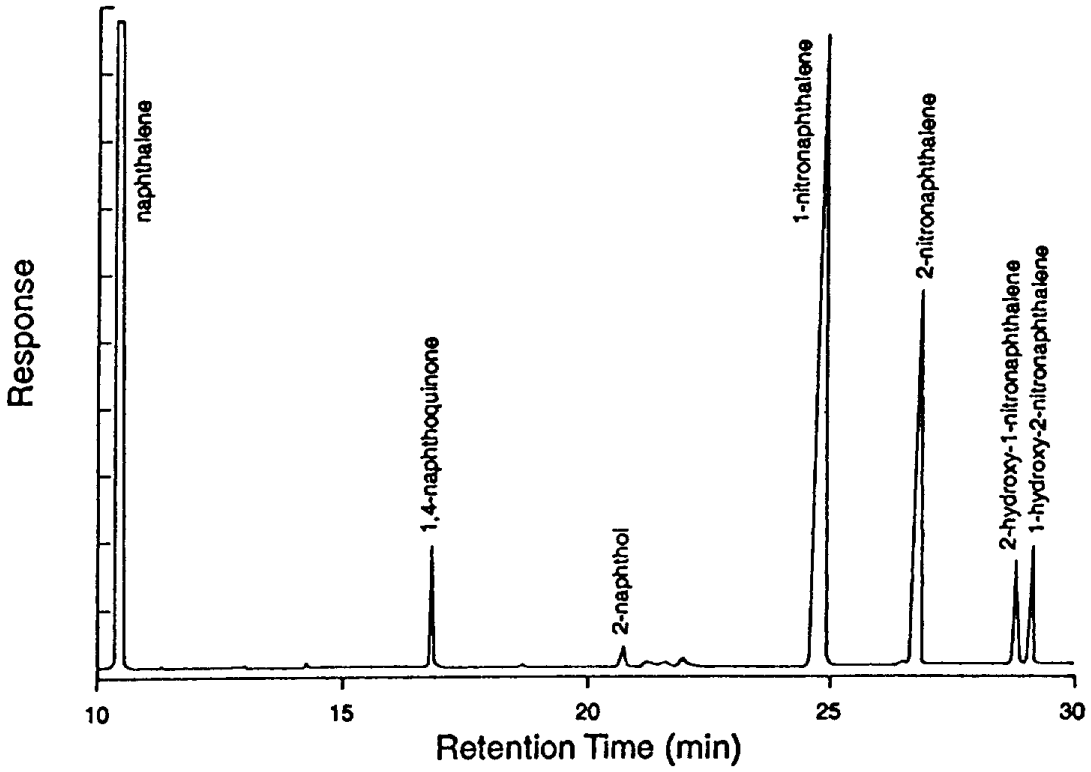

Figure 32. GC-FID chromatogram of the diethyl ether eluate of a sample collected on Tenax solid adsorbent from the gas-phase NO_3 radical-initiated reaction of naphthalene.

reactions showed that 1- and 2-nitronaphthalene, 1,4-naphthoquinone, 1-nitro-2-naphthol, 2-nitro-1-naphthol and 2-naphthol were products of the NO_3 radical-initiated reaction (the amounts of 2-naphthol formed were too low for quantification to be carried out).

API-MS and API-MS/MS analyses of reacted NO_3 - NO_2 - N_2O_5 - naphthalene - air and NO_3 - NO_2 - N_2O_5 - naphthalene-d_8 - air mixtures showed ion peaks at 115, 144, 155, 157, 159, 174 (dominant) and 189 u from the naphthalene reaction and at 122, 141, 151, 153, 161, 162, 163, 181 (dominant), 195, 199 and 209 u from the naphthalene-d_8 reaction. API-MS/MS parent ion and daughter ion spectra of these ion peaks formed in the naphthalene reaction indicated that products formed included naphthols ($[M]^+$ at 144 u), 1,4-naphthoquinone ($[M+H]^+$ at 159 u), nitronaphthalenes ($[M+H]^+$ at 174 u) and hydroxynitronaphthalenes ($[M]^+$ at 189 u). The corresponding ion peaks were observed in the naphthalene-d_8 reaction at 151, 165, 181 and 195 u, respectively, noting that rapid -OD to -OH exchange occurs for the naphthols and hydroxynitronaphthalenes.

The concentrations of these products were measured by GC-FID during the experiments, and the measured concentrations of 1- and 2-nitronaphthalene and the hydroxynitronaphthalenes were corrected for secondary reactions with the NO_3 radical using either measured (Atkinson, 1991) [for nitronaphthalenes] or estimated [for the hydroxynitronaphthalenes] NO_3 radical reaction rate constants. No correction was necessary for 1,4-naphthoquinone (Atkinson, 1991). Figure 33 shows plots of the amounts of 1- and 2-nitronaphthalene formed, corrected for reaction with the NO_3 radical, against the amounts of naphthalene reacted, and the formation yields of 1- and 2-nitronaphthalene and other products are given in Table 7. The formation yields of 1- and 2-nitronaphthalene from the NO_3 radical-initiated reaction of naphthalene have been measured previously in this laboratory (Pitts *et al.*, 1985; Atkinson *et al.*, 1987). The measured 1- and 2-nitronaphthalene formation yields reported from those studies, of 0.172 ± 0.034 and 0.075 ± 0.012, respectively (Pitts *et al.*, 1985; Atkinson *et al.*, 1987) and 0.153 ± 0.022 and 0.069 ± 0.021, respectively (Atkinson *et al.*, 1987), are 30-37% lower than the formation yields determined here, with the 1-nitronaphthalene/2-nitronaphthalene formation yield ratios from all three studies being in excellent agreement. Our previous studies (Pitts *et al.*, 1985; Atkinson *et al.*, 1987) involved HPLC analyses of extracts of samples collected on Tenax (Pitts *et al.*, 1985) or polyurethane foam (Atkinson *et al.*, 1987) solid adsorbents, and it is

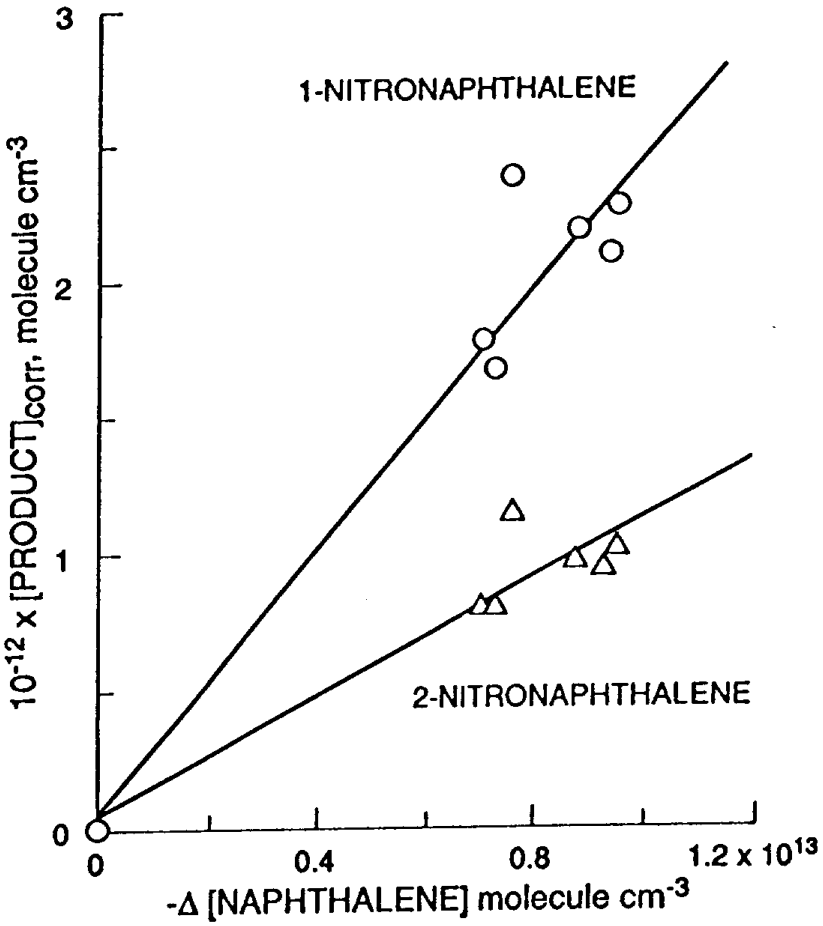

Figure 33. Plots of the amounts of 1- and 2-nitronaphthalene formed, corrected for reaction with the NO_3 radical (see text), against the amounts of naphthalene reacted with the NO_3 radical.

possible that some nitronaphthalene losses occurred in the overall analytical procedures in these previous studies.

The products quantified account for ~40% of the NO_3 radical reaction products, and potentially significantly more if naphthol formation is significant. The naphthols are expected to react rapidly with the NO_3 radical (Atkinson, 1991), with rate constants of $\sim 10^{-11}$ cm^3 $molecule^{-1}$ s^{-1}, and with rate constants of this magnitude secondary reactions of the naphthols with the NO_3 radical would be extremely important (with the measured concentrations needing to be corrected by a factor of 300-500 for the conditions employed in the present work). Scheme 7 shows possible reaction pathways leading to the observed products.

Conclusions

Our data show that a major fraction of the reaction of the OH radical with naphthalene in the presence of NO_x proceeds by ring-cleavage, leading to the formation of the unsaturated dicarbonyl 2-formylcinnamaldehyde. Moreover, our results show that this ring-cleavage product is highly reactive, both with respect to reacting with the OH radical and to photolysis. The ring-retaining products identified and quantified account for ~30% of the overall OH radical reaction products. The identified and quantified ring-retaining products of the OH radical reactions with benzene and the methyl-substituted benzenes (Atkinson, 1994; Kwok *et al.*, 1997) account for ~20-30% of the OH radical reaction proceeding by initial addition to the aromatic ring (Atkinson, 1994), and ring-cleavage to form α-dicarbonyls (plus the 1,4-unsaturated dicarbonyl co-products) and di-unsaturated-1,6-dicarbonyls (Atkinson, 1994; Kwok *et al.*, 1997) accounts for a large fraction of the overall reaction products. Hence the OH radical reaction with naphthalene is analogous to the corresponding reactions of the OH radical with the monocyclic aromatic hydrocarbons.

The major products identified and quantified from the reaction of the NO_3 radical with naphthalene are 1- and 2-nitronaphthalene, formed in a 1-nitronaphthalene/2-nitronaphthalene formation yield ratio of 2.2. These products and product yield data were obtained in the presence of sufficient NO_2 that the initially-formed nitrooxycyclohexadienyl radical reacted solely with NO_2 (Atkinson *et al.*, 1994c). An important question is whether or not these laboratory data are relevant to the atmosphere. We have previously shown that for the NO_3-naphthalene

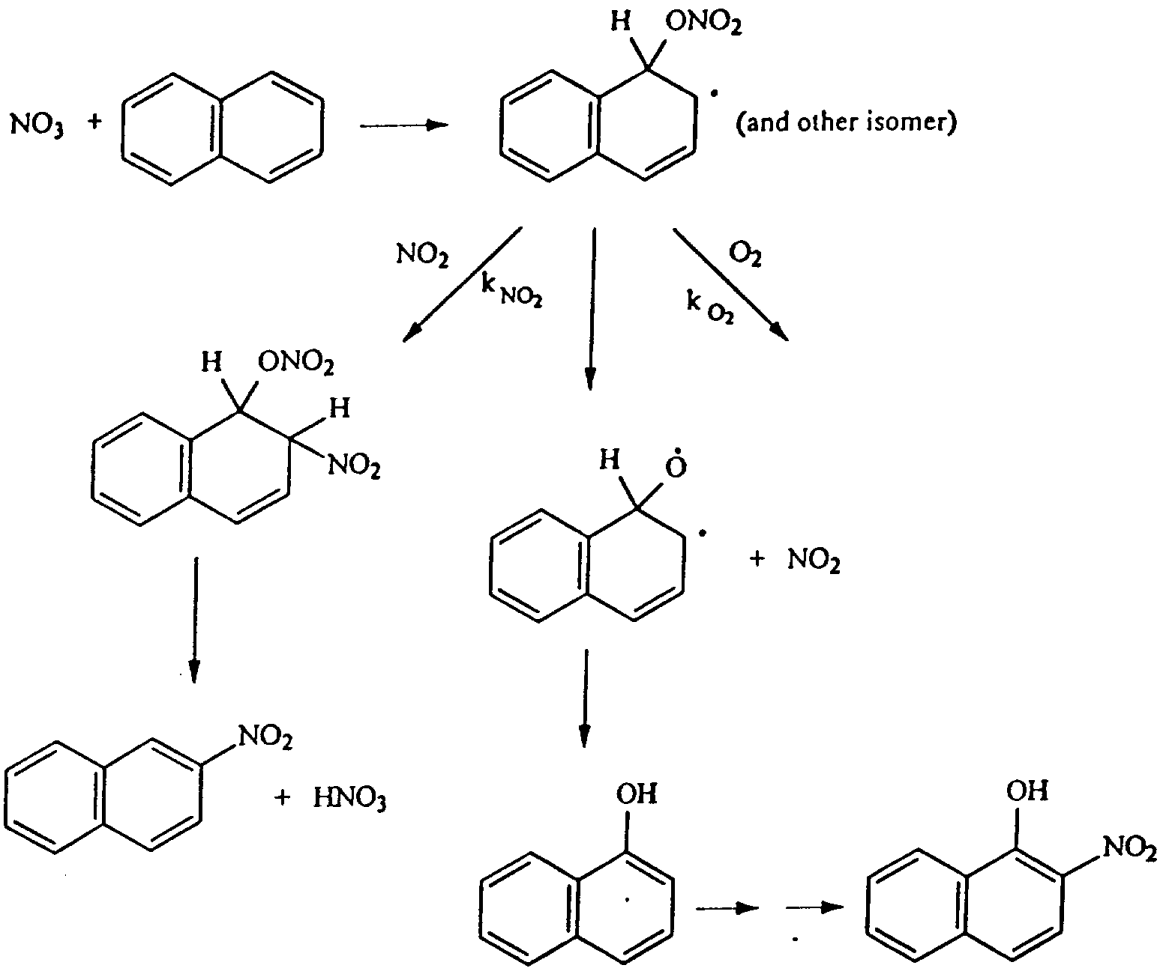

Reaction Scheme 7

adduct, the rate constant ratio for the O_2/NO_2 reactions is $k_d/k_c < 4 \times 10^{-7}$ (Reaction Scheme 5) (Atkinson *et al.*, 1994c), which results in dominant reaction of the nitrooxycyclohexadienyl radical with NO_2 for NO_2 mixing ratios >80 ppb (and possibly for much lower NO_2 mixing ratios). Ambient atmospheric measurements of 1- and 2-nitronaphthalene in an area downwind of the Los Angeles Air Basin (Gupta *et al.*, 1996; Gupta, 1996) showed that during nighttime hours 1- and 2-nitronaphthalene are formed with 1-nitronaphthalene/2-nitronaphthalene concentration ratios of ~2, very similar to those observed in our laboratory studies. Furthermore, ambient measurements of nitronaphthalenes, methylnitronaphthalenes and nitrofluoranthenes have shown distinctive nighttime isomer profiles which have been attributed to *in situ* formation from NO_3 radical reaction of the parent PAH (Atkinson and Arey, 1994; Gupta *et al.*, 1996). The magnitude of the nitronaphthalene formation yields from the NO_3 radical-initiated reaction of naphthalene presented here are consistent with this formation route and do not require the assumption of unrealistically high nighttime NO_3 radical concentrations.

6. PRODUCTS OF THE GAS-PHASE OH AND NO_3 RADICAL-INITIATED REACTIONS OF BIPHENYL AND 1- AND 2-METHYLNAPHTHALENE

Introduction

Biphenyl and 1- and 2-methylnaphthalene are polycyclic aromatic hydrocarbons which are of higher molecular weight than naphthalene and which are relatively abundant in ambient air [though less so than naphthalene] (Arey *et al.*, 1987, 1989). These three PAH exist in the lower troposphere essentially entirely in the gas phase (Arey *et al.*, 1987, 1989), and the rate constants for their gas-phase reactions with OH radicals, NO_3 radicals and O_3 have been measured (Atkinson and Arey, 1994). Biphenyl and 1- and 2-methylnaphthalene all react with the OH radical, and 1- and 2-methylnaphthalene also react at measurable rates with the NO_3 radical; no reactions have been observed for the O_3 reactions nor for the reaction of biphenyl with the NO_3 radical (Atkinson and Arey, 1994).

We have previously investigated the formation of nitrobiphenyls from the OH radical-initiated reaction of biphenyl and of the methylnitronaphthalenes from the OH radical- and NO_3 radical-initiated reactions of 1- and 2-methylnaphthalene (Atkinson *et al.*, 1987; Zielinska *et al.*, 1989). The formation of hydroxybiphenyls (mainly 2-hydroxybiphenyl) from the reaction of the OH radical with biphenyl was observed in $\sim$20% yield in the study of Atkinson *et al.* (1987). In this work, we have studied the atmospherically-important reactions of biphenyl and 1- and 2-methylnaphthalene using gas chromatographic (GC-FID and GC-MS) analyses as well as direct air sampling, atmospheric pressure ionization tandem mass spectrometry (API-MS) analyses.

Experimental

The experimental methods used were very similar to those used for the product study of the naphthalene reactions discussed in Section 5 above. Experiments were carried out in 6500-7900 liter all-Teflon chambers equipped with two parallel banks of blacklamps at 296 $\pm$ 2 K and 740 Torr total pressure of purified air at a relative humidity of $\sim$5%. Two series of experiments were carried out with analyses by GC with flame ionization (GC-FID) and mass spectrometric (GC-MS) detection and by API-MS, respectively, and these two sets of experiments used different reactant concentrations. The PAH were introduced into both chambers by flushing either a Pyrex tube packed with solid biphenyl, or a measured amount of

solid 2-methylnaphthalene or liquid 1-methylnaphthalene, with a stream of N_2 gas. The NO and initial NO_2 concentrations during these experiments were monitored using a Thermo Environmental Instruments, Inc., Model 42 chemiluminescence NO-NO_2-NO_x analyzer. For both series of experiments, OH radicals were generated by the photolysis of methyl nitrite (CH_3ONO) in air at wavelengths >300 nm (Atkinson *et al.*, 1981), and NO was added to the reactant mixtures to suppress the formation of O_3 and hence NO_3 radicals (Atkinson *et al.*, 1981). For both series of experiments, NO_3 radicals were generated from the thermal decomposition of N_2O_5 (Atkinson *et al.*, 1984), and NO_2 was added to the reactant mixtures to ensure that the NO_3-methylnaphthalene adducts reacted only with NO_2 and to minimize reactions of 1- and 2-methylnaphthalene with species other than NO_3 radicals.

Reactions with Gas Chromatographic Analyses. Reactions were carried out in a 7900 liter all-Teflon chamber. For the OH radical-initiated reactions, the initial reactant concentrations (in molecule cm^{-3} units) were: CH_3ONO, $\sim 2.4 \times 10^{14}$; NO, $\sim 2.4 \times 10^{14}$; biphenyl or 1- or 2-methylnaphthalene, $\sim 2.4 \times 10^{13}$; and 1,4-dichlorobenzene (as an internal standard), $\sim 2.4 \times 10^{13}$. Irradiations were carried out at 20% of the maximum light intensity for 20 min for the experiment with biphenyl and for 2-5 min for the experiments 1- and 2-methylnaphthalene. For the NO_3 radical-initiated reactions, the initial reactant concentrations (in molecule cm^{-3} units) were: NO_2, $\sim 5 \times 10^{13}$; 1- or 2-methylnaphthalene, $\sim 2.4 \times 10^{13}$; and 1,4-dichlorobenzene (an internal standard), $\sim 2.4 \times 10^{13}$. One addition of N_2O_5, corresponding to an initial concentration in the chamber of $(1.28\text{-}2.06) \times 10^{13}$ molecule cm^{-3}, was made to the chamber during these experiments.

During both the OH radical- and NO_3 radical-initiated experiments, biphenyl or 1- or 2-methylnaphthalene and 1,4-dichlorobenzene were analyzed by collecting 100 cm^3 volume gas samples from the chamber onto Tenax-TA solid adsorbent, with subsequent thermal desorption at ~ 225 °C onto a 60 m DB-5MS megabore column in a Hewlett Packard (HP) 5890 GC, initially held at 0 °C and then temperature programmed to 160 °C at 20 °C min^{-1} and then to 250 °C at 10 °C min^{-1}. Larger volume (~ 15 liter) gas samples were collected onto Tenax-TA solid adsorbent at ~ 0.45 liter min^{-1} for the quantification of biphenyl or 1- or 2-methylnaphthalene, 1,4-dichlorobenzene and reaction products, with subsequent elution with 1 m*l* of diethyl ether.

The eluate volume was reduced to ~500 μl, as measured with a 500 μl syringe, and a 2 μl aliquot was analyzed by GC-FID on a 60 m DB-5MS column (0.25 mm ID, 25 μm film thickness) in an HP 5890 GC, held at 40 °C and then temperature programmed to 120 °C at 20 °C min^{-1} and then to 280 °C at 6 °C min^{-1}. Replicate injections using the same temperature program and GC column type were carried out using an HP 5890 GC interfaced to an HP 5970 mass selective detector operated in the scanning mode to confirm the identities assigned to the product peaks. GC-FID response factors were measured using authentic standards when available, or were estimated using the calculated Effective Carbon Numbers (ECN) (Scanlon and Willis, 1985).

Reactions with API-MS Analyses. Reactions of biphenyl and 1- and 2-methylnaphthalene with OH radicals in the presence of NO_x were carried out in a 6500 liter all-Teflon chamber interfaced to a PE SCIEX API III MS/MS direct air sampling, atmospheric pressure ionization tandem mass spectrometer (API-MS). The initial CH_3ONO, NO and PAH concentrations were equal at either ~4.8 x 10^{13} molecule cm^{-3}, and irradiations were carried out for 2.5-3.5 min at the maximum light intensity for the experiments with biphenyl and for 1 min at 20% of the maximum light intensity for the experiments with 1- and 2-methylnaphthalene.

The 6500 liter Teflon chamber was interfaced to a PE SCIEX API III MS/MS instrument via a 25 mm diameter x 75 cm length Pyrex tube, with a sampling flow rate of ~20 liter min^{-1}. The operation of the API-MS in the MS (scanning) and MS/MS [with collision activated dissociation (CAD)] modes has been described elsewhere (Kwok *et al.*, 1995, 1996a,b; Atkinson *et al.*, 1995d). Use of the MS/MS mode with CAD allows the "daughter ion" or "parent ion" spectrum of a given ion peak observed in the MS scanning mode to be obtained (Kwok *et al.*, 1995, 1996a,b). The positive ion mode was used in all these API-MS and API-MS/MS analyses, with protonated water hydrates ($H_3O^+(H_2O)_n$) generated by the corona discharge in the chamber diluent gas being responsible for the protonation of analytes. Ions are drawn by an electric potential from the ion source through the sampling orifice into the mass-analyzing first quadrupole or third quadrupole. Neutral molecules and particles are prevented from entering the orifice by a flow of high-purity nitrogen ("curtain" gas), and as a result of the declustering

action of the curtain gas on the hydrated ions, the ions that are mass-analyzed are mainly protonated molecular ions ($[M+H]^+$).

Chemicals. The chemicals used, and their stated purities, were: biphenyl (99%), 1,4-dichlorobenzene (99+%), 1-methylnaphthalene (99%), 2-methylnaphthalene (98), 1-naphthaldehyde (97%), 2-naphthaldehyde (98%), 2-hydroxybiphenyl (99%), 3-hydroxybiphenyl (98%) and 4-hydroxybiphenyl (97%), Aldrich Chemical Company. Methyl nitrite and N_2O_5 were prepared and stored as described previously (Atkinson *et al.*, 1981, 1984), and NO_2 was prepared as needed by reacting NO with an excess concentration of O_2.

Results and Discussion

OH Radical Reaction with Biphenyl

API-MS analyses of irradiated CH_3ONO - NO - biphenyl - air mixtures showed the formation of product ion peaks, including ion peaks at 105, 161, 170, 177, 187 and 200 u. API-MS/MS daughter ion spectra of the 161, 177 and 200 u ion peaks indicated that the 105 u ion peak was a fragment ion of the 161 and 177 u ions. The 200 u ion peak showed fragment ions at 170 u (-NO), 154 u ($-NO_2$) and 153 u ($-HNO_2$), suggesting that the 200 u ion peak was the $[M+H]^+$ ion of M = nitrobiphenyl. The 177 u ion peak showed fragment ions at 159 u ($-H_2O$), 149 u (-CO) and 131 u ($-CO-H_2O$), while the 161 u ion peak showed fragment ions at 143 u ($-H_2O$) [weak], 133 u (-CO) [strong] and 115 u ($-CO-H_2O$). It is possible that the 161 u ion peak was the $[M+H]^+$ ion of M = $C_6H_5C(CHO)=CHCHO$ formed after ring-opening and with a glyoxal as a co-product.

Additional API-MS and API-MS/MS spectra were taken with added cyclohexanone to act as a chemical ionization agent to form heterodimers. While not completely unambiguous, this series of spectra suggested that ion peaks at 161, 177 and 187 u were products. These product ion peaks plus that at 200 u could be the $[M+H]^+$ ions of the products $C_6H_5C(CHO)=CHCHO$, a product of formula $C_6H_5CC_3H_3O_2$, $C_6H_5C(CHO)=CHCH=CHCHO$ (or isomer), and a nitrobiphenyl, respectively. The 170 u ion peak could be the $[M]^+$ ion of hydroxybiphenyl (note that hydroxynaphthalenes are observed as their $[M]^+$ ions; see section 5 above).

GC-FID and GC-MS analyses of ~ 15 liter volume samples collected from an irradiated CH_3ONO - NO - biphenyl - air mixture and eluted with diethyl ether showed the formation of 2-hydroxybiphenyl and 3-nitrobiphenyl. Because these products were identified and quantified in our previous product study of the OH radical reaction with biphenyl (Atkinson *et al.*, 1987), further experiments utilizing gas chromatographic analyses were not carried out. Our API-MS and GC data show that 2-hydroxybiphenyl and 3-nitrobiphenyl are ring-retaining products of the gas-phase reaction of the OH radical with biphenyl in the presence of NO_x, and that ring-opened products are also formed, analogous to the situation for monocyclic aromatic hydrocarbons (Atkinson, 1994; Kwok *et al.*, 1997).

OH Radical Reactions with 1- and 2-Methylnaphthalene

Irradiations of CH_3ONO - NO - methylnaphthalene - air mixtures were carried out with API-MS analyses. After the irradiations, both of the 1- and 2-methylnaphthalene reactions showed the presence of ion peaks (in addition to those of the pure air diluent and the 1- or 2-methylnaphthalene) at 149, 175 (strong), 191, 193, 209, 284, 323, 249, 365 and 367 u.

API-MS/MS "daughter" ion spectra of the 149 u ion peak showed fragment ions at 131 u ($-H_2O$), 103 u ($-H_2O$-CO) and 77 u ($[C_6H_5]^+$), and the "parent" ion spectra showed ion peaks at 297 u ($[148+148+H]^+$) and 323 u ($[148+174+H]^+$), indicating that the 149 u ion peak was the $[M+H]^+$ ion of a product of molecular weight 148 u and the presence of an additional product of molecular weight 174 u. API-MS/MS "daughter" ion spectra of the 175 u ion peak showed fragment ions at 157 u ($-H_2O$), 147 u (-CO), 129 u ($-H_2O$-CO) and 115 u ($[C_9H_7]^+$), and the "parent" ion spectra showed ion peaks at 193 u ($+H_2O$), 323 u ($[174+148+H]^+$), 349 u ($[174+174+H]^+$), 365 u ($174+190+H]^+$) and 367 u ($[174+174+H+H_2O]^+$), indicating that the 175 u ion peak was the $[M+H]^+$ ion of a product of molecular weight 174 u and the presence of additional product of molecular weight 148 u (see above) and 190 u. API-MS/MS "daughter" ion spectra of the 191 u ion peak showed fragment ions at 173 u ($-H_2O$), 145 u ($-H_2O$-CO), 131 u and 117 u, and the "parent" ion spectra showed ion peaks at 209 u ($+H_2O$), 365 u ($190+174+H]^+$) and 381 u ($[190+190+H]^+$), indicating that the 191 u ion peak was the $[M+H]^+$ ion of a product of molecular weight 190 u and the presence of the additional product of molecular weight 174 u (see above).

The identity of the 323 and 349 u ion peaks as $[148+174+H]^+$ and $[174+174+H]^+$ ion peaks was verified by API-MS/MS "daughter" ion spectra of these ion peaks. The 284 u ion peak is interpreted as a dimer of the [methylnaphthalene]$^+$ ion (at 142 u), consistent with the API-MS/MS "daughter" ion spectrum which showed only a 142 u ion peak. Therefore, API-MS analyses of the OH radical reaction with 1- and 2-methylnaphthalene in the presence of NO_x shows the formation of products of molecular weight 148, 174 and 190.

A series of experiments were also carried out with GC analyses of the diethyl ether eluates of ~15 liter volume gas samples collected from the chamber onto Tenax-TA solid adsorbent. GC-FID traces of the products of the 1- and 2-methylnaphthalene reactions are shown in Figures 34 and 35, respectively. Apart from 1- or 2-naphthaldehyde, for which matching of the GC retention times and mass spectra with those of the authentic standards could be carried out, the products are identified on Figures 34 and 35 by their molecular weight based on concurrent GC-MS analyses using electron impact (HP 5970 mass selective detector and a Varian 3000 GC-MS/MS) or chemical ionization (HP 5971 mass selective detector with CI module and a Varian 3000 GC-MS/MS). The products observed from both 1- and 2-methylnaphthalene by GC analyses are 1-naphthaldehydes from 1-methylnaphthalene, and a number of isomeric products of molecular weight 174 and a number of isomeric products of molecular weight 190 from both 1- and 2-methylnaphthalene (Figures 34 and 35). The observation of products of molecular weight 174 and 190 in the GC analyses is in agreement with the API-MS analyses discussed above; it is possible that the 148 u ion peak observed in the API-MS analyses is phthalic anhydride, which may be a secondary product of the 174 and/or 190 molecular weight species.

The 174 and 190 molecular weight products of the 1- and 2-methylnaphthalene reactions are presumably analogous to the 160 (primarily 2-formylcinnamaldehyde) and 176 molecular weight products observed from the corresponding naphthalene reaction (see Section 5), with the molecular weight 174 products being ring-opened products analogous to 2-formylcinnamaldehyde but containing a substituent methyl group. The molecular weight 174 and 190 products were quantified using the calculated ECNs relative to that for 1- and 2-naphthaldehyde for which GC-FID response factors were measured using the authentic compounds. Five experiments were carried out for 1-methylnaphthalene and four experiments for 2-methylnaphthalene, with the first

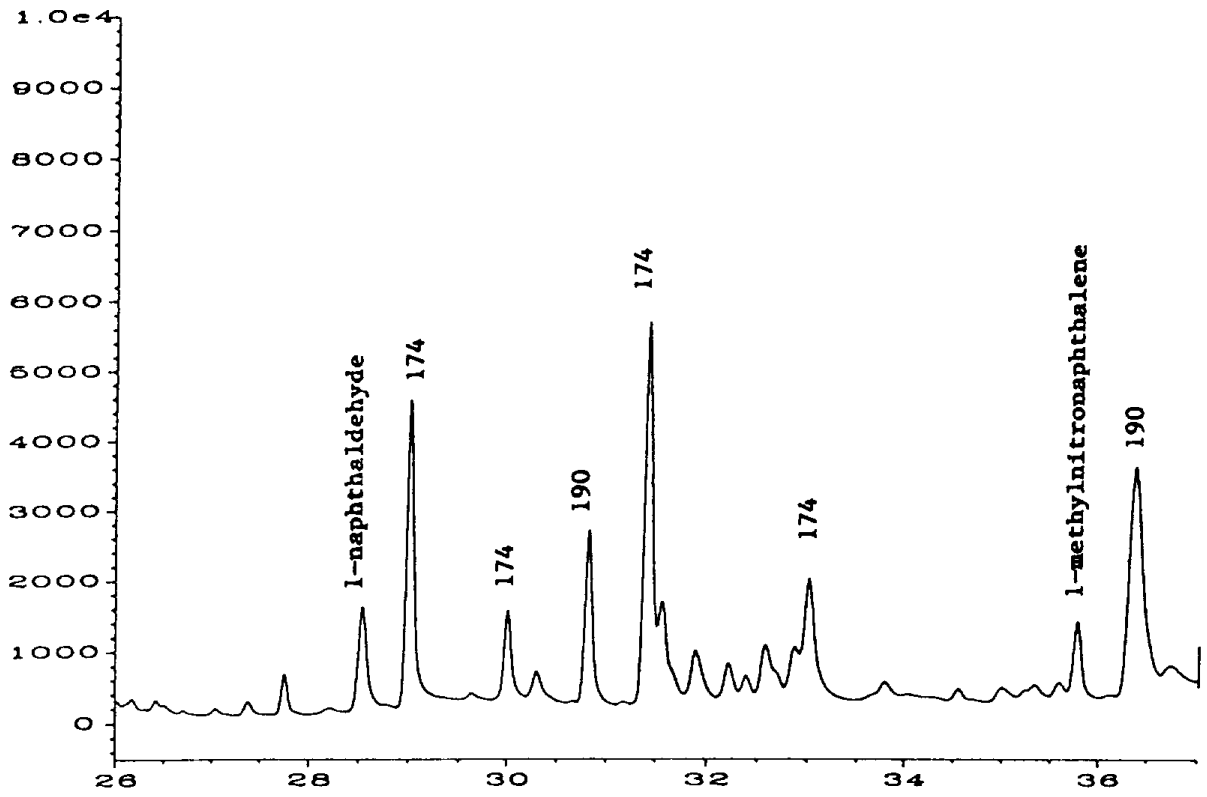

Figure 34. GC-FID chromatogram of the diethyl ether eluate of a sample collected on Tenax solid adsorbent from the gas-phase OH radical-initiated reaction of 1-methylnaphthalene.

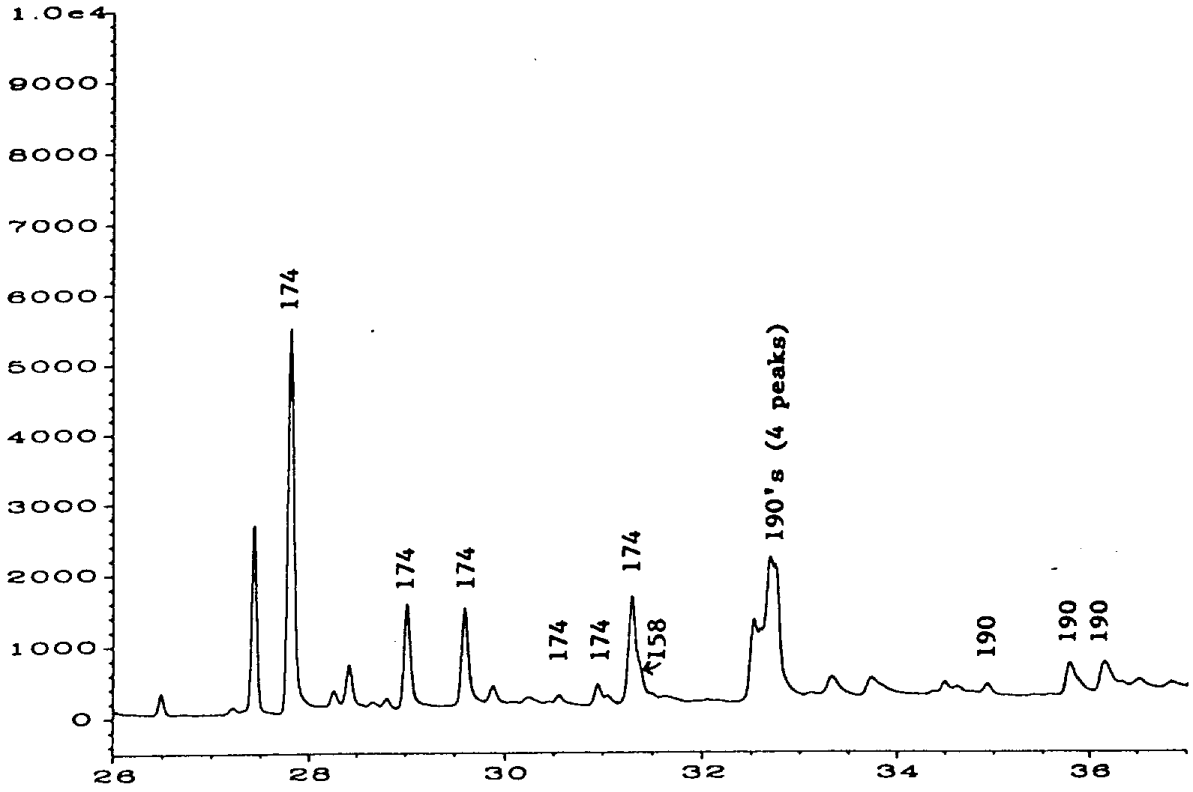

Figure 35. GC-FID chromatogram of the diethyl ether eluate of a sample collected on Tenax solid adsorbent from the gas-phase OH radical-initiated reaction of 2-methylnaphthalene.

experiment for 1-methylnaphthalene leading to product yields a factor of 2-4 lower than the subsequent experiments, with no obvious reason for the discrepancy. For the subsequent experiments, the irradiation times 2-5 min for 1-methylnaphthalene and 3-5 min for 2-methylnaphthalene, with the calculated product yields showing no obvious trend with the extent of reaction which ranged from 25-46% for the 1-methylnaphthalene reactions and from 34-50% for the 2-methylnaphthalene reactions. Neglecting the data from this first experiment, the molar product formation yields were, uncorrected for secondary reactions of the products by photolysis and/or reaction with the OH radical, from 1-methylnaphthalene:; 1-naphthaldehyde, 0.022 ± 0.018; molecular weight 174 products, 0.18 ± 0.09; and molecular weight 190 products, 0.11 ± 0.06; and from 2-methylnaphthalene: molecular weight 174 products, 0.17 ± 0.08; and molecular weight 190 products, 0.11 ± 0.02; where the indicated errors are the two least-squares standard deviations and do not include the uncertainties in the GC-FID response factors. 1-Naphthaldehyde is clearly formed after H-atom abstraction from the substituent methyl group [analogous to the formation of benzaldehyde from toluene (Atkinson, 1994)] and the percentage of the 1-methylnaphthalene reaction proceeding by H-atom abstraction is therefore ~2%. The molecular weight 174 and 190 products, uncorrected for further reactions, account for ~28-29% of the overall reaction products (and after correction for secondary reactions will account for >30% of the overall products).

NO_3 Radical Reactions with 1- and 2-Methylnaphthalene

A series of reactions of N_2O_5 - NO_2 - methylnaphthalene - air mixtures were carried out with GC-FID and GC-MS analyses, using the analytical procedures discussed above for the OH radical-initiated reactions. The products identified by GC and MS matching with authentic standards were mainly methylnitronaphthalenes (Zielinska *et al.*, 1989; Gupta, 1996). Figures 36 and 37 show GC-FID traces of the diethyl ether eluates of ~15 liter volume samples collected from the chamber onto Tenax-TA solid adsorbent from the 1- and 2-methylnaphthalene reactions, respectively. Quantification of the methylnitronaphthalenes from the NO_3 radical-initiated reactions of 1- and 2-methylnaphthalene led to molar methylnitronaphthalene formation yields of: 1-methyl-x-nitronaphthalenes from 1-methylnaphthalene, 0.27 ± 0.07; and 2-methyl-x-nitronaphthalenes from 2-methylnaphthalene, 0.39 ± 0.14, where the indicated errors are two

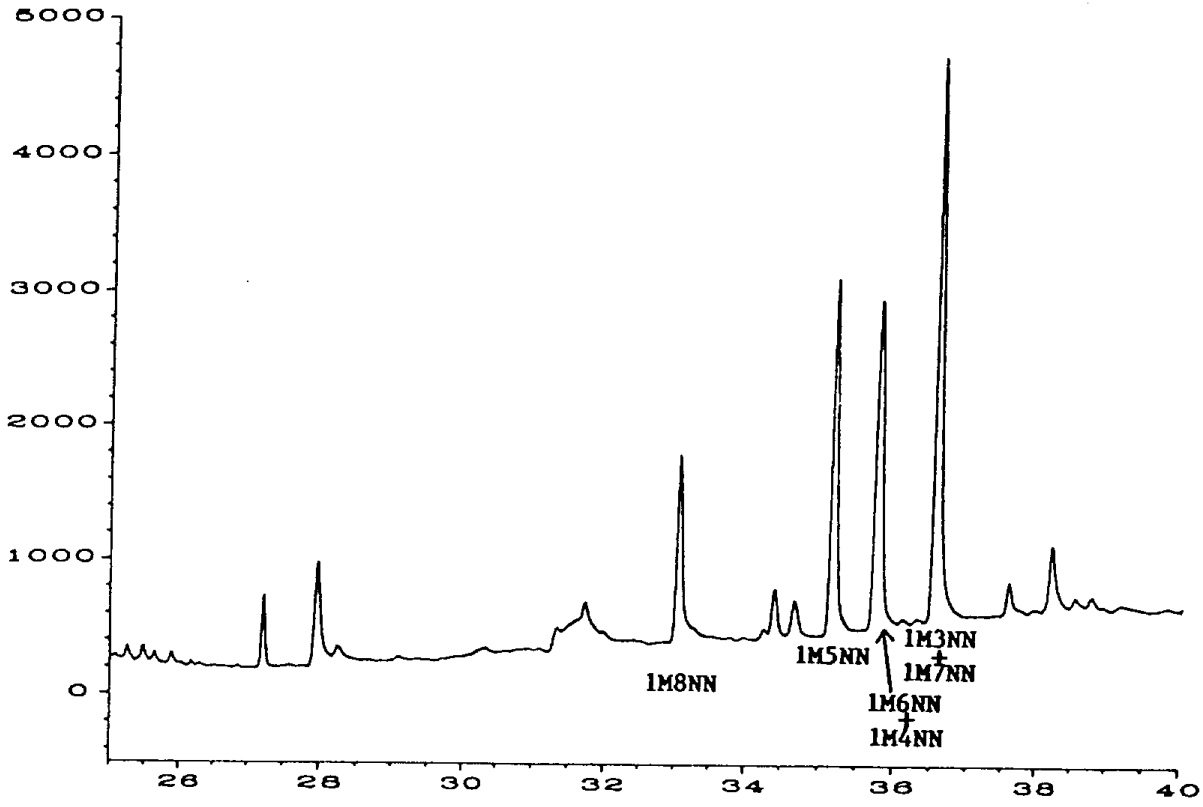

Figure 36. GC-FID chromatogram of the diethyl ether eluate of a sample collected on Tenax solid adsorbent from the gas-phase NO_3 radical-initiated reaction of 1-methylnaphthalene.

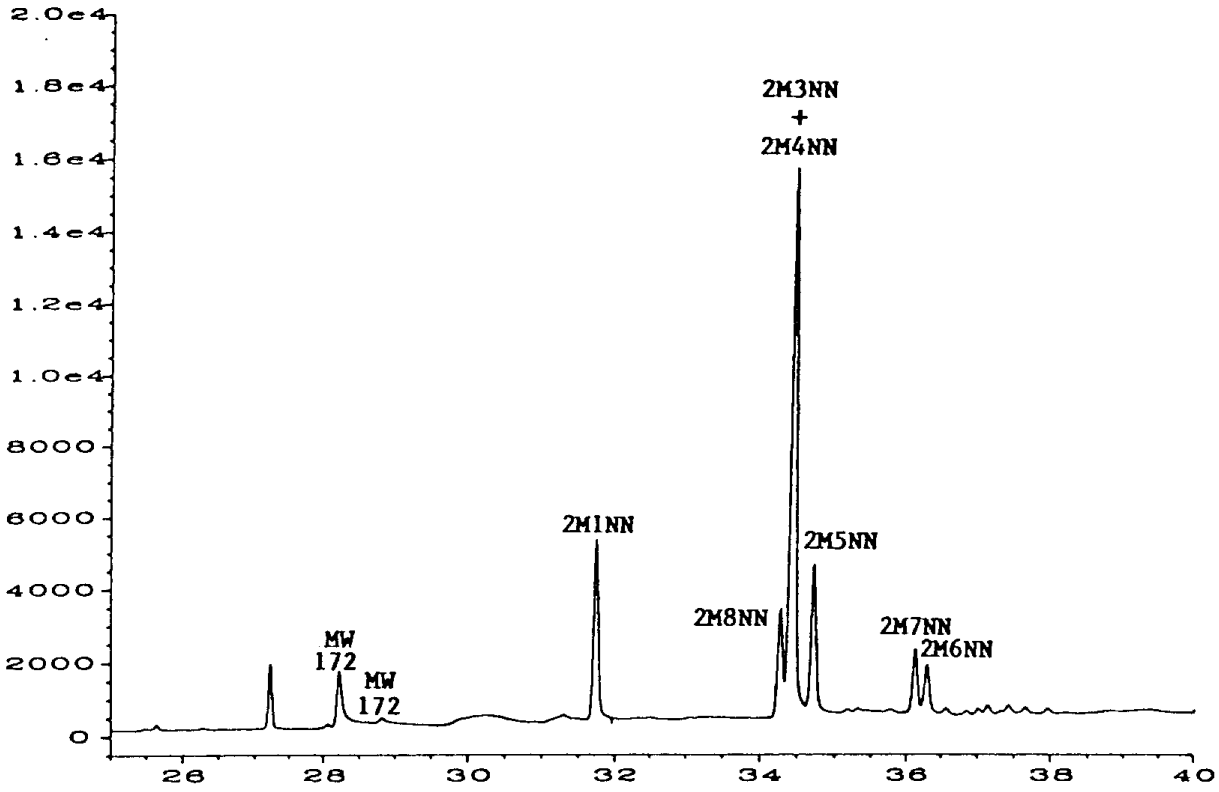

Figure 37. GC-FID chromatogram of the diethyl ether eluate of a sample collected on Tenax solid adsorbent from the gas-phase NO_3 radical-initiated reaction of 2-methylnaphthalene.

least-squares standard deviations and do not include the uncertainties in the GC-FID response factors. These methylnitronaphthalene formation yields from the NO_3 radical-initiated reactions of 1- and 2-methylnaphthalene are consistent with our earlier, qualitative, measurements (Zielinska *et al.*, 1989).

The OH radical- and NO_3 radical-initiated reactions of 1- and 2-methylnaphthalene are therefore analogous to the corresponding reactions of naphthalene discussed in Section 5.

7. CONCLUSIONS

The research carried out in this program and discussed in Sections 2 through 6 above have advanced our knowledge of the atmospheric reactions of alkenes and aromatic hydrocarbons.

Alkene Chemistry. We have developed an improved method for determining the yields of OH radicals from the reactions of O_3 with alkenes, utilizing 2-butanol to scavenge OH radicals and determining the OH radical formation yields from the amounts of 2-butanone formed. We have shown that this more accurate technique agrees well with the results of previous studies from our laboratory using cyclohexane to scavenge OH radicals and deriving the OH radical formation yields from the amounts of cyclohexanone plus cyclohexanol formed (Atkinson *et al.*, 1992; Atkinson and Aschmann, 1993).

Product studies of the reactions of O_3 with a series of methyl-substituted ethenes show that the sum of the primary carbonyls is unity (except where HCHO can be formed from secondary reactions of the biradical co-products), and a number of additional products (methane, methanol, ketene, glyoxal, CO and CO_2) were identified and quantified by *in situ* FTIR absorption spectroscopy. The yields of these products allows certain biradical decomposition pathways to be delineated.

Product studies of the reactions of the OH radical with 2-methylpropene, *cis*-2-butene, 2-methyl-2-butene and 2,3-dimethyl-2-butene in the presence of NO showed the formation of small amounts of organic nitrates from the $R\dot{O}_2$ + NO reactions, and the carbonyl products formed and their formation yields showed that the intermediate β-hydroxyalkoxy radicals undergo dominantly decomposition. API-MS analyses of the reacted mixtures showed no evidence for the formation of the β-hydroxycarbonyls which would be formed from reactions of the intermediate β-hydroxyalkoxy radicals with O_2. In the absence of NO_x, API-MS analyses indicated the formation of the products expected from the reactions of β-hydroxyalkyl peroxy radicals with organic peroxy radicals and HO_2 reactions (carbonyls, hydroxycarbonyls, dihydroxyalkanes and hydroxyhydroperoxides).

Aromatic Chemistry. Identification and quantification of the products of the reactions of the OH radical with naphthalene, 1- and 2-methylnaphthalene and biphenyl in the presence

of NO_x showed that these reactions are analogous to the OH radical-initiated reactions of monocyclic aromatic hydrocarbons, in that a major reaction pathway(s) lead to the formation of ring-opened products. The formation of 2-formylcinnamaldehyde from naphthalene was observed in high (~35%) yield, together with a number of other ring-opened and ring-retaining products. Although most of the products from the methylnaphthalene and biphenyl reactions were not specifically identified, the reactions appear to be quite similar to that for naphthalene. The NO_3 radical-initiated reactions of naphthalene and 1- and 2-methylnaphthalene lead to the formation of nitronaphthalenes and methylnitronaphthalenes in significant (~25-30%) yield. These product studies of two-ring polycyclic aromatic hydrocarbons reinforce the product data obtained for the monocyclic aromatic hydrocarbons (Atkinson, 1994; Kwok *et al.*, 1997).

References

Arey, J., B. Zielinska, R. Atkinson and A. M. Winer (1987): Polycyclic aromatic hydrocarbon and nitroarene concentrations in ambient air during a wintertime high-NO_x episode in the Los Angeles basin. *Atmos. Environ., 21*, 1437-1444.

Arey, J., R. Atkinson, B. Zielinska and P. A. McElroy (1989): Diurnal concentrations ofvolatile polycyclic aromatic hydrocarbons and nitroarenes during a photochemical air pollution episode in Glendora, California. *Environ. Sci. Technol., 23*, 321-327.

Aschmann, S. M., J. Arey and R. Atkinson (1996): OH radical formation from the gas-phase reactions of O_3 with methacrolein and methyl vinyl ketone. *Atmos. Environ., 30*, 2939-2943.

Aschmann, S. M., A. A. Chew, J. Arey and R. Atkinson (1997): Products of the gas-phase reaction of OH radicals with cyclohexane: Reactions of the cyclohexoxy radical. *Int. J. Chem. Kinet.*, to be submitted for publication.

Atkinson, R., W. P. L. Carter, A. M. Winer, and J. N. Pitts, Jr. (1981): An experimental protocol for the determination of OH radical rate constants with organics using methyl nitrite as an OH radical source. *J. Air Pollut. Control Assoc., 31*, 1090-1092.

Atkinson, R., S. M. Aschmann, W. P. L. Carter, A. M. Winer, and J. N. Pitts, Jr. (1982): Alkyl nitrate formation from the NO_x-air photooxidations of C_2-C_8 *n*-alkanes, *J. Phys. Chem., 86*, 4563-4569.

Atkinson, R. and W. P. L. Carter (1984): Kinetics and mechanisms of the gas-phase reactions of the gas-phase reactions of ozone with organic compounds under atmospheric conditions. *Chem. Rev., 84*, 437-470.

Atkinson, R., C. N. Plum, W. P. L. Carter, A. M. Winer and J. N. Pitts, Jr. (1984): Rate constants for the gas-phase reactions of nitrate radicals with a series of organics in air at 298 $\pm$ 1 K. *J. Phys. Chem., 88*, 1210-1215.

Atkinson, R., E. C. Tuazon and W. P. L. Carter (1985): Extent of H-atom abstraction from the reaction of the OH radical with 1-butene under atmospheric conditions. *Int. J. Chem. Kinet., 17*, 725-734.

Atkinson, R., J. Arey, B. Zielinska and S. M. Aschmann (1987): Kinetics and products of the gas-phase reactions of OH radicals and N_2O_5 with naphthalene and biphenyl. *Environ. Sci. Technol., 21*, 1014-1022.

Atkinson, R. (1988): *Atmospheric Transformations of Automotive Emissions*, In *Air Pollution, Public Health, and the Automobile*, Eds. Watson, A. Y.; Bates, R. R.; Kennedy, D., National Academy Press, Washington, DC, pp. 99-132.

Atkinson, R. (1989): Kinetics and mechanisms of the gas-phase reactions of the hydroxyl radical with organic compounds. *J. Phys. Chem. Ref. Data, Monograph 1*, 1-246.

Atkinson, R., E. C. Tuazon and J. Arey (1990): Reactions of naphthalene in N_2O_5-NO_3-NO_2-air mixtures. *Int. J. Chem. Kinet., 22*, 1071-1082.

Atkinson, R. (1991): Kinetics and mechanisms of the gas-phase reactions of the NO_3 radical with organic compounds. *J. Phys. Chem. Ref. Data, 20*, 459-507.

Atkinson, R., S. M. Aschmann, J. Arey and B. Shorees (1992): Formation of OH radicals in the gas phase reactions of O_3 with a series of terpenes. *J. Geophys. Res., 97*, 6065-6073.

Atkinson, R. and S. M. Aschmann (1993): OH radical production from the gas-phase reactions of O_3 with a series of alkenes under atmospheric conditions. *Environ. Sci. Technol., 27*, 1357-1363.

Atkinson, R. (1994): Gas-phase tropospheric chemistry of organic compounds. *J. Phys. Chem. Ref. Data, Monograph 2*, 1-216.

Atkinson, R. and J. Arey (1994): Atmospheric chemistry of gas-phase polycyclic aromatic hydrocarbons: Formation of atmospheric mutagens. *Environ. Health Perspect., 102(Suppl.4)*, 117-126.

Atkinson, R. and S. M. Aschmann (1994): Products of the gas-phase reactions of aromatic hydrocarbons: Effect of NO_2 concentration. *Int. J. Chem. Kinet., 26*, 929-944.

Atkinson, R., J. Arey, S. M. Aschmann and E. C. Tuazon (1994a): Formation of $O(^3P)$ atoms and epoxides from the gas-phase reaction of O_3 with isoprene. *Res. Chem. Intermed., 20*, 385-394.

Atkinson, R., S. M. Aschmann, J. Arey and E. C. Tuazon (1994b): Formation yields of epoxides and $O(^3P)$ atoms from the gas-phase reactions of O_3 with a series of alkenes. *Int. J. Chem. Kinet., 26*, 945-950.

Atkinson, R., E. C. Tuazon, I. Bridier and J. Arey (1994c): Reactions of NO_3-naphthalene adducts with O_2 and NO_2. *Int. J. Chem. Kinet., 26*, 605-614.

Atkinson, R., E. C. Tuazon, and S. M. Aschmann (1995a): Products of the gas-phase reactions of O_3 with alkenes. *Environ. Sci. Technol., 29*, 1860-1866.

Atkinson, R., E. C. Tuazon and S. M. Aschmann (1995b): Products of the gas-phase reactions of a series of 1-alkenes and 1-methylcyclohexene with the OH radical in the presence of NO. *Environ. Sci. Technol.*, *29*, 1674-1680.

Atkinson, R., J. Arey, S. M. Aschmann, S. B. Corchnoy and Y. Shu (1995c): Rate constants for the gas-phase reactions of *cis*-3-hexen-1-ol, *cis*-3-hexenylacetate, *trans*-2-hexenal, and linalool with OH and NO_3 radicals and O_3 at 296 $\pm$ 2 K, and OH radical formation yields from the O_3 reactions. *Int. J. Chem. Kinet.*, *27*, 941-955.

Atkinson, R., E. S. C. Kwok, J. Arey and S. M. Aschmann (1995d): Reactions of alkoxy radicals in the atmosphere. *Faraday Discuss. Chem. Soc.*, *100*, 23-37.

Atkinson, R. (1997a): Atmospheric reactions of alkoxy and β-hydroxyalkoxy radicals. *Int. J. Chem. Kinet. 29*, 99-111.

Atkinson, R. (1997b): Gas-phase tropospheric chemistry of organic compounds: 1. Alkanes and alkenes. *J. Phys. Chem. Ref. Data*, in press.

Bailey, P. S. and R. E. Erickson (1961): Diphenaldehyde (biphenyl, 2,2'-diformyl-). *Org. Synth.*, *41*, 41-45.

Bunce, N. L. and J. Zhu (1994): Products from photochemical reactions of naphthalene in air. *Polycyclic Aromatic Hydrocarbons, 5*, 123-130.

Blake, N. J., S. A. Penkett, K. C. Clemitshaw, P. Anwyl, P. Lightman, A. R. W. Marsh and G. Butcher (1993): Estimates of atmospheric hydroxyl radical concentrations from the observed decay of many reactive hydrocarbons in well-defined urban plumes. *J. Geophys. Res.*, *98*, 2851-2864.

Carter, W. P. L., K. R. Darnall, R. A. Graham, A. M. Winer and J. N. Pitts, Jr. (1979): Reactions of C_2 and C_4 α-hydroxy radicals with oxygen. *J. Phys. Chem.*, *83*, 2305-2311.

Carter, W. P. L. (1994): Development of ozone reactivity scales for volatile organic compounds. *J. Air Waste Manage. Assoc.*, *44*, 881-899.

Chameides, W. L., F. Fehsenfeld, M. O. Rodgers, C. Cardelino, J. Martinez, D. Parrish, W. Lonneman, D. R. Lawson, R. A. Rasmussen, P. Zimmerman, J. Greenberg, P. Middleton and T. Wang (1992): Ozone precursor relationships in the ambient atmosphere. *J. Geophys. Res.*, *97*, 6037-6055.

Dumdie, B. E. and R. J. O'Brien (1984): Toluene degradation products in simulated atmospheric conditions. *Nature, 311*, 248-250.

EPA/NIH (1980): EPA/NIH Mass Spectral Data Base, NSRDS-NBS 63, Suppl.1, U.S. Government Printing Office, Washington, D.C.

EPA (1990): Hewlett Packard HP 59963B, EPA Library FT-IR Spectra.

Garvin, D. and C. Schubert (1956): The vapor phase infrared spectra of the ozonides of ethylene, propylene and isobutylene. *J. Phys. Chem.*, *60*, 807-808.

Grosjean, D., E. Grosjean and E. L. Williams II (1994): Atmospheric chemistry of olefins: A product study of the ozone-alkene reaction with cyclohexane added to scavenge OH. *Environ. Sci. Technol.*, *28*, 186-196.

Grosjean, E. and D. Grosjean (1996a): Carbonyl products of the gas phase reaction of ozone with C_5-C_7 alkenes. *Environ. Sci. Technol.*, *30*, 1321-1327.

Grosjean, E. and D. Grosjean (1996b): Carbonyl products of the gas phase reaction of ozone with symmetrical alkenes. *Environ. Sci. Technol.*, *30*, 2036-2044.

Grosjean, E. and D. Grosjean (1996c): Carbonyl products of the gas phase reaction of ozone with 1,1-disubstituted alkenes. *J. Atmos. Chem.*, *24*, 141-156.

Grosjean, E. and D. Grosjean (1996d): Carbonyl products of the gas phase reaction of ozone with 1-alkenes. *Atmos. Environ.*, *30*, 4107-4113.

Grosjean, E., J. B. de Andrade and D. Grosjean (1996a): Carbonyl products of the gas-phase reaction of ozone with simple alkenes. *Environ. Sci. Technol.*, *30*, 975-983.

Grosjean, E., D. Grosjean and J. H. Seinfeld (1996b): Atmospheric chemistry of 1-octene, 1-decene, and cyclohexene: Gas-phase carbonyl and peroxyacyl nitrate products. *Environ. Sci. Technol.*, *30*, 1038-1047.

Gupta, P. (1996); "*The Contribution of Methylnitronaphthalenes to the Vapor-Phase Mutagenicity Observed in Ambient Air Samples Collected at Redlands, California*". M.S. Thesis, University of California, Riverside, CA.

Gupta, P., W. P. Harger and J. Arey (1996): The contribution of nitro- and methylnitronaphthalenes to the vapor-phase mutagenicity of ambient air samples. *Atmos. Environ.*, *30*, 3157-3166.

Hakola, H., B. Shorees, J. Arey and R. Atkinson (1993): Product formation from the gas-phase reactions of OH radicals and O_3 with β-phellandrene. *Environ. Sci. Technol.*, *27*, 278-283.

Hakola, H., J. Arey, S. M. Aschmann and R. Atkinson (1994): Product formation from the gas-phase reactions of OH radicals and O_3 with a series of monoterpenes. *J. Atmos. Chem., 18*, 75-102.

Halverson, F. and V. Z. Williams (1947): The infra-red spectrum of ketene. *J. Chem. Phys., 15*, 552-559.

Hatakeyama, S., H. Kobayashi and H. Akimoto (1984): Gas-phase oxidation of SO_2 in the ozone-olefin reactions. *J. Phys. Chem., 88*, 4736-4739.

Hatakeyama, S., H. Kobayashi, Z.-Y. Lin, H. Takagi and H. Akimoto (1986): Mechanism for the reaction of CH_2OO with SO_2. *J. Phys. Chem., 90*, 4131-4135.

Horie, O., P. Neeb and G. K. Moortgat (1994): Ozonolysis of *trans*- and *cis*-2-butenes in low parts-per-million concentration ranges. *Int. J. Chem. Kinet., 26*, 1075-1094.

Hu, J. and D. H. Stedman (1995): Atmospheric RO_x radicals at an urban site: Comparison to a simple theoretical model. *Environ. Sci. Technol., 29*, 1655-1659.

Koch, R., M. Siese, C. Fittschen and C. Zetzsch (1994): Addition and Regeneration of OH in the Presence of O_2 and NO: Results on Naphthalene, Isoprene and Acetylene. Presented at the Joint LACTOZ/HALIPP Workshop, Leipzig, Germany, September 20-22.

Knispel, R., R. Koch, M. Siese and C. Zetzsch (1990): Adduct formation of OH radicals with benzene, toluene, and phenol and consecutive reactions of the adducts with NO_x and O_2. *Ber. Bunsenges. Phys. Chem., 94*, 1375-1379.

Kwok, E. S. C. and R. Atkinson (1995): Estimation of hydroxyl radical reaction rate constants for gas-phase organic compounds using a structure-reactivity relationship: An update. *Atmos. Environ., 29*, 1685-1695.

Kwok, E. S. C., R. Atkinson and J. Arey (1995): Observation of hydroxycarbonyls from the OH radical-initiated reaction of isoprene. *Environ. Sci. Technol., 29*, 2467-2469.

Kwok, E. S. C., R. Atkinson and J. Arey (1996a): Isomerization of β-hydroxyalkoxy radicals formed from the OH radical-initiated reactions of C_4-C_8 1-alkenes. *Environ. Sci. Technol., 30*, 1048-1052.

Kwok, E. S. C., J. Arey and R. Atkinson (1996b): Alkoxy radical isomerization in the OH radical-initiated reactions of C_4-C_8 *n*-alkanes. *J. Phys. Chem., 100*, 214-219.

Kwok, E. S. C., S. M. Aschmann, J. Arey and R. Atkinson (1997): API-MS product study of the gas-phase OH radical-initiated reactions of *o*-, *m*- and *p*-xylene in the presence and absence of NO_x. *J. Chem. Soc. Faraday Trans.*, in press.

Lamb, B., D. Gay, H. Westberg and T. Pierce (1993): A biogenic hydrocarbon emission inventory for the U.S.A. using a simple forest canopy model. *Atmos. Environ.*, *27A*, 1673-1690.

Lane, D. A. and H. Tang (1994): Photochemical degradation of polycyclic aromatic compounds. I. Naphthalene. *Polycyclic Aromatic Hydrocarbons*, *5*, 131-138.

Larson, R. A., W. J. Garrison and K. A. Marley (1986): Preparation and photoisomerization of 2-formylcinnamaldehyde in solution. *Tetrahed. Lett.*, *27*, 3987-3990.

Lorenz, K. and R. Zellner (1983): Kinetics of the reactions of OH-radicals with benzene, benzene-d_6 and naphthalene. *Ber. Bunsenges. Phys. Chem.*, *87*, 629-636.

Lurmann, F. W. and H. H. Main (1992): *Analysis of the Ambient VOC Data Collected in the Southern California Air Quality Study*. Final Report to the California Air Resources Board Contract No. A832-130, Sacramento, CA, February.

Marley, K. A., R. A. Larson, P. L. Stapleton, W. J. Garrison and C. M. Klodnycky (1987): Ozonolysis of naphthalene derivatives in water and in kerosene films. *Ozone Sci. Eng.*, *9*, 23-36.

Martin, R. S., H. Westberg, E. Allwine, L. Ashman, C. J. Farmer and B. Lamb (1991): Measurement of isoprene and its atmospheric oxidation products in a central Pennsylvania deciduous forest. *J. Atmos. Chem.*, *13*, 1-32.

Miyoshi, A., S. Hatakeyama and N. Washida (1994): OH radical-initiated photooxidation of isoprene: An estimate of global CO production. *J. Geophys. Res.*, *99*, 18779-18787.

Montzska, S. A., M. Trainer, P. D. Goldan, W. C. Kuster and F. C. Fehsenfeld (1993): Isoprene and its photooxidation products, methyl vinyl ketone and methacrolein, in the rural troposphere. *J. Geophys. Res.*, *98*, 1101-1111.

Muthuramu, K., P. B. Shepson and J. M. O'Brien (1993): Preparation, analysis, and atmospheric production of multifunctional organic nitrates. *Environ. Sci. Technol.*, *27*, 1117-1124.

Nelson, L., O. Rattigan, R. Neavyn, H. Sidebottom, J. Treacy and O. J. Nielsen (1990): Absolute and relative rate constants for the reactions of hydroxyl radicals and chlorine atoms with a series of aliphatic alcohols and ethers at 298 K. *Int. J. Chem. Kinet.*, *22*, 1111-1126.

Niki, H., P. D. Maker, C. M. Savage and L. P. Breitenbach (1977): Fourier transform IR spectroscopic observation of propylene ozonide in the gas phase reaction of ozone-*cis*-2-butene-formaldehyde. *Chem. Phys. Lett.*, *46*, 327-330.

Niki, H., P. D. Maker, C. M. Savage and L. P. Breitenbach (1978): Mechanism for hydroxyl radical initiated oxidation of olefin-nitric oxide mixtures in parts per million concentrations. *J. Phys. Chem.*, *82*, 135-137.

Niki, H., P. D. Maker, C. M. Savage and L. P. Breitenbach (1981): An FTIR study of mechanisms for the HO radical-initiated oxidation of C_2H_4 in the presence of NO: Detection of glycolaldehyde. *Chem. Phys. Lett.*, *80*, 499-503.

Niki, H., P. D. Maker, C. M. Savage, L. P. Breitenbach and R. I. Martinez (1984): Fourier transform infrared study of $^{18}O_3$ with *trans*-CHCl=CHCl in $^{16}O_2$-rich mixtures. Branching ratio for O-atom production via dissociation of the primary Criegee intermediate. *J. Phys. Chem.*, *88*, 766-769.

Niki, H., P. D. Maker, C. M. Savage, L. P. Breitenbach, and M. D. Hurley (1987): FTIR spectroscopic study of the mechanism for the gas-phase reaction between ozone and tetramethylethylene. *J. Phys. Chem.*, *91*, 941-946.

Paulson, S. E., and J. H. Seinfeld (1992): Atmospheric photochemical oxidation of 1-octene: OH, O_3, and $O(^3P)$ reactions. *Environ. Sci. Technol.*, *26*, 1165-1173.

Paulson, S. E., R. C. Flagan, and J. H. Seinfeld (1992a): Atmospheric photooxidation of isoprene. Part II: The ozone-isoprene reaction. *Int. J. Chem. Kinet.*, *27*, 103-125.

Paulson, S. E., R. C. Flagan and J. H. Seinfeld (1992b): Atmospheric photooxidation of isoprene. Part I: The hydroxyl radical and ground state atomic oxygen reactions. *Int. J. Chem. Kinet.*, *24*, 79-101.

Pitts, J. N., Jr., R. Atkinson, J. A. Sweetman and B. Zielinska (1985): The gas-phase reaction of naphthalene with N_2O_5 to form nitronaphthalenes. *Atmos. Environ.*, *19*, 701-705.

Pouchert, C. J. (1989): The Aldrich Library of FT-IR Spectra, Edition 1, Vol. 3, Vapor Phase, Aldrich Chemical Co., Inc., Milwaukee, WI.

Riemer, D. D., P. J. Milne, C. T. Farmer and R. G. Zika (1994): Determination of terpene and related compounds in semi-urban air by GC-MSD. *Chemosphere*, *28*, 837-850.

Rowley, D. M., P. D. Lightfoot, R. Lesclaux and T. J. Wallington (1991): UV absorption spectrum and self-reaction of cyclohexylperoxy radicals. *J. Chem. Soc. Faraday Trans.*, *87*, 3221-3226.

Scanlon, J. T. and D. E. Willis (1985): Calculation of flame ionization detector relative response factors using the effective carbon number concept. *J. Chromat. Sci.*, *33*, 333-340.

Seila, R. L., W. A. Lonneman and S. A. Meeks (1989): *Determination of C_2 to C_{12} Ambient Air hydrocarbons in 39 U.S. Cities, from 1984 through 1986.* U.S. Environmental Protection Agency Report EPA/600/3-89/058, Atmospheric Research and Exposure Assessment Laboratory, Research Triangle Park, NC, September.

Shepson, P. B., E. O. Edney, T. E. Kleindienst, J. H. Pittman, G. R. Namie and L. T. Cupitt (1985): The production of organic nitrates from hydroxyl and nitrate radical reaction with propylene. *Environ. Sci. Technol., 19,* 849-854.

Shu, Y. and R. Atkinson (1994): Rate constants for the gas-phase reactions of O_3 with a series of terpenes and OH radical formation from the O_3 reactions with sesquiterpenes at 296 $\pm$ 2 K. *Int. J. Chem. Kinet., 26,* 1193-1205.

Smith, A. M., E. Rigler, E. S. C. Kwok and R. Atkinson (1996): Kinetics and products of the gas-phase reactions of 6-methyl-5-hepten-2-one and *trans*-cinnamaldehyde with OH and NO_3 radicals. *Environ. Sci. Technol., 30,* 1781-1785.

Taylor, W. D., T. D. Allston, M. J. Moscato, G. B. Fazekas, R. Kozlowski and G. A. Takacs (1980): Atmospheric photodissociation lifetimes for nitromethane, methyl nitrite, and methyl nitrate. *Int. J. Chem. Kinet., 12,* 231-240.

Tuazon, E. C. and R. Atkinson (1990): A product study of the gas-phase reaction of isoprene with the OH radical in the presence of NO_x. *Int. J. Chem. Kinet., 22,* 1221-1236.

Wallington, T. J., P. Dagaut, R. Liu and M. J. Kurylo (1988): Rate constants for the gas phase reactions of OH with C_5 through C_7 aliphatic alcohols and ethers: Predicted and experimental values. *Int. J. Chem. Kinet., 20,* 541-547.

Zielinska, B., J. Arey, R. Atkinson and P. A. McElroy (1989): Formation of methylnitronaphthalenes from the gas-phase reactions of 1- and 2-methylnaphthalene with OH radicals and N_2O_5 and their occurrence in ambient air. *Environ. Sci. Technol., 23,* 723-729.

Glossary of Terms, Abbreviations and Symbols

API-MS	atmospheric pressure ionization tandem mass spectroscopy
C_2H_5ONO	ethyl nitrate
CH_3ONO	methyl nitrite
GC	gas chromatographic
GC-FID	GC with flame ionization
GC-FTIR	GC with Fourier transform infrared spectroscopy
GC-MS	GC with mass spectrometric
ECN	Effective Carbon Numbers
FTIR	Fourier transform infrared
HO_2	hydroperoxyl radical
HP	Hewlett Packard
NMOC	non-methane organic compounds
NO	nitric oxide
NO_2	nitrogen dioxide
NO_3	nitrate radical
N_2O_5	Dinitrogen pentoxide
O_3	ozone
OH	hydroxyl radical
PAH	polycyclic aromatic hydrocarbons
$\dot{R}$	alkyl or substituted-alkyl radical
$R\dot{O}$	alkoxy or substituted-alkoxy radical
$R\dot{O}_2$	alkyl peroxy or substituted-alkyl peroxy radical
$RONO_2$	alkyl nitrate or hydroxyalkyl nitrate